Exploration of enzymatic strategies for synergistic degradation of lignocellulosic substrates

賈, 麗麗

出版情報：九州大学, 2016, 博士（工学）, 課程博士
バージョン：
権利関係：

Exploration of enzymatic strategies for synergistic degradation of lignocellulosic substrates

Lili JIA

Department of Applied Chemistry

Graduate School of Engineering

Kyushu University

Contents

Chapter 1 Introduction

Chapter 2 Effect of pretreatment methods on the synergism of cellulase and xylanase during the hydrolysis of bagasse

Chapter 3 Synergistic degradation of arabinoxylan by free and immobilized xylanases and arabinofuranosidase

Chapter 4 Construction of a novel polymeric proteinaceous scaffold for ratio-controllable binary artificial hemicellulosome

Chapter 5 Conclusions

Chapter 1 Introduction

1. The energy problem and development of alternative energy

1.1 The scenarios of world energy consumption

After the first industrial revolution, people started changing their way of working from hand production to machines, which improved the efficiency of productivity. However, this change inevitably increased the demands of usage of energy. According to a report from International Energy Agency (IEA), the energy consumption of the whole world in 2013 was approximately 9000 Mtoe (million tons of oil equivalent), with coal and oil taking the lead [1]. Campbell and Laherrere evaluated the amount of oil has been extracted until then and estimated the reserves, and predicted the quantity of conventional oil that remains to be discovered and exploited. They concluded that the amount of annual oil production would fall to one fifth of current production until year of 2050 [2]. Besides, severe environmental problems caused by fossil fuels consuming, such as greenhouse gas (GHG) emission and ozone layer depletion, have also raised the widespread concerns of public. Therefore, since the end of last century, people started to seek clean and renewable fuels to alter the relying on fossil fuels.

1.2 The development of renewable energy and bioenergy

The renewable fuels are generally defined as the energies that collected from resources which are naturally renewed in a short time, such as sunlight, wind, water, tides, geothermal heat. However, almost all these resources are limited by the distribution of area. Therefore, the biofuels made from the agricultural or industrial residues, such as wheat straw, corn stover, and sugarcane bagasse, etc., have attracted enormous focus due to its advantages of widely-distributed, high combustion efficiency.

1.3 The production process of bioethanol from lignocellulosic biomass

At present, the ethanol is the most widely used clean energy for vehicles. Brazil and the USA are the two major ethanol producers account for about 85% of the bioethanol production all over the world in 2015 from the report of Renewable Fuels Association (RFA). For these two countries, the main raw materials to make ethanol in large-scale are sucrose from sugarcane and corn [3]. However, these crops are not desirable due to their food and feed value, it causes competition against food for human being consumption. Thus, the second generation of bioethanol made from lignocellulsic biomass started to be studied.

Lignocellulosic materials are renewable, widely distributed and abundantly available, including agricultural residues, pulp waste and wood chips, and recently popularized seaweed [4]. The major operations for production of bioethanol from lignocelluloses are four steps: pretreatment for delignification and loose the structure of hemicellulose and cellulose; hydrolysis of cellulose and hemicellulose to produce fermentable sugars; fermentation of sugars to ethanol by microorganisms; and distillation [5]. The challenges of bioethanol production are mainly focused on the improvement of the efficiency of pretreatment and saccharification.

2. The structure of lignocellulosic biomass

Lignocellulosic biomass is mainly composed of three constituents, cellulose, hemicellulose and lignin. Cellulose is most abundant natural polymer and it is purely composed of D-glucose linked by β-1,4 glycoside bond. Between the fibril, intra- and inter-molecular hydrogen bonding network is formed in highly crystalline structure. Therefore, it is difficult for enzyme to degrade.

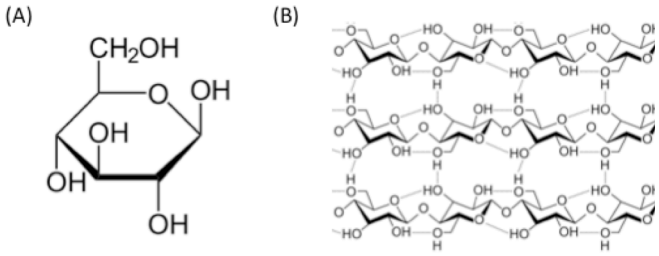

Fig.1-1 The structure of (A) β-D glucose (B) cellulose chain

Hemicelluloses are hetero-polymer consist of varieties of pentoses (such as xylose and arabinose) and hexoses (such as mannose and galactose). The xylose units are crosslinked by β-1,4 glycoside bond as the backbone, and with arabinose, mannose, glucuronic acid, etc., substituted as the side chain (Fig. 1-3) [6,7].

The type of hemicellulose is varied from different species of plant. Arabinoxylans are the main form of hemicellulose in plant cell walls, especially in cereal grains such as wheat [6]. While in softwood, the main component is mannose [8]. The lignin matrix covers the bundles of cellulose and

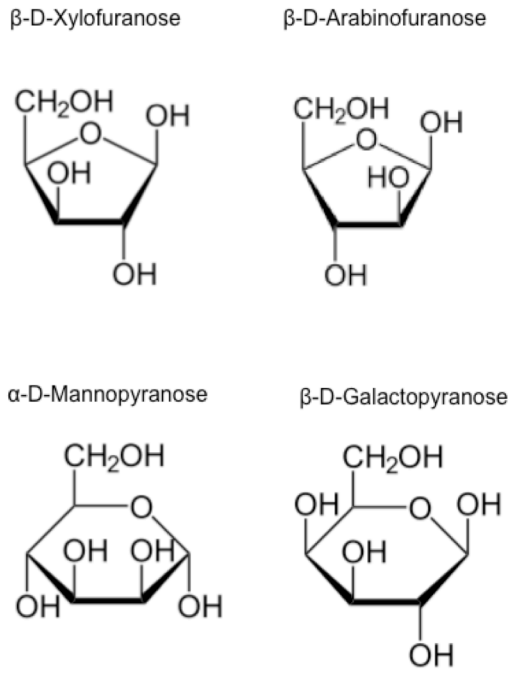

Fig. 1-2 Structure of representative hemicellulose monomers

hemicellulose, and affords the chemical and physical strength of the plant tissues [9].

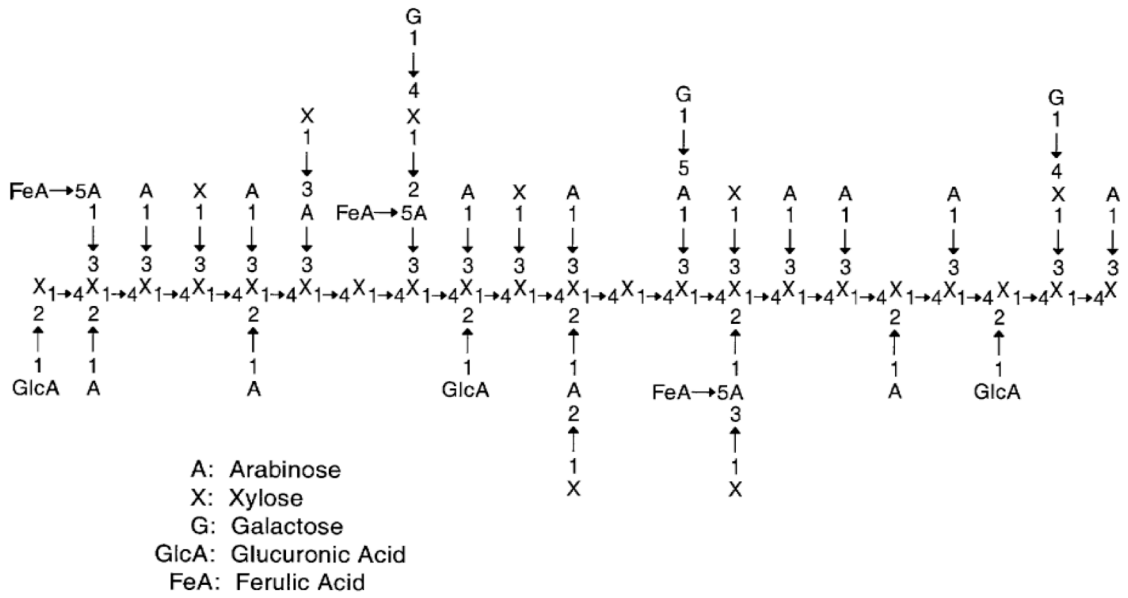

Fig. 1-3 Illustration of structure of hemicelllulose [7].

7-Reprinted from *Carbohydr. Polym.* Vol. 26, Saulnier *et al.*, Cell wall polysaccharide interactions in maize bran, 279-287, Copyright 1995, with permission from Elsevier.

3. The pretreatment of lignocellulosic biomass

Because of the rigid structure of these three components, pretreatment is needed to break the matrix and decrease the crystallinity of cellulose and remove the unfermentable lignin. There are several key factors for an effective pretreatment method: (i) greatly improving the accessibility of cellulose to enzymes, (ii) avoiding the formation of inhibitory products, (iii) reducing energy demands and (iv) minimum heat and power requirements [10]. Physical, chemical, physicochemical and biological treatments are the most fundamental types of pretreatment techniques employed at present. The advantages and disadvantages of each pretreatment was listed in Table 1-1 [10-12].

Table 1-1 The advantages and disadvantages of different pretreatment methods.

Classification	Pretreatment method	Advantages	Disadvantages
Physical	Milling, grinding or chipping	1) Reduce the particle size and polymerization	1) Power requirement
Chemical	Alkali	1) Effectively remove lignin; 2) Less cellulose and hemicellulose loss; 3) Increase the porosity of biomass	1) Generate inhibitors for subsequent process; 2) Long processing time; 3) Neutralization of the pretreated slurry
	Acid	1) Solubilize hemicellulose; 2) Increase the porosity of biomass	1) Loss of fermentable sugars; 2) Equipment corrosion; 3) Acid recovery; 4) Generate inhibitors for subsequent process
	Ionic liquid	1) Decrease the crystallinity of cellulose; 2) Remove lignin; 3) Less inhibitory	1) Expensive, recovery process is needed
Physico-chemical	Steam explosion: SO_2-Steam explosion	1) Lignin transformation and hemicellulose hydrolysis; 2) Possibility of using high chip size; 3) High sugar recovery	1) Fermentable sugar loss; 2) Generation of toxic compounds
	Ammonia fiber explosion (AFEX)	1) Short time needed; 2) Decrease cellulose crystallinity; 3) Less inhibitor generated	1) Efficient ammonia recovery and recycling is needed; 2) Not suitable for high lignin biomass; 3) High cost of
Biological		1) Environmental friendly; 2) Low energy consumption; 3) Low-capital cost	1) Long process time; 2) Large space requirement

4. The enzymatic hydrolysis of cellulose and hemicellulose

The enzymatic hydrolysis of lignocellulose has attracted enormous attentions from industrial and academic area, due to its mild degradation conditions and less inhibitory compounds formation, compared with the acid hydrolysis [13]. As introduced before, the main components of lignocellulose contain cellulose, hemicellulose and lignin. Complete degradation of cellulose and hemicellulose components require a variety of specific enzymes to degrade. Generally these enzymes are classified into two categories: cellulase and hemicellulase.

4.1 Cellulase

Due to the simplicity of the cellulose component, only three types enzymes are needed in complete degradation of cellulose. Cellobiohydrolase (CBH, EC 3.2.1.91) progressively attacks the end of cellulose chain and release cellobiose at the same time. CBH I and II attack the cellulose chain from reducing end and non-reducing end, respectively. Endoglucanase (EG, EC 3.2.1.4) can cut intramolecular β-1,4 glycoside bond of the cellulose chain from amorphous site. β-Glucosidase (BGL, EC 3.2.1.21) preferably hydrolyze cellobiose into glucose [14].

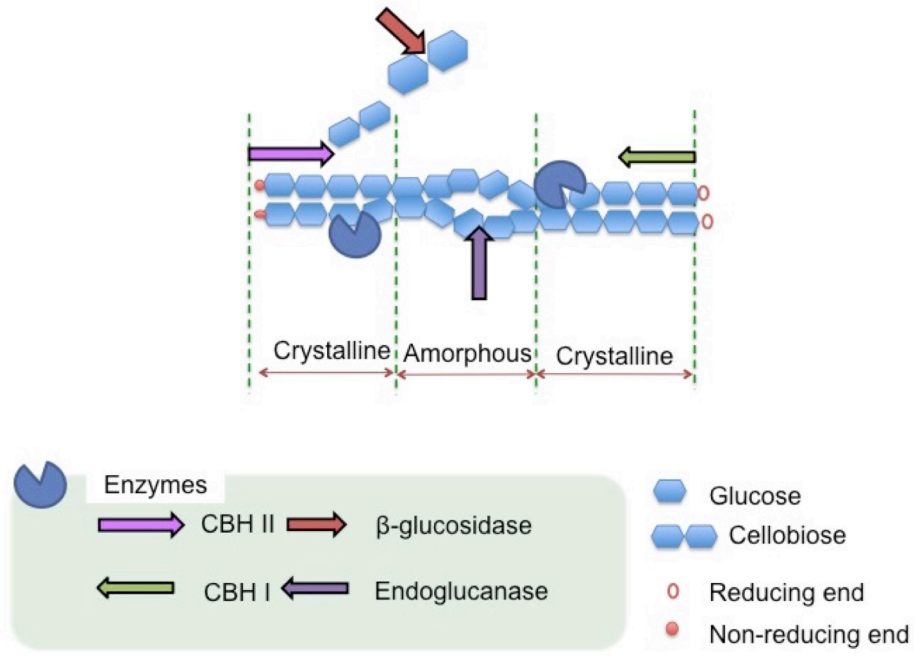

Fig. 1-4 The schematic illustration of three types of cellulase

4.2 Hemicellulase

Unlike cellulase, to effectively degrade hemicellulase needs a large number of enzymes, because of the heterogeneity and complexity of hemicellulose structure. Generally, hemicellulase can be classified as depolymerizing enzyme and debranching enzyme, representing the enzyme digest xylan backbone, and the substitutions of xylan backbone, respectively [14].

4.2.1 Depolymerizing enzyme

Xylanase

Xylanases comprise of endoxylanase (EX, EC 3.2.1.8), which digest the β-1,4 glycoside linkage of xylan backbone and release xylooligomers at the same time. β-xylosidase (BXL, EC 3.2.1.37) can digest xylooligomers into xylose [15]. Endoxylanases are generally belong to glycoside hydrolase (GH) family 5, 8, 10 and 11 [16]. Endo-xylanase from GH family 10 (GH10) and GH11 are most intensively studied enzymes. Endoxylanase from GH10 has a broad substrate specificity compared to endoxylanase from GH11. It can attack not only linear chain of xylan, but also the decorated sites, such as methylglucuronic acid, arabinose and feruloyl-arabinose, of heteroxylans [16]. Some endoxylanase from GH10 even has ability on digesting low molecular mass cellulose substrate, like cello-oligosaccharides [15]. Endoxylanase from GH11 has exclusive activity on xylan backbone. It can only digest on the sites that has three consecutive unsubstituted xylose residues [16].

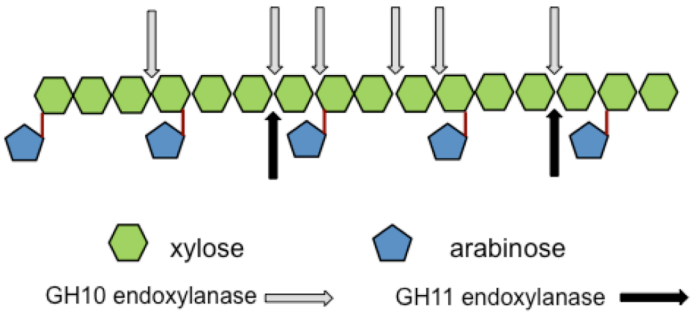

Fig. 1-5 The illustration of the action of endoxylanase from GH10 and GH11.

Mannanase

Another depolymerizing enzyme, mannanase can digest mannan, which is the most hemicellulose component in softwood, has been characterized. Similar to xylans, mannans are also hetero-polymers: 1) linear mannan, 2) glucose linked with mannan, so-called linear glucomannans, 3) galactose decorated mannan, so-called branched galactomanan, and 4) with glucose, galactose decorated mannan, galactoglucomannan [17]. Major enzymes involved in

hydrolysis of mannan are β-mannanases (EC 3.2.1.78), β-mannosidases (EC 3.2.1.25) and β-glucosidases (EC 3.2.1.21) [17,18]. Recent study has shown the inhibition of mannan in cellulose degradation, and this inhibition increased with loading and galactose substituents of mannose backbone [19].

4.2.2 Debranching enzyme

α-Arabinofuranosidase

Arabinoxylans are the main form of hemicellulose in plant cell walls, especially in cereal grains such as wheat. They consist of a xylan backbone with arabinose residues linked to its O-2 or O-3 positions [20]. Arabinofuranosidase (Araf), hydrolyzing arabinofuranosyl moieties from arabinan and xylans, was assigned to different GH families, GH 3, GH 43, GH 51, GH 54 and GH 62, based on their amino acid sequence similarities [21]. For completely degrade arabinoxylan, besides Araf, other hemicellulases, like β-xylosidase and endoxylanase are needed [20,22,23].

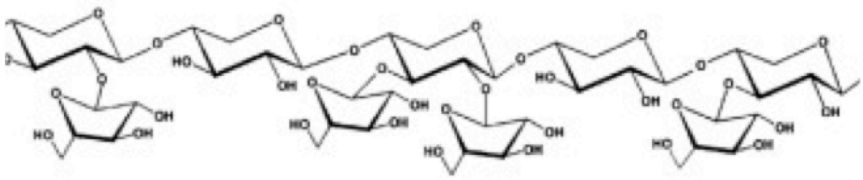

Fig. 1-6 Arabinose substitution of xylan backbone [20]

20-Reprinted from *Biotechnol. Adv.* Vol. 32, Lagaert *et al.*, β-Xylosidases and α-l-arabinofuranosidases: Accessory enzymes for arabinoxylan degradation, 316-332, Copyright 2014, with permission from Elsevier.

Hemicellulolytic esterase

Hemicellulolytic esterases consist of acetyl xylan esterase (AXE, EC 3.1.1.72) and ferulic acid esterase (FAE, EC 3.1.1.73), that hydrolyze acetyl substituents and ester bond between ferulic acid and arabinose [18,24], respectively. Feruloyl ester bond has shown to be involved in the crosslinking between xylan and lignin, addition of this esterase can release the lignin from hemicellulose and improve the efficiency of lignocellulose degradation [18,25].

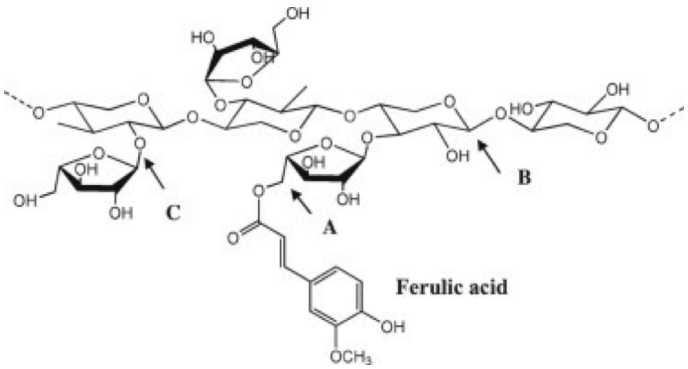

Fig. 1-7 Structure of ferulic acid substituted to arabinoxylan. (A) Ferulic acid linked to arabinose side chain of xylan backbone; (B) β-1,4 linked xylan backbone; (C) α-1,2-linked arabinose to xylan backbone [24].

24-Reprinted from *Mol. Plant.* Vol. 2, Marcia, Feruloylation in grasses: current and future perspective, 861-872. Copyright 2009, with permission of Elsevier.

5. Enzymatic strategy for improving efficiency of biodegradation of lignocellulose

It was reported that the cost of enzymes is still the main obstacle that impeding the biofuel production [26]. Besides optimizing the cost of enzyme production, developing the strategies to improve the enzyme performance and reusability to achieve high bioethanol yield at low enzyme loadings is urgently needed. Thus, in the following context, the enzymatic strategies that focus on improving reducing sugars production are stated.

5.1 Synergism between enzymes

As the complicated structure and crosslinking between each component of lignocellulose, effective degradation of lignocellulose needs a consortium of enzymes that work cooperatively. The definition of synergism is the products released by mixture of enzymes are greater than the sum of products released by single enzymes using separately. Calculation of the degree of synergy (DS) is an effective way to quantitatively evaluate the synergism. As shown in Equation 1, if the DS value is more than 1, the synergism exists between tested enzymes; if the DS value is less than 1, antagonism may happen between tested enzymes.

$DS = Y_{1+2+3} / (\alpha Y_1 + \beta Y_2 + \gamma Y_3)$ [27]

Where α, β, γ correspond to ratio of each single enzyme to whole mixture, and Y_{1+2+3} correspond to the yield of products released by enzyme mixture, and Y_1, Y_2 and Y_3 correspond to the yield of products released by each single enzyme.

Many synergism studies using commercial enzymes or crude enzyme mixtures to optimize the hydrolysis of substrate, usually lignocellulosic biomass, aiming at high yield of reducing

sugars production. In the contrary, some studies using pure enzymes in hydrolysis of model substrate or lignocellulosic biomass, to obtain more information about the one-on-one interaction between enzymes. The synergism between purified enzymes was studied to optimize the 'minimum enzymatic mixture' for efficient degradation of lignocellulosic substrate [14].

Studies about synergistic effect between cellulases, hemicellulases, and cellulase-hemicellulase, in degradation of model substrates and lignocellulosic biomass will be clarified in detail below.

5.1.1 Synergism between cellulases

As introduced before, cellulases consist of three enzymes, EG, CBH and BGL. Each enzyme specifically hydrolyze the 1,4 -β-bond of different substrate. The synergism between endo- and exo- cellulases, EG and CBH, is most widely studied [28-30]. EG can randomly cut the glycosidic bond at the amorphous part of cellulose, resulting the new available hydrolysis site for the action of CBH [31]. Moreover, the synergism between CBH I and II [32,33], between endoglucanases [34], and between these three components and BGL [31] in hydrolysis of model substrates have also been investigated.

Beside, some studies have shown the synergism between cellulase and non-hydrolytic enzymes. Han and Chen separated one protein from fresh postharvest corn stover, and then this protein (Zea h) was subjected to synergism study together with commercial cellulase of *Trichoderma reesei*. It is shown that 2-fold more glucose was produced from filter paper, when using Zea h and cellulase together than using cellulase alone [35]. The possible mechanism for this phenomenon is Zea h could weaken the inter- or intra-molecular hydrogen bond intensity of substrate and increase the adsorption of cellulase onto a filter paper [35].

5.1.2 Synergism between hemicellulases

The synergism between hemicellulases has been intensively studied in applications of conversion of biomass to biofuels and bleaching process of pulp industry. As introduced before, hemicellulases are divided into two groups: depolymerizing enzyme and debranching enzyme. Thus the synergism between hemicellulases could be assigned as synergism between depolymerizing enzymes, synergism between debranching enzymes, and synergism between depolymerizing and debranching enzymes.

In the case of depolymerizing enzymes, due to the various specificity on different substrate, synergism between xylanases from different families, was studied. Because of endoxylanases from GH10 and GH11 can be active in digesting different sites of xylan backbone, the

synergism between GH10 and GH11 was studied on different substrates, such as pretreated bagasse [36]. While other studies, however, shown the absence of the synergism between these two endoxylanases on some substrates, such as wheat bran arabinoxylan [37]. Moreover, studies on the synergism between xylanase that from same GH family were also reported. For example, Clarke and coworkers have studied the synergistic effect between two xylanases from GH10 in bleaching of softwood and hardwood pulp. Two xylanases from GH10 families showed synergistic effect in boosting release of reducing sugars and bleachability. The synergistic interaction between these two enzymes probably because of the cooperation in attacking the reprecipitated fiber and inter-fiber xylan of the pulp [38]. The synergism between other depolymerizing enzymes, such as xylanases and mannanase, was also carried out, especially in the studies of degradation of softwood [39].

The synergism between debranching enzymes, however, was relatively less studied. It has been reported that a recombinant Araf worked synergistically with an endo-arabinanase in the degradation of arabinan [40]. Recently, an Araf from GH43 was shown synergism after addition with Araf from GH51, since Araf from GH51 hydrolyzes the 1,2- and 1,3-linked arabinose singly substituted xylan, whereas Araf from GH43 hydrolyzes 1,3-linked arabinose doubly substituted xylan only. In the presence of two kinds of Arafs resulted in fully debranching of arabinoxylan [23].

Mixing debranching enzyme together with depolymerizing enzyme usually has an enhanced yield of reducing sugars production. The removal of side-chains of xylan backbone by debranching enzymes favors the action of depolymerizing enzymes, due to the steric hindrance caused by substituents. Many studies have investigated the synergism between debranching and depolymerizing enzymes, for example, xylanase and arabinofunosidase in degradation of model substrate, such as soluble and insoluble arabinoxylan [22,23], oatspelt xylan [41], wheat and rye arabinoxylan [42]. Conversely, other studies about xylanase and hemicellulolytic esterase were also investigated. Feruloyl ester bond has found to be related with the association of lignin and hemicellulose, thus feruloyl esterase can work synergistically with endoxylanases in hydrolysis of hemicellulose component in biomass [43].

5.1.3 Synergism between cellulase and hemicellulase

Different from the model substrates used in studies of synergistic effect between cellulases or hemicellulases, the study of synergism between cellulase and hemicellulase was always carried out on lignocellulosic biomass. It has been reported that the addition of xylanases, can remarkably improve the degradation of cellulose [44,45]. In addition, the removal of xylan was demonstrated to be linearly correlated with the cellulose degradation [46]. Because of the

crosslinked structure, removing the cover of xylan can generate more available sites for cellulase, and vice versa. Besides xylanases, other hemicellulases were also evaluated as the accessory enzymes in biomass degradation. Selig et al., investigated the synergistic effect of addition of EX, AXE and FAE to CBH I in hydrolysis of hot-water pretreated corn stover. The improvement of cellobiose production after addition of EX and AXE was probably due to the removal of ester linkage in cell wall matrix by these accessory enzymes, thus resulting in the expose of cellulose fiber [47]. Gao and coworkers have mixed six core glycosyl hydrolases, EG I, CBH I and II, BGL, EX and BXL, in hydrolysis of AFEX pretreated corn stover. The optimal ratio of this six-component mixture was CBH I (28.4%): CBH II (18%): EG I (31%): EX (14.1%): BGL (4.7%): BXL (3.8%) based on percentage of protein mass loading using response surface models [48].

5.1.4 Factors that affect synergism

One factor that affecting synergism is the property of substrates, such as cellulose crystallinity, substitution of side chain of hemicellulose. Substrates with high cellulose crystallinity or highly substituted hemicellulose structure tend to have high synergism between enzymes [14,29,30,49], but not always [27,50]. Kumar and Wyman have tested the synergism between commercial xylanase and cellulase in degradation of corn stover pretreated by six different kinds of methods, including acid, base, AFEX and so on. Different xylan proportion and cellulose crystallinity in the corn stover was observed. In the hydrolysis process, substrate with high cellulose crystallinity had the lowest improvement of xylose release. The pretreated substrates, with less xylan and cellulose crosslinking disrupted, resulted a higher improvement of xylose release [49]. Hu et al. observed the same phenomenon when adding EX to a CBH in hydrolysis of different pretreated substrates. The synergism between EX and CBH was more predominant in hydrolysis of substrate with less branched xylan [44].

Another factor that affecting synergism is the specificity of the enzyme. Hu et al. have observed higher synergism between EX from GH10 and CBH than EX from GH11 did in hydrolysis of pretreated corn stover [45]. The possible reason might be the stronger hydrolytic ability and higher affinity to branched xylan of EX from GH10 than EX from GH11.

The other factor that affecting synergism is maybe the loading of enzymes. Woodward et al. have mixed EG, CBH I and II, and excess amount of BGL, at enzyme loading of 360 μg/mL in hydrolysis of microcrystalline cellulose, however, the synergism was negligible. When the enzyme loading decreased to 20 μg/mL, the degree of synergy reached highest value of 2.03.

This phenomenon indicated that with high enzyme loading, the substrates get saturated with enzyme, thus, the synergistic improvement will be reduced. Similar observations also reported elsewhere [28].

5.2 Construction of enzyme assemblies

Assembling enzymes together possesses the advantages of shorten the distance between enzymes that work cooperatively, form the substrate channel to increase the local concentration of the intermediate product and providing kinetic driving forces that promote the reaction. For efficient degradation of lignocellulose, there is a perfect example in nature, that is cellulosome.

In 1980s, Bayer and coworkers has identified a huge enzyme assembly from some anaerobic bacteria, so-called cellulosome, that can efficiently degrade lignocellulose under mild conditions. All the hydrolases are assembled onto a protein scaffold, that consists of six to ten cohesins, through site-specific and species-specific cohesin-dockerin interaction (Fig. 1-8) [51].

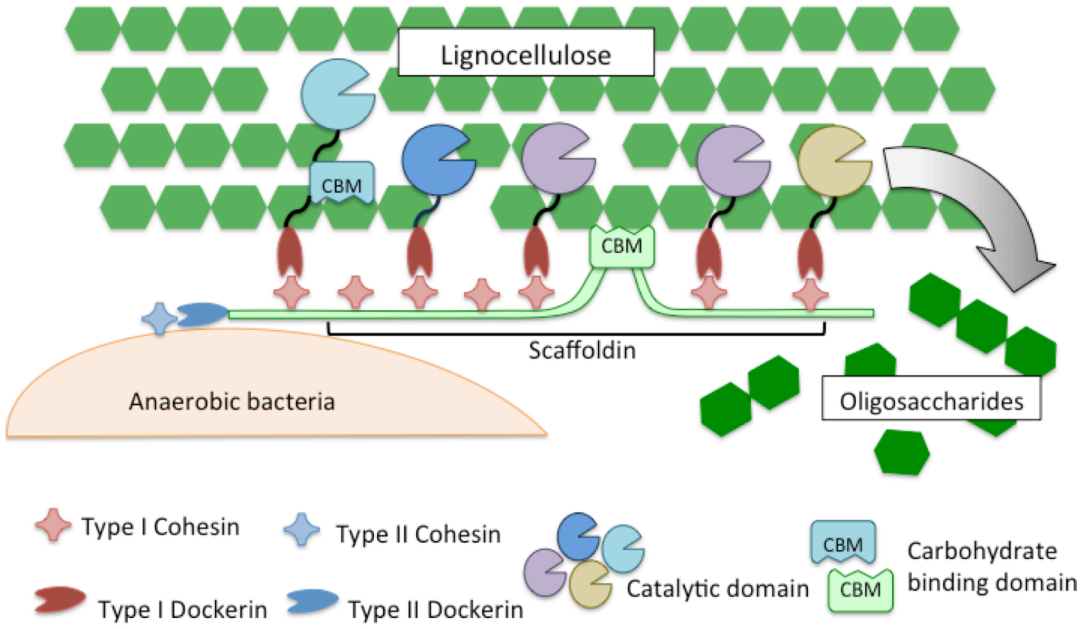

Fig. 1-8 Illustration of the structure of cellulosome

With the advances of genetic engineering methodologies and conjugation technologies, artificial cellulosomes have been proposed to mimic the characteristics of this natural enzyme assembly [52,53]. Many attempts that adopted from this technique have developed to

integrate enzymes onto variety of synthetic scaffolds, such as protein [54], DNA [55] and nanoparticle [56].

5.2.1 Artificial cellulosome assembled on protein scaffold

Taken the advances of genetically programmable, highly biocompatible and versatile post-translational modification methods, therefore, protein as binding scaffold for fabrication enzyme assembly has been intensively studied. The artificial cellulosome was proposed by Bayer and colleagues that employed the cohesin-dockerin system [51]. Unlike natural cellulosome, the scaffold of artificial cellulosome can be constructed by linking cohesins from different microorganisms. As talked before, cohesin-dockerin system is species-specific, as a result, the order of enzyme can be controlled to induce the cascade reaction between enzymes (Fig. 1-9).

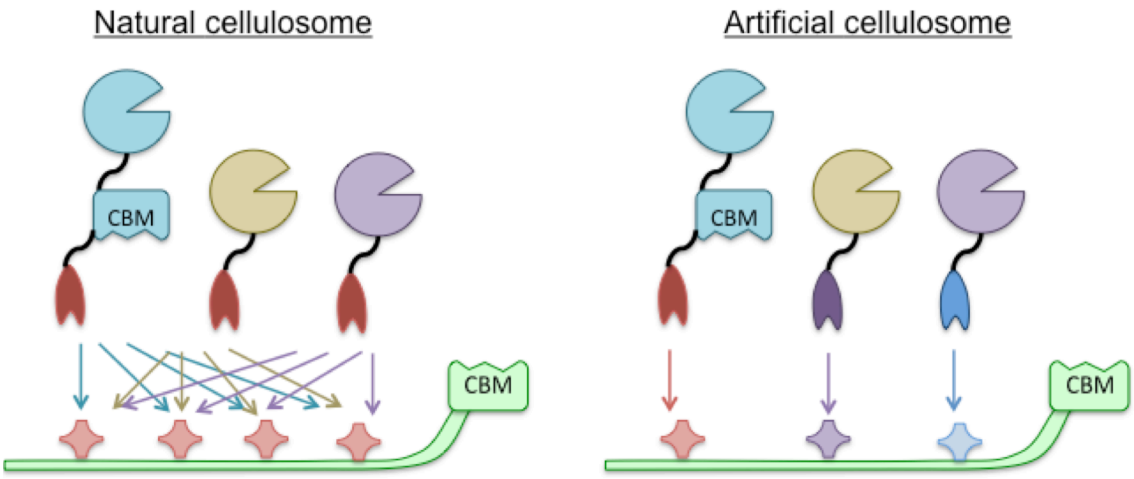

Fig. 1-9 Difference between natural cellulosome and artificial cellulosome

In the first report of artificial cellulosome, chimeric scaffoldins consist of two cohesin modules from different microorganisms were constructed and assembled with two selected enzymes fused with dockerins from corresponding microorganisms in vitro. The assembled two endocellulase CelA and CelF converted 1.5-fold reducing sugars than free enzymes did [57]. After that, with great dedicated effort, artificial cellulosome was developed towards increasing the types and numbers of enzyme conjugated [54, 58-60].

For the conjugation that using synthetic protein scaffold, as reported, most natural scaffolds contain about six to nine cohesins. Recently, it was shown that enzymes conjugated on longer scaffold presenting nine cohesin modules exhibited better synergistic effect than a truncated

scaffold contains two cohesin modules in hydrolysis of Avicel [61]. However, the employment of genetic method to express larger scaffold protein is quite difficult because proper protein folding and the full retention of all the protein function are becoming difficult to achieved. Therefore, the studies aiming at developing synthetic scaffold by post-translational modification was demonstrated. Matsumoto et al. constructed a twigged streptavidin polymer by crosslinking the tyrosine tag appended to C-termini of streptavidin via horseraddish peroxidase (HRP). In the meanwhile, G tag, could be recognized by sortase A, was introduced at the N-termini of streptavidin. Endoglucanase and CBH, fused with LPETG sequence and biotin acceptor peptide, respectively, were site-specifically conjugated onto the polymer through the sortase A catalysis and avidin-biotin interaction, respectively. Enhancement of reducing sugars conversion in hydrolysis of phosphoric acid swollen cellulose (PASC) and Avicel was observed [62].

Besides the genetically constructed chimeric scaffoldins and scaffoldins formed by post-translational protein modification, other natural self-assembly protein complexes as the scaffold for artificial cellulosome have also been investigated. Linking the four dockerin-containing cellulases onto rosettasome have about 2.4-fold improvement than these enzymes in free form in hydrolysis of Avicel [63].

5.2.2 Artificial cellulosome assembled on DNA/RNA scaffold

DNA and RNA are one kind of the ideal scaffolds with advantages of easily programmable, synthesized and highly biocompatible and stable [64]. The secondary structure formed by DNA or RNA molecules have been applied to assembly enzymes with spatial organization in vivo or in vitro [65,66]. This strategy was first applied to assemble cellulase by Mori et al. to construct an artificial cellulosome via site-specific transglutaminase catalysis. 5.7-fold enhancement in reducing sugars production was observed after conjugated endoglucanase and CBM onto a double-stranded DNA [55]. Afterwards, Chen's lab investigated other different conjugation methods, such as zinc finger protein-guided [67], and halo-tag mediated [68] techniques, to construct the artificial cellulosome. Compared with free enzymes, the reducing sugars produced by the enzymes assembled onto DNA scaffold was remarkably improved.

5.2.3 Artificial cellulosome assembled on nanoparticle scaffold

Generally, after the immobilization of enzymes onto nanoparticle scaffold, the stability of the enzymes against high temperature, long time storage or inappropriate pH has been greatly improved [69,70]. Besides, the advances of easy separation and high reusability of immobilized enzymes are very appealing to applying this strategy into industrial uses [71].

Table 1-2 summarized the studies that assembled cellulase or hemicellulase onto different nanoparticle scaffolds for reducing sugars production.

The protein immobilization through chemical reaction is strong that proteins are covalently bound to appropriately modified supports through functional side groups exposed on protein surface. However, in some cases, this immobilization way may cause the alteration of protein structures, as a result, part of protein functions would lose [69,72,77]. Thus, recently, site-specific conjugation methods by using the affinity between protein and protein or other molecules have been applied to retain the enzymatic activity and improve the reusability and stability at the same time [74-76]. Kim et al. have site-specifically conjugated biotinylated endoglucanase and CBM onto streptavidin coated CdSe nanoparticles. The results showed that after clustering the enzyme and CBM closely, a remarkable enhancement (7.2-fold) of reducing sugar production, compared with free enzymes, was observed [78].

Table 1-2 Summary of enzymes immobilized on nanoparticles

Materials	Coupling method	Enzymes	Substrates	Activity	Recycling	Reference
Graphene oxide decorated iron oxide nanoparticles (SPGO)	Cyanuric chloride	Commercial xylanase	Beechwood xylan	91% activity was retained	After 10 times recycle, 66% of activity was retained	[72]
Synthesized polyaniline (PANI)	Glutaraldehyde and amino group of enzyme	Commercial xylanase	Birchwood xylan	Km_{free} =1.86, $Km_{immobilized}$=1.07 mg/mL, $Vmax_{free}$ = 1.44 $Vmax_{immonilized}$= 0.44 mg/mL/min	72% activity was retained after 15 cycles	[73]
Iron oxide particles	Silane-derived hydroxyl with primary amine	Commercial cellulase	Avicel	39% activity was retained	-	[69]
Au nanoparticles (AuNP)/Au-doped magnetic silica nanoparticles (AuMSNP)	Cystein-gold affinity	EG, CBH and BGL	p-nitrophenyl β-D-glucopyranoside, CMC and filter paper	Almost 100% activity was remained in both cases	Scaffold reused four times of seven cycles, about 70% activity was retained	[70]
Chitin	Site-specific chitin binding domain	Chimeric trifunctional hemicellulase (Xylosidase-arabinosidase-xylanase)	Corncob xylan and corncob xylan hydrolysate	100% activity was retained	More than 60% activity was retained after 19 cycles	[74]
Artificial oil bodies (AOBs)	Oleosin-phospholipid affinity	EG, CBH and BGL	PASC	-	80% activity was retained after four cycles	[75]
Polystyrene particle	Sortase A-mediated or EDC/NHS coupling	BGL	p-nitrophenyl β-D-glucopyranoside	80% and 60% activity was retained respectively	After 10 cycles, 86.8% and 74.6% activity was retained, respectively	[76]

5.2.4 Artificial cellulosome formed by crosslinking enzyme aggregates (carrier-free)

Although assembling enzymes onto certain scaffolds, such as DNA, nanoparticles, have the merits described above, it still has some drawbacks; notably, the tedious preparation process and high cost of the scaffolds. Therefore, in the early 1960s, studies that using functional chemical linker, mostly glutaraldehyde, reacting with the primary amine on the protein surface to form the insoluble crosslinked enzyme crystals (CLEs) or crosslinked enzyme aggregates (CLEAs) was developed [79]. The process of fabricating CLEAs basically consist of two steps, firstly, precipitation of enzyme by adding salt or organic solvent; secondly, addition of the crosslinking reagent to form the aggregate [80]. Dalal et al. have prepared CLEAs from a commercial enzyme mixture, which contains pectinase, xylanase and cellulase, and investigated the enzymatic activity, stability, and reusability of three crosslinked enzymes. It was shown that almost 100% of the enzymatic activity was retained for three enzymes, and the thermostability of enzymes, especially pectinase, was remarkably improved [81].

Considering the difficulties of the separation of CLEAs from insoluble substrate, magnetic CLEAs (mag-CLEAs) was recently developed. Bhattacharya and Pletschke have prepared xylanase-mag-CLEAs by mixing xylanase supernatant with silanized magnetic nanopaticle. Interestingly, the activity and stability of xylanase after forming mag-CLEAs were considerably enhanced probably due to the interaction between metal ions and enzymes [82].

5.2.5 Artificial cellulosome assembled onto cells

Besides the strategies as described above, another strategy was developed based on the modification of the cells, that is engineering the non-cellulolytic microorganisms to secret and/or surface-display cellulolytic hydrolases, to improve the degradation of biomass and proceed saccharification and fermentation simultaneously. This whole-cell biocatalyst for lignocellulosic substrate degradation was first proposed by fusing the gene of β-glucosidase and carboxymethylcellulase (CMCase) to the C-termini of yeast α-agglutinin, which is considered as an anchor protein that can deliver the fusing protein onto the cell surface [83]. After displayed the enzymes onto the surface of *Saccharomyces cerevisiae*, this yeast strain obtained the ability of assimilating cellooligosaccharides and due to the reproductive characteristics of yeast, the number of surface-displayed enzymes can increase with the cell growth. Not longer the studies of immobilizing other cellulases, and hemicellulases onto yeast surface that can degrade the real biomass were developed [84,85].

Similar to yeast, *Escherichia coli* is a promising bacterium, since its well-understood genetic information and metabolism, and easy culturing process. With the advances of genetic technologies, we can control the production of one or several specific targets by *E. coli* via

manipulating its metabolic pathway. Recently, the surface-display of biomass degrading enzymes onto *E. coli* was proposed in production of cadaverine [86], fatty-acid ethyl esters, butanol, and monoterpene pinene [87].

6. Objectives and outline of the thesis

The main objective of the presenting thesis is to develop and evaluate several feasible enzymatic strategies that can maximize the degradation of cellulose and hemicellulose, and thus, achieving final goal to contribute a sustainable society through the biorefinery concept.

The main content of this thesis is consist of the following chapters:

In Chapter 2, the effect of two pretreatment methods on the synergism between three purified cellulase and xylanases was investigated. The physical structure and chemical components of bagasse before and after two individual pretreatment methods, peracetic acid and ionic liquid, were systematically investigated. Afterwards, two endoglucanase, XynZ and Xyn11A, were selected and mixed with an endoglucanase Cel6A for demonstrating the relationship between substrate property and synergism between enzymes.

In Chapter 3, three hemicellulases, XynZ, Xyn11A and Araf51A, was selected and covalently immobilized on the magnetic nanoparticles. The synergism between immobilized hemicellulases was studied in degradation of insoluble arabinoxylan. Moreover, the changes of synergism between immobilized enzymes in recycling was also investigated.

In Chapter 4, an universal protein polymer scaffold was constructed by crosslinking two tyrosine residues at N- and C-termini of SpyCatcher protein via horseradish peroxidase-catalyzed reaction. Subsequently, assembling hemicellulases, XynZ and Araf51A, on to this hyperbranching protein polymer scaffold via site-specific SpyCatcher-SpyTag was demonstrated. The synergism between closely conjugated XynZ and Araf51A was evaluated in hydrolysis of soluble arabinoxylan.

In Chapter 5, the main contents of this thesis were summarized and future perspective regarding the sustainable development by biocatalytic degradation of lignocellulosic substrate was also discussed.

Reference

[1] International Energy Agency, Key World Energy Statistics, (2015).

[2] C.J. Campbell, J.H. Laherrère, The End of Cheap Oil, Sci. Am. 278 (1998) 78–83.

[3] H.L. Chum, E. Warner, J.E.A. Seabra, I.C. Macedo, A comparison of commercial ethanol production systems from Brazilian sugarcane and US corn, Biofuels, Bioprod. Biorefining. 6 (2014) 205–223.

[4] Uju, A.T. Wijayanta, M. Goto, N. Kamiya, Great potency of seaweed waste biomass from the carrageenan industry for bioethanol production by peracetic acid-ionic liquid pretreatment, Biomass and Bioenergy. 81 (2015) 63–69.

[5] M. Balat, Production of bioethanol from lignocellulosic materials via the biochemical pathway: A review, Energy Convers. Manag. 52 (2011) 858–875.

[6] B.C. Saha, Hemicellulose bioconversion., J. Ind. Microbiol. Biotechnol. 30 (2003) 279–291.

[7] L. Saulnier, C. Marot, E. Chanliaud, J. Thibault, Cell wall polysaccharide interaction in maize bran, Carbohydr. Polym. 26 (1995) 279–287.

[8] M. Galbe, G. Zacchi, A review of the production of ethanol from softwood., Appl. Microbiol. Biotechnol. 59 (2002) 618–628.

[9] J.H. Grabber, How do lignin composition, structure, and cross-linking affect degradability? A review of cell wall model studies, Crop Sci. 45 (2005) 820–831.

[10] P. Alvira, E. Tomás-Pejó, M. Ballesteros, M.J. Negro, Pretreatment technologies for an efficient bioethanol production process based on enzymatic hydrolysis: A review., Bioresour. Technol. 101 (2010) 4851–4861.

[11]S. Haghighi Mood, A. Hossein Golfeshan, M. Tabatabaei, G. Salehi Jouzani, G.H. Najafi, M. Gholami, M. Ardjmand, Lignocellulosic biomass to bioethanol, a comprehensive review with a focus on pretreatment, Renew. Sustain. Energy Rev. 27 (2013) 77–93.

[12] G. Brodeur, E. Yau, K. Badal, J. Collier, K.B. Ramachandran, S. Ramakrishnan, Chemical and physicochemical pretreatment of lignocellulosic biomass: a review., Enzyme Res. 2011 (2011) 787532.

[13] A. Aden, T. Foust, Technoeconomic analysis of the dilute sulfuric acid and enzymatic hydrolysis process for the conversion of corn stover to ethanol, Cellulose. 16 (2009) 535–545.

[14] J.S. Van Dyk, B.I. Pletschke, A review of lignocellulose bioconversion using enzymatic hydrolysis and synergistic cooperation between enzymes--factors affecting enzymes, conversion and synergy, Biotechnol. Adv. 30 (2012) 1458–1480.

[15] T. Collins, C. Gerday, G. Feller, Xylanases, xylanase families and extremophilic xylanases., FEMS Microbiol. Rev. 29 (2005) 3–23.

[16] A. Pollet, J. a Delcour, C.M. Courtin, Structural determinants of the substrate specificities of xylanases from different glycoside hydrolase families., Crit. Rev. Biotechnol. 30 (2010) 176–191.
[17] W.H. van Zyl, S.H. Rose, K. Trollope, J.F. Görgens, Fungal β-mannanases: Mannan hydrolysis, heterologous production and biotechnological applications, Process Biochem. 45 (2010) 1203–1213.
[18] D. Shallom, Y. Shoham, Microbial hemicellulases, Curr. Opin. Microbiol. 6 (2003) 219–228.
[19] R. Kumar, C.E. Wyman, Strong cellulase inhibition by Mannan polysaccharides in cellulose conversion to sugars., Biotechnol. Bioeng. 111 (2014) 1341–1353.
[20] S. Lagaert, A. Pollet, C.M. Courtin, G. Volckaert, β-Xylosidases and α-l-arabinofuranosidases: Accessory enzymes for arabinoxylan degradation, Biotechnol. Adv. 32 (2014) 316–332.
[21] E.J. Taylor, N.L. Smith, J.P. Turkenburg, S. D'Souza, H.J. Gilbert, G.J. Davies, Structural insight into the ligand specificity of a thermostable family 51 arabinofuranosidase, Araf51, from *Clostridium thermocellum*, Biochem. J. 395 (2006) 31–37.
[22] T. Hashimoto, Y. Nakata, Synergistic degradation of arabinoxylan with α-L-arabinofuranosidase, xylanase and β-xylosidase from soy sauce koji mold, *Aspergillus oryzae*, in high salt condition, J. Biosci. Bioeng. 95 (2003) 164–169.
[23] H.R. Sørensen, S. Pedersen, C.T. Jørgensen, A.S. Meyer, Enzymatic hydrolysis of wheat arabinoxylan by a recombinant "minimal" enzyme cocktail containing β-xylosidase and novel endo-1,4-β-xylanase and α-L-arabinofuranosidase activities, Biotechnol. Prog. 23 (2007) 100–107.
[24] M.M. Marcia, Feruloylation in grasses: Current and future perspectives, Mol. Plant. 2 (2009) 861–872.
[25] D.L. Blum, I. a. Kataeva, X.-L. Li, L.G. Ljungdahl, Feruloyl Esterase Activity of the *Clostridium thermocellum* Cellulosome Can Be Attributed to Previously Unknown Domains of XynY and XynZ, J. Bacteriol. 182 (2000) 1346–1351.
[26] D. Klein-Marcuschamer, P. Oleskowicz-Popiel, B.A. Simmons, H.W. Blanch, The challenge of enzyme cost in the production of lignocellulosic biofuels, Biotechnol. Bioeng. 109 (2012) 1083–1087.
[27] N. Andersen, K.S. Johansen, M. Michelsen, E.H. Stenby, K.B.R.M. Krogh, L. Olsson, Hydrolysis of cellulose using mono-component enzymes shows synergy during hydrolysis of phosphoric acid swollen cellulose (PASC), but competition on Avicel, Enzyme Microb. Technol. 42 (2008) 362–370.

[28] J. Medve, J. Karlsson, D. Lee, F. Tjerneld, Hydrolysis of microcrystalline cellulose by cellobiohydrolase I and endoglucanase II from *Trichoderma reesei*: Adsorption, sugar production pattern, and synergism of the enzymes, Biotechnol. Bioeng. 59 (1998) 621–634.
[29] Y.-H.P. Zhang, L.R. Lynd, Toward an aggregated understanding of enzymatic hydrolysis of cellulose: noncomplexed cellulase systems., Biotechnol. Bioeng. 88 (2004) 797–824.
[30] P. Väljamäe, V. Sild, A. Nutt, G. Pettersson, G. Johansson, Acid hydrolosis of bacterial cellulose reveals different modes of synergistic action between cellobiohydrolase I and endoglucanase I, Eur. J. Biochem. 266 (1999) 327–334.
[31] J. Woodward, M. Lima, N.E. Lee, The role of cellulase concentration in determining the degree of synergism in the hydrolysis of microcrystalline cellulose., Biochem. J. 255 (1988) 895–899.
[32] T.M. Wood, S.I. McCrae, The cellulase of *Penicillium pinophilum*, Biochem. J. 99 (1986) 93–99.
[33] P. Tomme, V. Heriban, M. Claeyssens, Adsorption of two cellobiohydrolase from *Trichodema reesei* to Avicel: Evidence for exo-exo'' synergism and possible loose complex'' formation, Biotechnol. Lett. 12 (1990) 525–530.
[34] S. Zhou, L.O. Ingram, Synergistic hydrolysis of carboxymethyl cellulose and acid-swollen cellulose by two endoglucanases (CelZ and CelY) from *Erwinia chrysanthemi*, J. Bacteriol. 182 (2000) 5676–5682.
[35] Y.J. Han, H.Z. Chen, Synergism between corn stover protein and cellulase, Enzyme Microb. Technol. 41 (2007) 638–645.
[36] G.A.L. Gonçalves, Y. Takasugi, L. Jia, Y. Mori, S. Noda, T. Tanaka, H. Ichinose, N. Kamiya, Synergistic effect and application of xylanases as accessory enzymes to enhance the hydrolysis of pretreated bagasse, Enzyme Microb. Technol. 72 (2015) 16–24.
[37] J. Beaugrand, G. Chambat, V.W.K. Wong, F. Goubet, C. Rémond, G. Paës, S. Benamrouche, P. Debeire, M. O'Donohue, B. Chabbert, Impact and efficiency of GH10 and GH11 thermostable endoxylanases on wheat bran and alkali-extractable arabinoxylans., Carbohydr. Res. 339 (2004) 2529–2540.
[38] J.H. Clarke, J.E. Rixon, a Ciruela, H.J. Gilbert, G.P. Hazlewood, Family-10 and family-11 xylanases differ in their capacity to enhance the bleachability of hardwood and softwood paper pulps., Appl. Microbiol. Biotechnol. 48 (1997) 177–183.
[39] S. Malgas, J.S. van Dyk, B.I. Pletschke, A review of the enzymatic hydrolysis of mannans and synergistic interactions between β-mannanase, β-mannosidase and α-galactosidase, World J. Microbiol. Biotechnol. 31 (2015) 1167–1175.

[40] H. Yang, H. Ichinose, M. Nakajima, H. Kobayashi, S. Kaneko, Synergy between an α-L-arabinofuranosidase from *Aspergillus oryzae* and an endo-arabinanase from *Streptomyces coelicolor* for degradation of arabinan, Food Sci. Technol. Res. 12 (2006) 43–49.
[41] M. Tuncer, a S. Ball, Co-operative actions and degradation analysis of purified xylan-degrading enzymes from *Thermomonospora fusca* BD25 on oat-spelt xylan., J. Appl. Microbiol. 94 (2003) 1030–5.
[42] A. Valls, P. Diaz, F.I. Javier Pastor, S. V Valenzuela, A newly discovered arabinoxylan-specific arabinofuranohydrolase. Synergistic action with xylanases from different glycosyl hydrolase families, Appl. Microbiol. Biotechnol. 100 (2015) 1743–1751.
[43] C.B. Faulds, G. Mandalari, R.B. Lo Curto, G. Bisignano, P. Christakopoulos, K.W. Waldron, Synergy between xylanases from glycoside hydrolase family 10 and family 11 and a feruloyl esterase in the release of phenolic acids from cereal arabinoxylan., Appl. Microbiol. Biotechnol. 71 (2006) 622–629.
[44] J. Hu, V. Arantes, A. Pribowo, J.N. Saddler, The synergistic action of accessory enzymes enhances the hydrolytic potential of a “cellulase mixture” but is highly substrate specific., Biotechnol. Biofuels. 6 (2013) 112.
[45] J. Hu, V. Arantes, J.N. Saddler, The enhancement of enzymatic hydrolysis of lignocellulosic substrates by the addition of accessory enzymes such as xylanase: is it an additive or synergistic effect?, Biotechnol. Biofuels. 4 (2011) 36.
[46] J. Zhang, L. Viikari, Impact of xylan on synergistic effects of xylanases and cellulases in enzymatic hydrolysis of lignocelluloses., Appl. Biochem. Biotechnol. 174 (2014) 1393–1402.
[47] M.J. Selig, E.P. Knoshaug, W.S. Adney, M.E. Himmel, S.R. Decker, Synergistic enhancement of cellobiohydrolase performance on pretreated corn stover by addition of xylanase and esterase activities., Bioresour. Technol. 99 (2008) 4997–5005.
[48] D. Gao, S.P.S. Chundawat, C. Krishnan, V. Balan, B.E. Dale, Mixture optimization of six core glycosyl hydrolases for maximizing saccharification of ammonia fiber expansion (AFEX) pretreated corn stover., Bioresour. Technol. 101 (2010) 2770–2781.
[49] R. Kumar, C.E. Wyman, Effect of xylanase supplementation of cellulase on digestion of corn stover solids prepared by leading pretreatment technologies., Bioresour. Technol. 100 (2009) 4203–4213.
[50] H.P. Fierobe, E.A. Bayer, C. Tardif, M. Czjzek, A. Mechaly, A. Bélaïch, R. Lamed, Y. Shoham, J.P. Bélaïch, Degradation of cellulose substrates by cellulosome chimeras: Substrate targeting versus proximity of enzyme components, J. Biol. Chem. 277 (2002) 49621–49630.
[51] E. a Bayer, E. Morag, R. Lamed, The cellulosome - a treasure-trove for biotechnology, Trends Biotechnol. 12 (1994) 259–265.

[52]G. Gonçalves, Y. Mori, N. Kamiya, Biomolecular assembly strategies to develop potential artificial cellulosomes, Sustain. Chem. Process. 2 (2014) 19.
[53]S.P. Smith, E. a Bayer, Insights into cellulosome assembly and dynamics: from dissection to reconstruction of the supramolecular enzyme complex., Curr. Opin. Struct. Biol. 23 (2013) 686–694.
[54]S. Moraïs, Y. Barak, Y. Hadar, D. Wilson, Y. Shoham, R. Lamed, E. a. Bayer, Assembly of xylanases into designer cellulosomes promotes efficient hydrolysis of the xylan component of a natural recalcitrant cellulosic substrate, MBio. 2 (2011) e00233-11.
[55]Y. Mori, S. Ozasa, M. Kitaoka, S. Noda, T. Tanaka, H. Ichinose, N. Kamiya, Aligning an endoglucanase Cel5A from *Thermobifida fusca* on a DNA scaffold: potent design of an artificial cellulosome., Chem. Commun. (Camb). 49 (2013) 6971–6973.
[56]S.L. Tsai, M. Park, W. Chen, Size-modulated synergy of cellulase clustering for enhanced cellulose hydrolysis, Biotechnol. J. 8 (2013) 257–261.
[57]H.P. Fierobe, A. Mechaly, C. Tardif, A. Belaich, R. Lamed, Y. Shoham, J.P. Belaich, E.A. Bayer, Design and production of active cellulosome chimeras. Selective incorporation of dockerin-containing enzymes into defined functional complexes, J. Biol. Chem. 276 (2001) 21257–21261.
[58]L. Davidi, S. Moraïs, L. Artzi, D. Knop, Y. Hadar, Y. Arfi, E.A. Bayer, Toward combined delignification and saccharification of wheat straw by a laccase-containing designer cellulosome, Proc. Natl. Acad. Sci. 113 (2016) 201608012.
[59]J. Caspi, Y. Barak, R. Haimovitz, D. Irwin, R. Lamed, D.B. Wilson, E. a Bayer, Effect of linker length and dockerin position on conversion of a *Thermobifida fusca* endoglucanase to the cellulosomal mode., Appl. Environ. Microbiol. 75 (2009) 7335–7342.
[60]M. Park, Q. Sun, F. Liu, M.P. DeLisa, W. Chen, Positional assembly of enzymes on bacterial outer membrane vesicles for cascade reactions, PLoS One. 9 (2014) 1–6.
[61]K. Hirano, S. Nihei, H. Hasegawa, M. Haruki, N. Hirano, Stoichiometric Assembly of Cellulosome Generates Maximum Synergy for the Degradation of Crystalline Cellulose, as Revealed by *In Vitro* Reconstitution of the *Clostridium thermocellum* Cellulosome., Appl. Environ. Microbiol. 81 (2015) AEM.00772-15.
[62]T. Matsumoto, Y. Isogawa, K. Minamihata, T. Tanaka, A. Kondo, Twigged streptavidin polymer as a scaffold for protein assembly, J. Biotechnol. 225 (2016) 61–66.
[63]S. Mitsuzawa, H. Kagawa, Y. Li, S.L. Chan, C.D. Paavola, J.D. Trent, The rosettazyme: A synthetic cellulosome, J. Biotechnol. 143 (2009) 139–144.
[64]P.W.K. Rothemund, Folding DNA to create nanoscale shapes and patterns, Nature. 440 (2006) 297–302.

[65]C.J. Delebecque, A.B. Lindner, P.A. Silver, F.A. Aldaye, Organization of Intracellular reactions with rationally designed RNA assemblies, Science. 333 (2011) 470–474.
[66]J. Fu, M. Liu, Y. Liu, N.W. Woodbury, H. Yan, Interenzyme substrate diffusion for an enzyme cascade organized on spatially addressable DNA nanostructures, J. Am. Chem. Soc. 134 (2012) 5516–5519.
[67]Q. Sun, B. Madan, S.-L. Tsai, M.P. DeLisa, W. Chen, Creation of artificial cellulosomes on DNA scaffolds by zinc finger protein-guided assembly for efficient cellulose hydrolysis., Chem. Commun. (Camb). 50 (2014) 1423–1425.
[68]Q. Sun, W. Chen, HaloTag mediated artificial cellulosome assembly on a rolling circle amplification DNA template for efficient cellulose hydrolysis, Chem. Commun. (2016).
[69]A. Garcia, S. Oh, C.R. Engler, Cellulase Immobilization on Fe_3O_4 and Characterization, Biotechnol. Bioeng. 33 (1989) 321–326.
[70]Q. Wang, Y. Xue, X. Wu, Characterization of a novel thermostable chitin-binding domain and its application in immobilization of a multifunctional hemicellulase, J. Agric. Food Chem. 61 (2013) 3074–3081.
[71]R. DiCosimo, J. McAuliffe, A.J. Poulose, G. Bohlmann, Industrial use of immobilized enzymes, Chem. Soc. Rev. 42 (2013) 6437−6474.
[72]M. Royvaran, A. Taheri-Kafrani, A. Landarani Isfahani, S. Mohammadi, Functionalized superparamagnetic graphene oxide nanosheet in enzyme engineering: A highly dispersive, stable and robust biocatalyst, Chem. Eng. J. 288 (2016) 414–422.
[73]S. Madakbas, O. Danis, S. Demir, M.V. Kahraman, s, Xylanase immobilization on functionalized polyaniline support by covalent attachment, Starch/Starke. 65 (2013) 146–150.
[74]E.J. Cho, S. Jung, H.J. Kim, Y.G. Lee, K.C. Nam, H.-J. Lee, H.-J. Bae, Co-immobilization of three cellulases on Au-doped magnetic silica nanoparticles for the degradation of cellulose, Chem. Commun. 48 (2012) 886.
[75]C.-J. Chiang, P.T. Chen, C.Y. Yeh, Z.W. Wang, Y.-P. Chao, A useful method integrating production and immobilization of recombinant cellulase., Appl. Microbiol. Biotechnol. 97 (2013) 9185–9192.
[76]Y. Hata, T. Matsumoto, T. Tanaka, A. Kondo, C-Terminal-oriented Immobilization of Enzymes Using Sortase A-mediated Technique, Macromol. Biosci. 15 (2015) 1375–1380.
[77]A. Soozanipour, A. Taheri-Kafrani, A. Landarani Isfahani, Covalent attachment of xylanase on functionalized magnetic nanoparticles and determination of its activity and stability, Chem. Eng. J. 270 (2015) 235–243.

[78]D.-M. Kim, M. Umetsu, K. Takai, T. Matsuyama, N. Ishida, H. Takahashi, R. Asano, I. Kumagai, Enhancement of cellulolytic enzyme activity by clustering cellulose binding domains on nanoscaffolds., Small. 7 (2011) 656–664.

[79]R.A. Sheldon, Characteristic features and biotechnological applications of cross-linked enzyme aggregates (CLEAs), Appl. Microbiol. Biotechnol. 92 (2011) 467–477.

[80]R.A. Sheldon, S. Van Pelt, Enzyme immobilisation in biocatalysis: why, what and how, Chem. Soc. Rev. 42 (2013) 6223–6235.

[81]S. Dalal, A. Sharma, M.N. Gupta, A multipurpose immobilized biocatalyst with pectinase, xylanase and cellulase activities., Chem. Cent. J. 1 (2007) 16.

[82]A. Bhattacharya, B.I. Pletschke, Magnetic cross-linked enzyme aggregates (CLEAs): A novel concept towards carrier free immobilization of lignocellulolytic enzymes, Enzyme Microb. Technol. 61–62 (2014) 17–27.

[83]T. Murai, M. Ueda, T. Kawaguchi, M. Arai, A. Tanaka, Assimilation of cellooligosaccharides by a cell surface-engineered yeast expressing β-glucosidase and carboxymethylcellulase from *Aspergillus aculeatus*, Appl. Environ. Microbiol. 64 (1998) 4857–4861.

[84]Y. Fujita, S. Takahashi, M. Ueda, A. Tanaka, H. Okada, Y. Morikawa, T. Kawaguchi, M. Arai, H. Fukuda, A. Kondo, Direct and Efficient Production of Ethanol from Cellulosic Material with a Yeast Strain Displaying Cellulolytic Enzymes, Appl. Environ. Microbiol. 26 (2002) 668–673.

[85]S. Katahira, Y. Fujita, A. Mizuike, H. Fukuda, A. Kondo, Construction of a xylan-fermenting yeast strain through codisplay of xylanolytic enzymes on the surface of xylose-utilizing *Saccharomyces cerevisiae* cells, Appl. Environ. Microbiol. 70 (2004) 5407–5414.

[86]N. Ikeda, M. Miyamoto, N. Adachi, M. Nakano, T. Tanaka, A. Kondo, Direct cadaverine production from cellobiose using β-glucosidase displaying Escherichia coli., AMB Express. 3 (2013) 67.

[87]G. Bokinsky, P.P. Peralta-Yahya, a. George, B.M. Holmes, E.J. Steen, J. Dietrich, T. Soon Lee, D. Tullman-Ercek, C. a. Voigt, B. a. Simmons, J.D. Keasling, Synthesis of three advanced biofuels from ionic liquid-pretreated switchgrass using engineered *Escherichia coli*, Proc. Natl. Acad. Sci. 108 (2011) 19949–19954.

Chapter 2 Effect of pretreatment methods on the synergism of cellulase and xylanase during the hydrolysis of bagasse

1. Introduction

Second-generation bioethanol, produced from agriculture residues, as a substitute for fossil fuels has received widespread attention since the end of the last century. Owing to the prior abundance and appreciable polysaccharides percentage, sugarcane bagasse is considered an ideal substrate for biorefineries [1]. However, because of the complex matrix of polysaccharides and lignin within the structure of the plant cell wall, pretreatment becomes an indispensable step to accelerate the degradation of the lignin–carbohydrate complex and to ensure that bioethanol production is a competitive and sustainable process [2].

1.1 Peracetic acid pretreatment and ionic liquid pretreatment

Studies aimed at improving monosaccharide production from sugarcane bagasse include the use of acid, base, hydrogen peroxide and steam explosive processes [3,4]. Peracetic acid (PAA) is a powerful oxidant reagent and was used as cotton-bleaching reagent in the early 40's [5]. Previous studies showed that peracetic acid (PAA) has good delignification ability, because PAA generates the hydroxonium ion, HO^+, which electrophilic attacks lignin related structure via an electrophilic reaction. The mechanism of HO^+ generation is [6]:

$$HCOOOH + H^+ \rightarrow HCO_2H + HO^+$$

The involved reactions include: (1) ring hydrolxylation, (2) oxidative demethylation, (3) oxidative ring opening, (4) displacement of side-chains, (5) cleavage of β-arylether bonds, and (6) epoxidation (Fig. 2-1) [7-9]. After PAA pretreatment, the lignin structure in biomass would be disrupted and dissolved in the solution. It was reported that the digestibility of bagasse was greatly improved after pretreated with PAA at loading of 50% (based on initial dry materials), liquid/solid (l/s) ratio of 6:1 at 80 °C for 2 h [10].

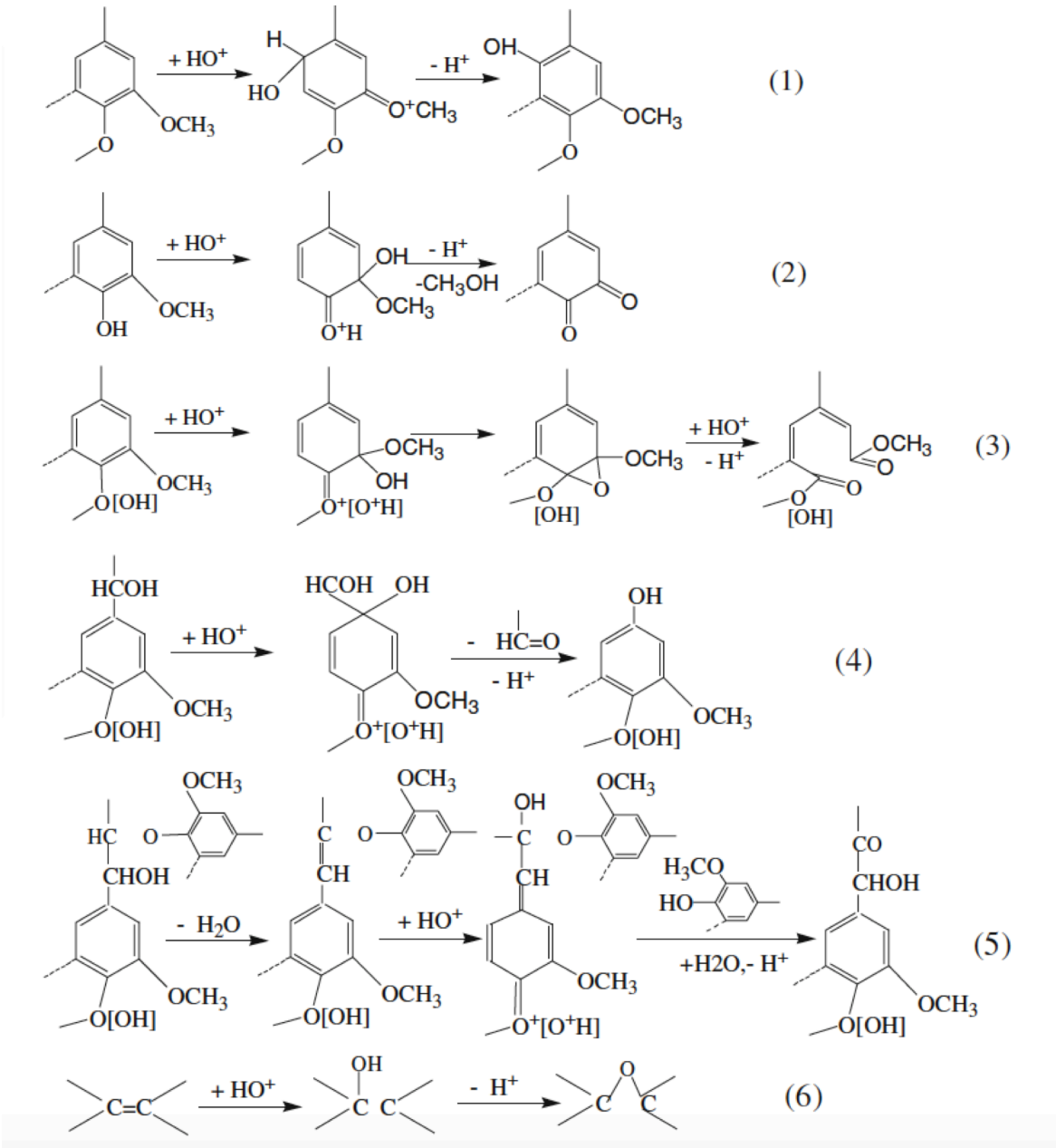

Fig. 2-1 Reactions of lignin-related structure with HO^+ generated by peracetic acid (PAA) [9]

9-Reprinted from *Appl. Microbiol. Biotechnol.* Vol. 82, Zhao et al., Organosolv pretreatment of lignocellulosic biomass for enzymatic hydrolysis, 815-827., Copyright 2009, with permission from Springer.

Ionic liquids (IL) as emerging reagents for biomass pretreatment have been extensively studied because of their excellent characteristics, like thermal stability, easy recyclability, and unique cellulose dissolution capability [11,12]. This dissolution is induced by the formation of the electron donor-acceptor complex between the anion of IL and the free hydroxyl group on cellulose, and between the cation of IL and the hydroxyl oxygen atoms on the cellulose

chain [13]. Singh and coworkers have observe the swelling of cell wall of switchgrass by confocal fluorescence microscopy. After treated at 120 °C for 120 min, the structure of sclerenchyma, which contains large amount of lignin, was completely destroyed (Fig. 2-2) [14].

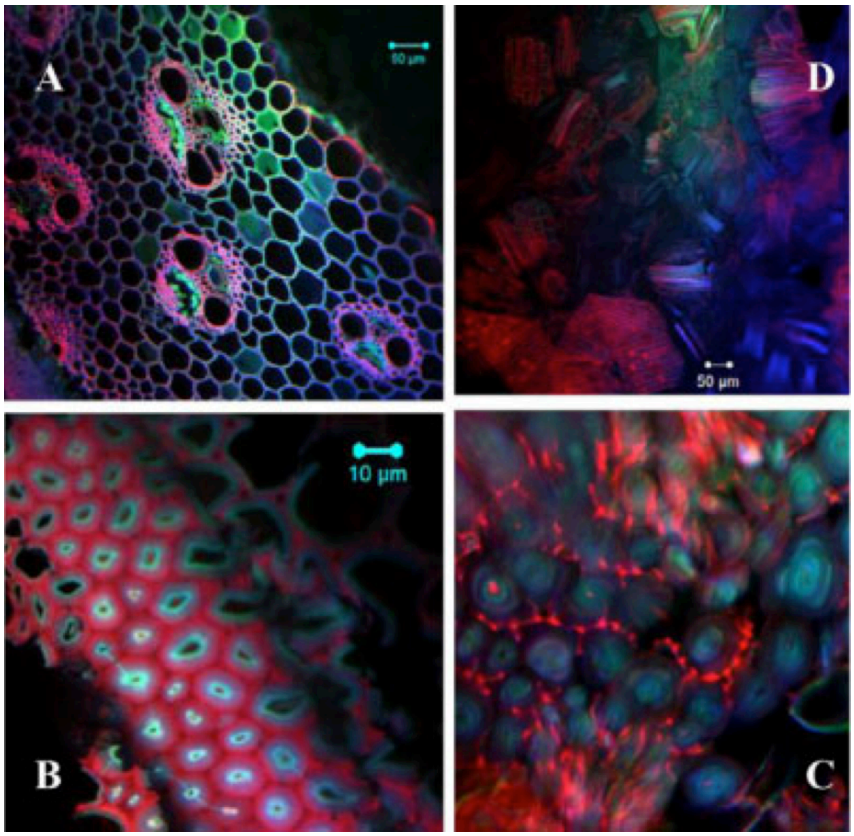

Fig. 2-2 The confocal fluorescence image showing the dissolution of switchgrass stem in [Emim][OAc]. (A) before pretreatment; (B) after pretreatment at 120 °C for 20 min; (C) after pretreatment at 120 °C for 50 min; (D) complete breakdown of the cell after pretreated at 120 °C for 120 min. [14]

14-Reprinted from *Biotechnol. Bioeng.* Vol. 104, Singh *et al.*, Visualization of biomass solubilization and cellulose regeneration during ionic liquid pretreatment of switchgrass, Copyright 2009, with permission from John Wiley & Sons, Ltd.

It has been summarized that until the year of 2010, more than 97 kinds of ionic liquids have been synthesized that possessing the ability in cellulose dissolution [15]. Among the different ILs, 1-Ethyl-3-methylimidazolium acetate ([Emim][OAc]) has proven to be one of the most effective in solubilizing cellulose [12]. The studies using [Emim][OAc] to pretreat various substrates were listed in Table 2-1.

Table 2-1 Summary of published studies using [Emim][OAc] in pretreatment process

Substrate	Pretreatment conditions	Morphology and component change	Conversion yield	Reference
Bagasse	bagasse/IL 1:20 (wt%), 120 °C, 120min	20.7% weight loss during pretreatment	80% by 15 FPU Acremonium cellulase/gram substrate, including 0.2% (v/v) OptimashTM BG	[4]
Avicel	2% (w/w), 110°C 40 min	Disrupted surface, crystallinity index change	More than 60% cellulose was degraded by 10 mg cellulase/200 mg cellulose	[16]
Bagasse	5% (w/w), 120 °C, 30min	32% lignin removal, 8% glucan and 14% xylan loss, reduction of cellulose crystallinity	87.0% glucan and 64.3% xylan conversion by Spezyme CP at 30 FPU/g glucan and Novozyme 188 at 30 CBU/g glucan	[17]
Maple wood flour	5% (W/W), 90 °C, 24h	40% lignin removal, reduction of cellulose crystallinity	>90% of the cellulose degradted by 34 U/mL cellulase	[18]
Rice straw, Avicel	5% (W/W), 120 °C, 24h	Not described	80% and 100% conversion of rice straw and Avicel by 4 U cellulase/mg substrates	[19]
Bagasse	4% (W/V), 145 °C 15min	Reduction of cellulose crystallinity and partial dissolution of hemicellulose	70% cellulose conversion by 30 FPU/gCellulase Onozuka R-10	[20]

1.2 Addition of xylanase as accessory enzyme to synergistically improve sugar production

Naturally, xylans are highly cross-linked with cellulose fibrils by diferulic bridges, contributing to the firm cell wall matrix (Fig. 2-3) [21,22]. As a result, access to cellulose by cellulase is generally prevented and this reduction in cellulose activity can hamper downstream successive enzymatic hydrolysis processes. Nonetheless, hemicellulose is a desired polysaccharide that can also be yielded from biomass conversion. The addition of accessory enzymes, especially xylanases, to degrade the hemicellulose content is an alternative approach to make cellulose more accessible to cellulases, and to yield more

saccharides simultaneously.

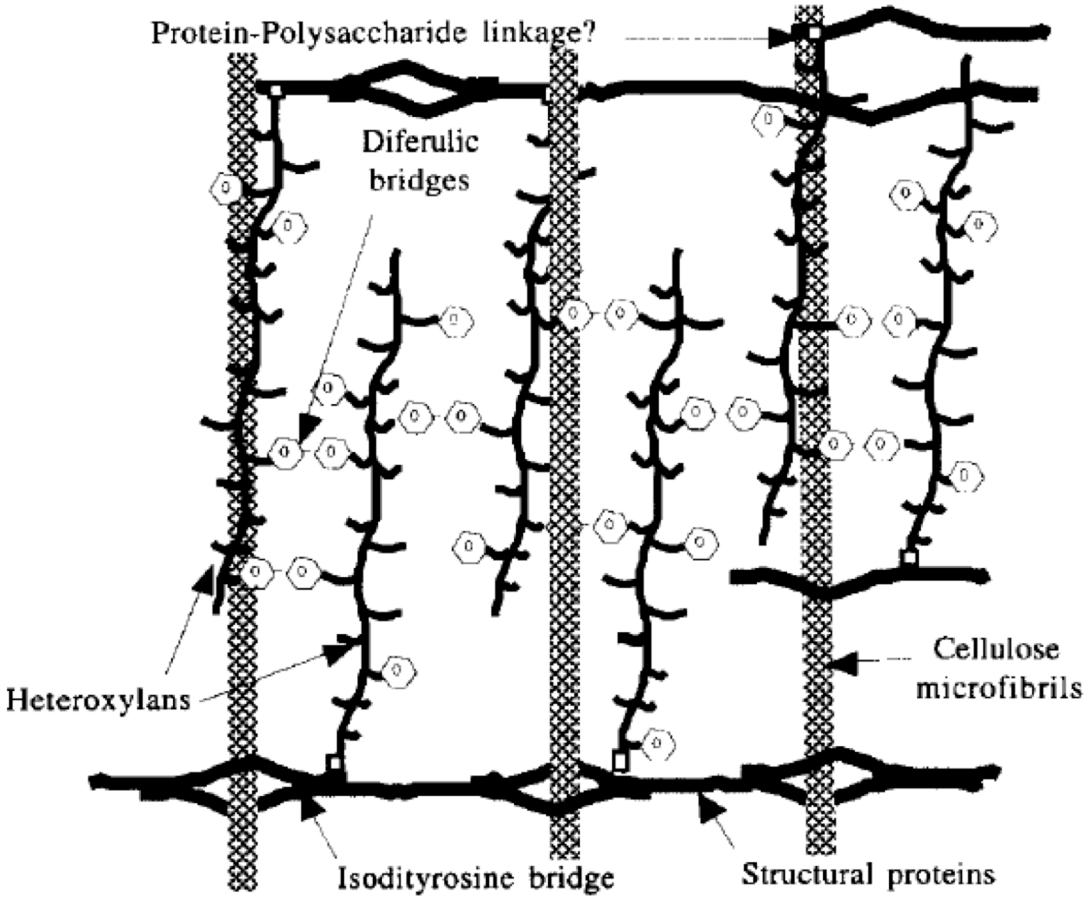

Fig. 2-3 The crosslinked structure of cellulose and hemicellulose [22]

22-Reprinted from *J. Sci. Food. Agric.*, Vol. 79, Saulnier *et al.*, Ferulic acid and diferulic acids as components of sugar-beet pectins and maize bran heteroxylan, Copyright 1999, with permission from John Wiley & Sons, Ltd.

Endoxylanases (EX) from GH10 and GH11 are two intensively studied xylanase families. As introduced in Chaper 1, EX from GH10 generally have a broad substrate specificity. The structure of the catalytic domain of GH10 xylanases is $(\alpha/\beta)_8$ barrel fold, and the active site is small [23]. Unlike the structure of GH10 xylanase, catalytic domain of xylanase from GH11 is a β-jelly roll structure and consists of two twisted antiparallel β-sheets and a single α-helix [23]. The shape of the GH11 xylanase looks like a gesture of 'C'. EX from GH11 mostly can only digest the sites without substitution of side-groups.

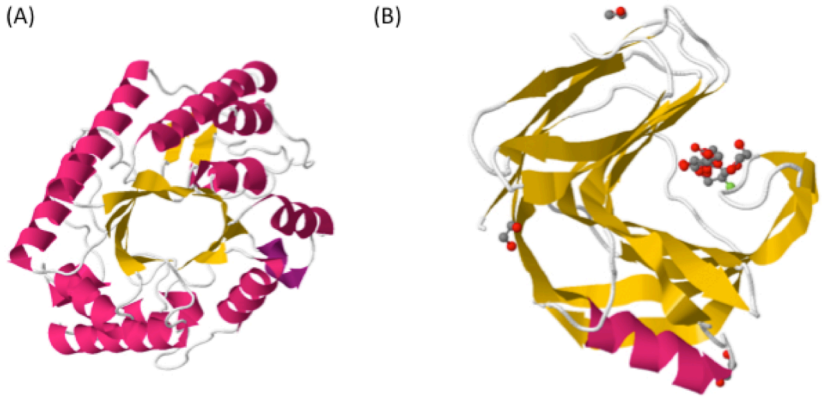

Fig. 2-4 Structures of EXs. (A) XynZ, from GH10, *Clostridium thermocellum* (PDB: 1XYZ) (B) Xyn11A, from GH11, *Thermobifida fusca* (PDB: 3ZSE)

Previous work has shown the use of bagasse as a substrate to study the synergistic effect between cellulase and xylanase. High synergy (6.3) between EX, Xyn11A from *Cellulomonas flavigena* and endoglucanase (EG), Cel7B from *Trichoderma reesei*, for reducing sugars production has been reported during the hydrolysis of alkaline pretreated bagasse [24]. Nonetheless, a recent report using four types of reagents to pretreat bagasse observed distinct synergism between cellulase and xylanase. Steam exploded bagasse, NaOH and H_2O_2 pretreated bagasse showed obvious synergy between cellulase and xylanase for glucose and xylose production, whereas H_2SO_4 pretreated bagasse did not [25]. Thus, it appeared that synergism between cellulase and xylanase was specific to the substrate and the pretreatment method used.

1.3 Objective of this Chapter

In the present work, the physical structure and chemical composition of bagasse after PAA and 1-Ethyl-3-methylimidazolium acetate ([Emim][OAc]) pretreatments were determined to verify the potential synergistic effect between EG and EX. For rationalizing the action of the hydrolases with different catalytic properties, one EG, Cel6A (GH6, with a CBM) from *Thermobifida fusca*, and two different EXs, XynZ (GH10, without CBM) from *Clostridium thermocellum* and Xyn11A (GH11, with a XBM) from *T. fusca*, were selected. The performance of each enzyme with varied molecular structure in the hydrolysis of pretreated bagasse with different chemical and physical properties was systematically investigated.

2. Materials and methods

2.1 Materials and enzymes

The biomass bagasse with an average particle size of 200 μm was purchased from Toyota

Tsusho Corporation (Nagoya, Japan). [Emim][OAc] was purchased from Kanto Kagaku, Tokyo, Japan. PAA was supplied by the Mitsubishi Gas Chemical Company, Inc., Japan. The enzymes used in the present study, Xyn11A was provided from Professor Tanaka, Kobe University. XynZ and Cel6A were provided from Professor Ichinose, Kyushu University. The detail information of these three enzymes are listed below. The enzyme purities were confirmed by SDS-PAGE.

Table 2-2 The detail information of XynZ, Xyn11A and Araf51A

Enzyme	Classification	CBM	Microorganism	Mw (kDa)	pI	Family
XynZ	EX	-	*Clostridium thermocellum*	38.2	5.3	10
Xyn11A	EX	*XBM	*Thermobifida fusca*	36.4	9.5	11
Cel6A	EG	+	*Thermobifida fusca*	43	5.7	6

*XBM: bind to cellulose and xylan; EX: Endoxylanase; EG: Endoglucanase.

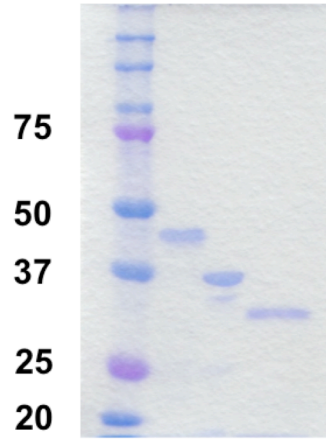

Fig. 2-5 SDS-PAGE of purified enzymes. Lane 1, marker; lane 2, Cel6A; lane 3, XynZ; lane 4, Xyn11A.
Reproduced from *Bioresour. Technol.*, 2015, 185, 158-164 with permission of Elsevier.

2.2 Biomass pretreatments and regeneration

Fifty milligrams of bagasse was added to 1 g [Emim][OAc] or 1 mL deionized water that includes 50 μL of a 40% (w/w) PAA solution. The mixture was heated at 80 °C with stirring (200 rpm) for 3 h. After the reaction, 5 mL deionized water was added into the tubes to precipitate the regenerated cellulose with vigorous shaking. Subsequently, the regenerated bagasse and solution were separated by centrifugation at 25 °C (5,800 g, 20 min). The regenerated water was kept at −18 °C for further investigation. In order to remove the residual reagent, the regenerated cellulose was washed with 5 mL deionized water three times. The

regenerated cellulose was then dried by lyophilization overnight. All pretreatment experiments were carried out in triplicates. The dry mass of the regenerated cellulose was weighed and the yield of the regenerated biomass was calculated by the following equation [8]:

$$YRB\ (\%) = M_{\text{pretreated biomass}}/M_{\text{initial biomass}} \times 100\%$$

2.3 Chemical composition of bagasse and sugar loss in regenerated water during the pretreatment process

The chemical composition of untreated, PAA pretreated and [Emim][OAc] pretreated bagasse was measured following the protocol (LAP TP-510-42619, 42618, 42622) from the National Renewable Energy Laboratory [26-28]. Measuring sugar loss in regenerated water was performed with small modifications. Briefly, the samples were treated with 72% sulfuric acid at 30 °C for 1 h, then diluted to 4% and incubated in an autoclave at 121 °C for 1 h. After cooling the sample, calcium carbonate was used for neutralizing the pH to 7. Analysis of the sugar content was performed using a high-performance liquid chromatography (HPLC) system equipped with a Shodex sugar KS-801 column (8.0 × 300 mm, Showa Denko Co., Tokyo, Japan) and a RI detector at 80 °C with HPLC-grade water as the eluent at a flow rate of 1 mL/min. The remaining acid insoluble lignin was measured after oven-drying overnight at 45 °C and the amount of acid soluble lignin was determined by measuring the absorbance at 240 nm against a deionized water blank using Jasco UV-Vis spectrophotometer V-550 (Jasco, Tokyo, Japan).

2.4 Analytical methods

Scanning electron microscopy (SEM) was employed to observe the changes in the surface of bagasse before and after PAA and [Emim][OAc] pretreatments. The equipment, Shimadzu SS-550 scanning electron microscope (Shimadzu Co., Kyoto, Japan), was operated at 40 kV to image the samples. X-ray diffraction (XRD) measurements were conducted using a Rigaku MultiFlex Diffractometer (Rigaku Co., Tokyo, Japan) operating at 40 kV and 30 mA. The samples were scanned in a 2θ range from 5 to 50° using steps of 0.02°. The calculation of cellulose crystallinity (*CCr*) was derived from the XRD spectra according to Xu et al. [29]:

$$CCr = (I_{002} - I_{am})/I_{002}/C \times 100\%$$

where *CCr* is the cellulose crystallinity, I_{002} is the maximum intensity of the (002) lattice diffraction, I_{am} is the peak of the amorphous part evaluated as the minimum intensity between (101) and (002) lattice planes and C is the cellulose percentage of the biomass.

2.5 Enzymatic hydrolysis and sugars analysis of hydrolysates

The hydrolysis experiments were carried out with 0.25 wt% of the biomass at 50 °C and 1,000 rpm, in 2 mL of sodium phosphate buffer (50 mM, pH 7.0). In each tube the total enzyme loading was held constant at 2 mg protein/g biomass. For the binary mixtures, each enzyme loading was 1 mg/g, and for the ternary mixture, 1 mg/g Cel6A was supplemented with 0.5 mg/g XynZ and 0.5 mg/g Xyn11A. One hundred microliter samples were taken at 0, 3, 6, 12, 24, 48 and 72 h time points and were analyzed for reducing sugars (glucose as the standard) by the dinitrosalicylic acid method [30]. The samples after 72 h enzymatic hydrolysis were analyzed by HPLC using the ABEE (4-aminobenzoic acid ethyl ester) derivation method described by Yasuno et al. [31]. Hydrolysis experiments were carried out in triplicates.

2.6 Calculation method of the degree of synergy

The calculation of the degree of synergy (DS) was determined using the equation [32]:

$DS = Y_{1+2}/(\alpha Y_1 + \beta Y_2)$ or $DS = Y_{1+2+3}/(\alpha Y_1 + \beta Y_2 + \gamma Y_3)$

where α, β and γ correspond to the mass ratios of the enzymes. For example, for the binary mixture α and β are 0.5. Y_{1+2} represents the glucan or xylan conversion of the mixture by two enzymes working simultaneously, whereas Y_1 and Y_2 indicate the glucan or xylan conversion achieved by each enzyme working individually. When XynZ, Xyn11A and Cel6A are mixed together in the reaction, the α and β values are 0.25 and the γ value is 0.5, respectively. Y_{1+2+3}, indicates the glucan or xylan conversion of the mixture by the three enzymes working simultaneously, whereas Y_1, Y_2 and Y_3 indicate the glucan or xylan conversion achieved by each enzyme working individually.

3. Results and Discussion

3.1 Effect of pretreatment methods on chemical composition and physical structure of bagasse

Different pretreatment methods with distinct mechanisms usually have different effects on the same biomass. The chemical compositions of unpretreated, PAA pretreated and [Emim][OAc] pretreated bagasse, are summarized in Table 2-3. After PAA and [Emim][OAc] pretreatments the cellulose percentage did not show any clear change. Nevertheless, 5.8% of lignin and 11.7% of hemicellulose (xylan and arabinan) were removed from the bagasse after PAA pretreatment. Zhao et al. [10] reported that 80% of lignin was removed under conditions of 50% PAA charge, l/s ratio 6:1, 80 °C for 2 h. However, 59.6% of the hemicellulose was removed at the same time. In our study, increasing the amount of water diluted the concentration of PAA and aided the preservation of the hemicellulose. For comparison

purposes, [Emim][OAc] pretreatment was carried out under the same conditions. The results showed that, in this case, the [Emim][OAc] pretreatment method removed more lignin (26.7%) than the PAA pretreatment and, interestingly, it retained a large amount of the hemicellulose (33.7%), especially arabinan (7.2%). However, this phenomenon was not observed if the [Emim][OAc] was used under high temperature conditions, such as 120 °C [17].

Table 2-3 Chemical composition of unpretreated, PAA and [Emim][OAc] pretreated bagasse and the yield of regenerated bagasse

	Unpretreated	PAA pretreated	[Emim][OAc] pretreated
Glucan	37.7 ± 1.1	38.6 ± 0.4	38.9 ± 1.6
Xylan	22.0 ± 5.6	21.0 ± 0.7	26.5 ± 1.0
Arabinan	2.8 ± 0.8	0.9 ± 0.3	7.2 ± 0.6
Ash	3.7 ± 0.4	2.7 ± 0.5	2.3 ± 0.6
Extractives	13.1 ± 1.6	11.5 ± 0.4	9.3 ± 0.9
Acid insoluble lignin	20.2 ± 0.8	14.9 ± 2.5	12.0 ± 3.0
Acid soluble lignin	2.3 ± 0.1	6.3 ± 0.3	4.5 ± 0.1

The results of the yield of regenerated biomass (YRB) indicated that a higher solid content (79%) was preserved after [Emim][OAc] pretreatment when compared with 63% preservation following PAA pretreatment (Fig 2-6a). Few monosaccharides were dissolved in PAA and [Emim][OAc] regenerated water. After acid hydrolysis, long soluble oligomers were degraded to monosaccharides, and thus the loss of saccharides with respect to the percentage of total glucan and xylan of untreated bagasse in regenerated water after PAA and [Emim][OAc] pretreatment were measured (Fig. 2-6b). After PAA pretreatment, 10.8% of glucan and 20.9% of xylan from untreated bagasse were dissolved, whereas [Emim][OAc] pretreatment gave a lower loss of glucan (4.3%) and xylan (2.8%). This result can be explained by the different mechanisms by which PAA and IL pretreatments disrupt the structure of cellulose. IL pretreatment dissolves cellulose by forming new hydrogen bonds with cellulose [8,12,33]. As a result, more glucan remains in the liquid phase after IL pretreatment. However, the mechanism of PAA degradation of lignocellulosic biomass involves the selective attack of the hydroxonium ion on lignin. As a result, partial hemicellulose content, cross-linked with lignin, is removed [10].

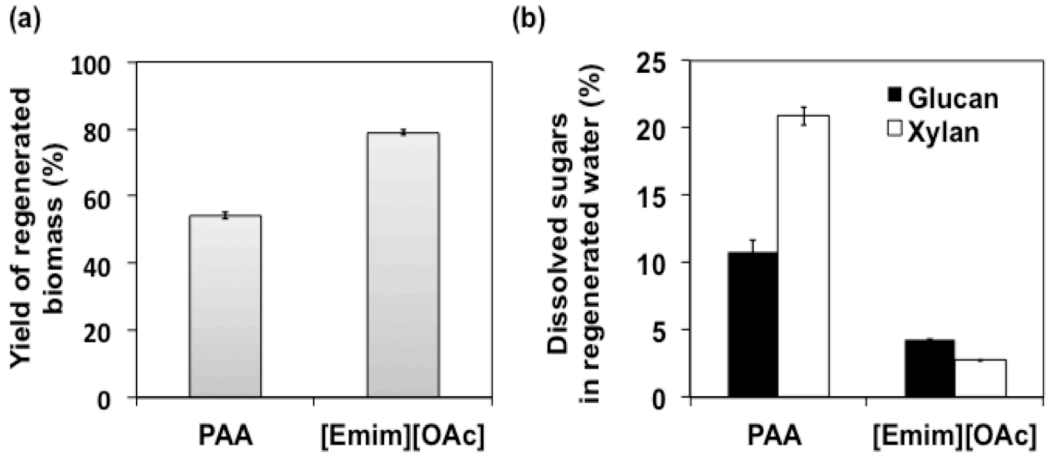

Fig 2-6 Comparison of the effect of PAA and [Emim][OAc] pretreatments on: (a) the yield of regenerated biomass. (b) The percentages of glucan and xylan lost in regenerated water to total glucan and xylan contents in untreated bagasse.

Reproduced from *Bioresour. Technol.*, 2015, 185, 158-164 with permission of Elsevier.

The effect of PAA and [Emim][OAc] pretreatments on the structure of bagasse was evaluated by SEM and XRD analyses. After both PAA and [Emim][OAc] pretreatments, the biomass surface and fibrils became rough and disordered, which could be due to the removal of lignin and part of the carbohydrates. Compared with the significantly altered surface of PAA pretreated bagasse, the surface of bagasse after [Emim][OAc] pretreatment preserved the major microfibrous cellulose structure, however, the surface was disrupted (Fig. 2-7).

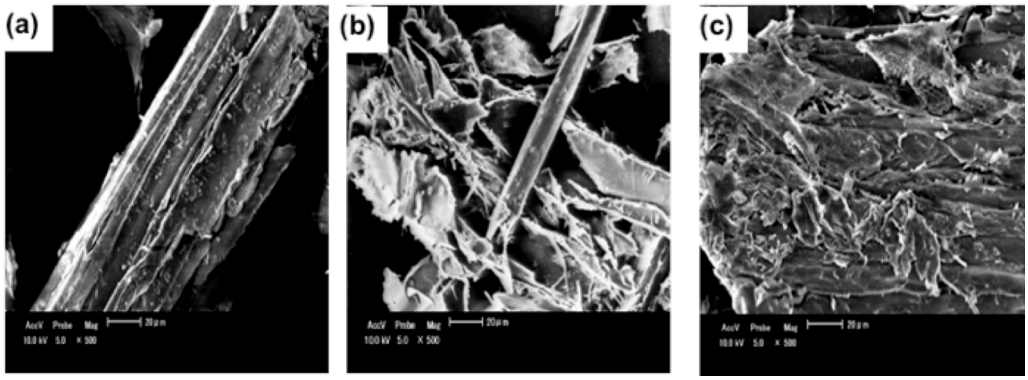

Fig. 2-7 SEM images of (a) unpretreated bagasse, (b) PAA pretreated bagasse and (c) [Emim][OAc] pretreated bagasse under 500 × magnification

Reproduced from *Bioresour. Technol.*, 2015, 185, 158-164 with permission of Elsevier.

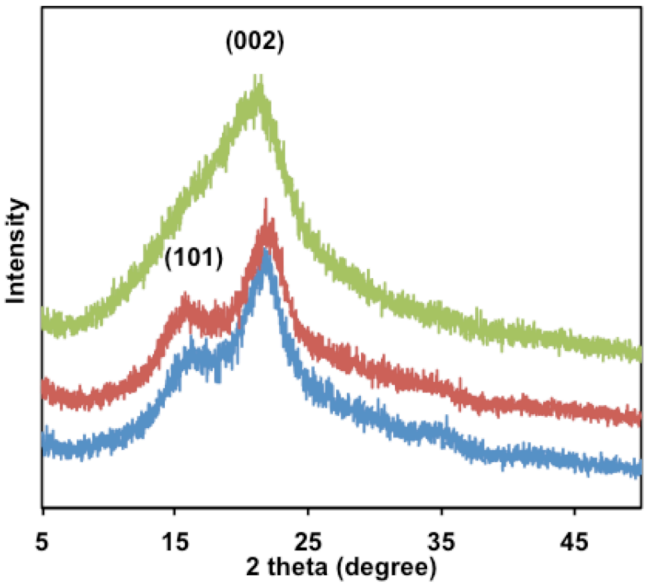

Fig. 2-8 X-ray diffraction spectra of unpretreated bagasse (blue line), PAA pretreated bagasse (red line), [Emim][OAc] pretreated bagasse (green line).

Reproduced from *Bioresour. Technol.*, 2015, 185, 158-164 with permission of Elsevier.

As shown in Fig. 2-8, the XRD peak pattern from untreated to [Emim][OAc] pretreated bagasse showed clear changes. The (101) peak of [Emim][OAc] pretreated bagasse disappeared and the (002) peak became broad. This observation is similar to a previous report from Qiu et al. [17], suggesting the expansion of the cellulose I lattice and the disruption of hydrogen bonds between cellulose fibers [34]. Based on the XRD pattern, cellulose crystallinity (*CCr*), which represents the ratio of the crystalline cellulose to the whole cellulose part, was calculated. The *CCr* value of unpretreated bagasse was 136, whereas [Emim][OAc] pretreated bagasse gave a *CCr* value of 68 and PAA pretreated bagasse gave a value of 116. The decrease in the *CCr* value indicates that part of crystalline cellulose changed form to amorphous cellulose following pretreatment. The lower *CCr* value of [Emim][OAc] pretreated bagasse indicates that more amorphous cellulose was recovered after pretreatment and may facilitate enzymatic hydrolysis efficiency [33,34].

3.2 Production of total sugars from pretreated bagasse

Enzymatic hydrolysis of PAA and [Emim][OAc] pretreated bagasse by Cel6A, XynZ and Xyn11A, solely or mixed together at a fixed loading of 2 mg protein/g bagasse was carried out (Fig. 2-9).

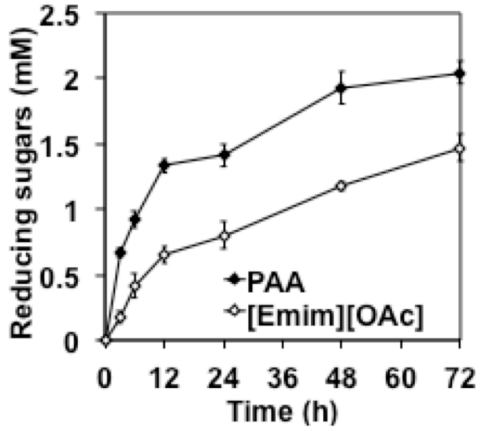

Fig. 2-9 Determination of reducing sugars concentration after 3-, 6-, 12-, 24-, 48- and 72 h hydrolysis of PAA pretreated bagasse and [Emim][OAc] pretreated bagasse by mixture of Cel6A, XynZ and Xyn11A. The error bars represent the standard deviations for three independent trials.

In general, the results showed that PAA pretreated bagasse released more reducing sugars by enzymatic hydrolysis when compared with the amount of reducing sugars released from [Emim][OAc] pretreated bagasse. After 72 h hydrolysis, 1.4-fold more reducing sugars were released from PAA pretreated bagasse than [Emim][OAc] pretreated bagasse when the three enzymes were used in combination. The reducing sugars are a mixture of several kinds of sugars with reducing ends, including glucose, xylose, cellobiose and so on. Since there are several different potential applications of hexoses and pentoses, and to understand the synergistic effect of cellulase and xylanase on C-5 and C-6 sugars production, further determination of monosaccharides and oligosaccharides released in hydrolysates was performed.

The soluble sugars released from pretreated bagasse after enzymatic hydrolysis by individual or combined enzymes for 72 h were analyzed by HPLC. Note that higher polymerized oligomers have not been determined (Fig. 2-10). The products consisted mostly of cellobiose, xylobiose and xylotriose, with small quantities of glucose and xylose detected. In general, Cel6A converted only a minor amount of glucan from both PAA and [Emim][OAc] pretreated bagasse, even though it has a CBM. The absence of other major components, such as β-glucosidase and CBH, appears to affect the efficiency of the EG, even though the EG has a CBM [35,36]. In the case of PAA pretreated bagasse, glucan conversions by all the enzymatic combinations were low (< 3%) for the tested conditions. Surprisingly, higher

glucan conversion was observed for [Emim][OAc] pretreated bagasse (Fig. 2-10b). Cel6A alone converted 4% of glucan from [Emim][OAc] pretreated bagasse, which was four times higher than from PAA pretreated bagasse. This result reflects the impact of cellulose crystallinity in the conversion of glucan during the hydrolysis process. [Emim][OAc] pretreated bagasse with low crystallinity was converted by a higher value than PAA pretreated bagasse, because the EG randomly cut the cellulose chain from the amorphous region [36]. Following the addition of xylanase(s) into cellulase, the glucan conversion from PAA pretreated bagasse increased by > 2-fold, even though the amount of Cel6A had been halved. For [Emim][OAc] pretreated bagasse, combining Cel6A with an EX(s) gave a 1.5-fold improvement in conversion. The highest glucan conversion, 8%, was reached when using the ternary mixture at 72 h from [Emim][OAc] pretreated bagasse. Similarly, for PAA pretreated bagasse, the highest glucan conversion, 2.5 %, was also observed when using the ternary mixture. Since XynZ and Xyn11A only released little cellobiose or glucose from pretreated bagasse, the improvement of glucan conversion by mixing Cel6A and xylanase(s) was mostly contributed by the synergistic effect. This observation shows that the removal of xylan favors the action of Cel6A.

In the case of xylan conversion, at least 2-fold more xylan was converted from PAA pretreated bagasse than from [Emim][OAc] pretreated bagasse by the same enzyme(s). This observation is possibly a result of the high arabinose percentage in [Emim][OAc] pretreated bagasse inhibiting the xylanases. In non-woody biomass, arabinose is generally present as a substituent in arabinoxylans and is tightly connected to other hemicellulose components [37]. Thus, the high percentage of arabinose in the substrate likely protects the substrate from xylanase activity, and this may explain the observed low xylan conversion from [Emim][OAc] pretreated bagasse. XynZ without the CBM converted similar amounts of xylan from PAA pretreated bagasse as Xyn11A; however, in the case of [Emim][OAc] pretreated bagasse, Xyn11A achieved a 1.7-fold higher xylan conversion when compared with the results using XynZ. This result demonstrates that the presence of a CBM appears to play an important role in xylan conversion.

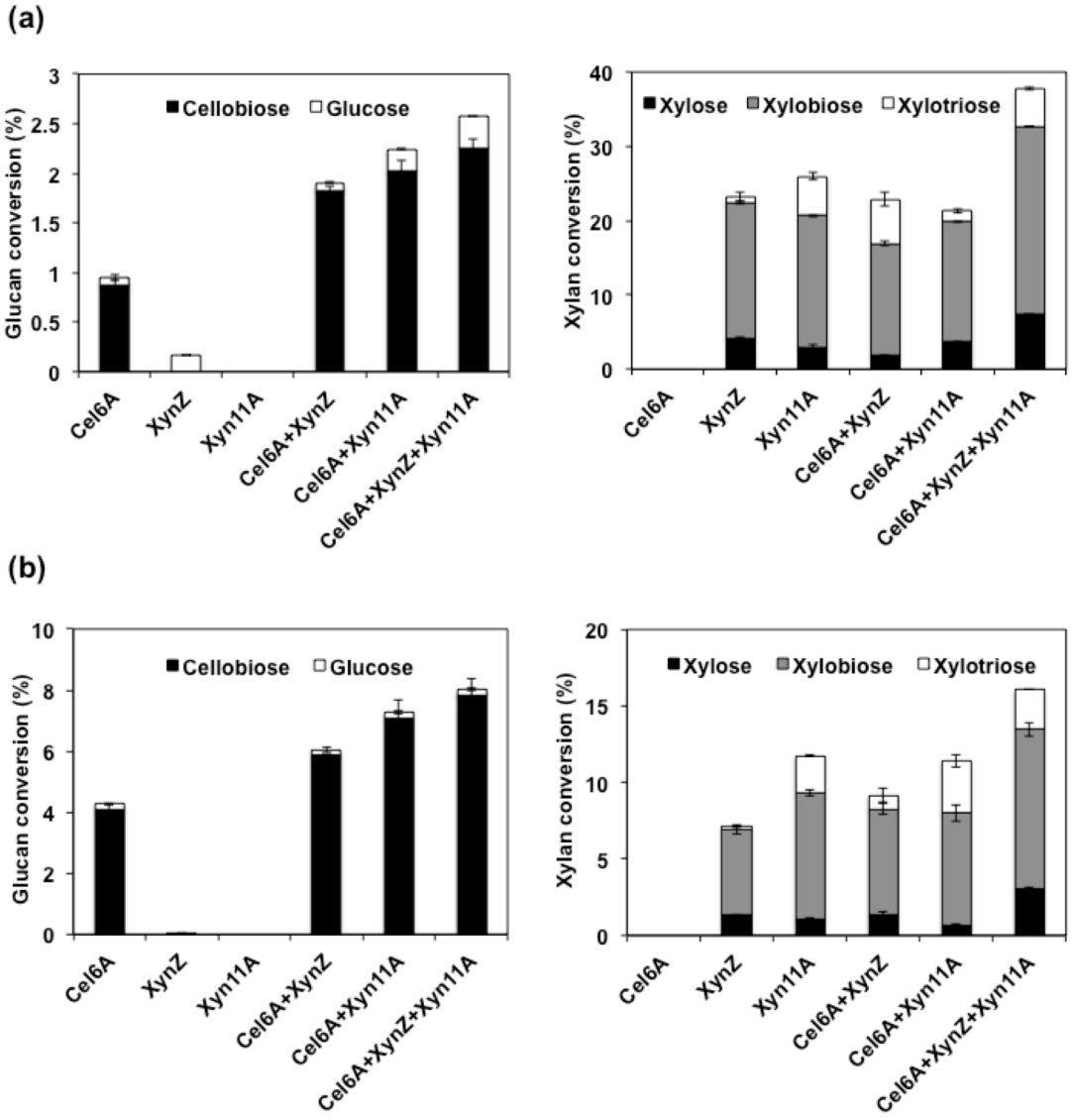

Fig. 2-10 Glucan conversion and xylan conversion after 72 h hydrolysis of (a) PAA pretreated bagasse (b) [Emim][OAc] pretreated bagasse by individual or different combinations of endoglucanase, Cel6A from *T. fusca* and xylanases, XynZ and Xyn11A, from *C. thermocellum* and *T. fusca*. For each trial, the enzyme loading was held constant at 2 mg protein/g biomass. The error bars represent standard deviations for three independent trials.

Reproduced from *Bioresour. Technol.*, 2015, 185, 158-164 with permission of Elsevier.

The CBM facilitates the interaction of the enzyme with the substrate and therefore increases the local concentration of the enzyme on the insoluble biomass substrate. In the present study, Xyn11A with a XBM could potentially increase the accessibility of the catalytic domain of Xyn11A to the substrate. On the other hand, the low arabinan amount in

PAA pretreated bagasse indicates the high accessibility of the substrate to xylanase. Thus, even XynZ without any binding module could convert similar amounts of xylan from PAA pretreated bagasse compared to Xyn11A. Improving the conversion of xylan after xylanase replacement was not as apparent as glucan conversion. For PAA pretreated bagasse, after combining with Cel6A, Xyn11A converted less xylan (21.3%) than the enzyme achieved individually (25.9%). Correspondingly, in the case of [Emim][OAc] pretreated bagasse, the combination of Cel6A and Xyn11A yielded a similar xylan conversion amount when compared with the amount converted using Xyn11A alone. This is probably because of the competition of the two binding modules. Finally, the ternary mixture converted the maximum amount of xylan (37.8% and 16.1%) from PAA and [Emim][OAc] pretreated bagasse, respectively.

3.3 Synergy between EXs and EG on pretreated bagasse

The addition of EXs into EG improved both glucan and xylan conversions. The relationships between xylan removal and glucan conversion for the different enzyme combinations (Cel6A, XynZ and/orXyn11A) are shown in Fig. 2-11.

This linear relationship confirmed the postulate that the removal of xylan from the cellulose matrix had a positive effect on glucan conversion, because the hemicellulose is highly cross-linked by diferulic bridges and cellulose fibrils are likely incorporated [7,21,36,38,39]. The slope of [Emim][OAc] pretreated bagasse was steeper than PAA pretreated bagasse. [Emim][OAc] pretreated bagasse presented a lower *CCr* value, which indicates that the more amorphous cellulose forms are exposed the easier the cellulase hydrolysis, and thus high cellulose conversion could be observed. We hypothesize that for the [Emim][OAc] pretreated bagasse, once a small amount of xylan is removed the conversion may yield high cellulose conversion. In contrast, PAA pretreated bagasse exposed cellulose that was more crystalline, and thus only a small incremental improvement in cellulose conversion, induced by xylan removal, was observed.

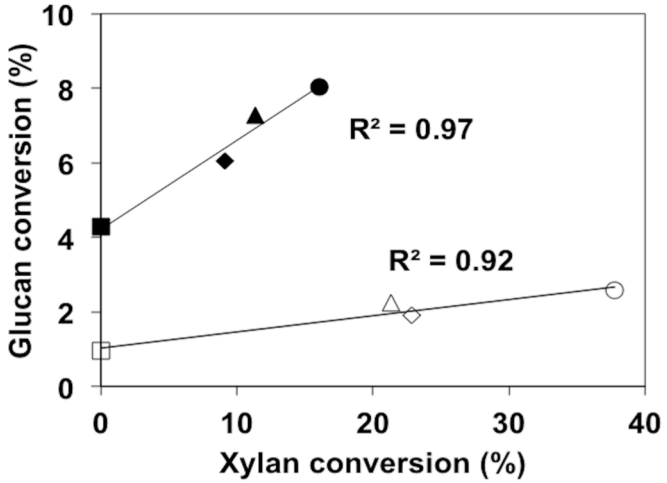

Fig. 2-11 Relationship between glucan and xylan conversion during the hydrolysis of PAA pretreated bagasse (white symbol) and [Emim][OAc] pretreated bagasse (black symbol) by Cel6A alone (square), Cel6A + XynZ (diamond), Cel6A + Xyn11A (triangle) and Cel6A + XynZ + Xyn11A (circle) after 72 h hydrolysis.

Reproduced from *Bioresour. Technol.*, 2015, 185, 158-164 with permission of Elsevier.

The observed improvement of glucan and xylan conversion in the hydrolysis of pretreated bagasse, after combining Cel6A and xylanase(s) demonstrates the synergism between cellulase and xylanase(s). The calculation of the degree of synergy is a direct way to evaluate the synergism between enzymes. In general, when the value of *DS* is higher than 1, the synergism between cellulase and xylanase is active. In the present study, *DS* was calculated based on the percentage of glucan and xylan conversion from different pretreated bagasses after 72 h of hydrolysis (Fig. 2-12). The *DS* values for glucan conversion were higher than the *DS* values for xylan conversion in the hydrolysis of both PAA and [Emim][OAc] pretreated bagasse. This indicates that the synergistic effect between EG and EX is stronger for glucan conversion than for the conversion of xylan.

In general, the physical structure and chemical composition of the substrate is noticeably altered after pretreatment [12,36,41]. Previous reports showed that pretreatment methods significantly affect the synergism of cellulase and xylanase [25,40]. In the present study, all the combinations showed a more evident synergism (over 3.4) for glucan conversion in the hydrolysis of PAA pretreated bagasse, whereas a higher *DS* value for xylan conversion was achieved from hydrolyzing the [Emim][OAc] pretreated bagasse. For PAA pretreated bagasse, a relatively larger amount of xylan was converted after the addition of xylanase(s) (Fig. 2-12a); thus, because more degradable cellulose fractions were exposed, the *DS* values for

glucan conversion were high. However, because of the high crystallinity of cellulose in PAA pretreated bagasse, low glucan conversion was observed. Only a small amount of xylan was exposed from the interaction between EG and EX, and as a consequence the *DS* values for xylan conversion were low. In the case of [Emim][OAc] pretreated bagasse, because of the highly cross-linked structure of hemicellulose but low crystallinity of cellulose, a higher *DS* value for xylan conversion and a lower DS value for glucan conversion were observed.

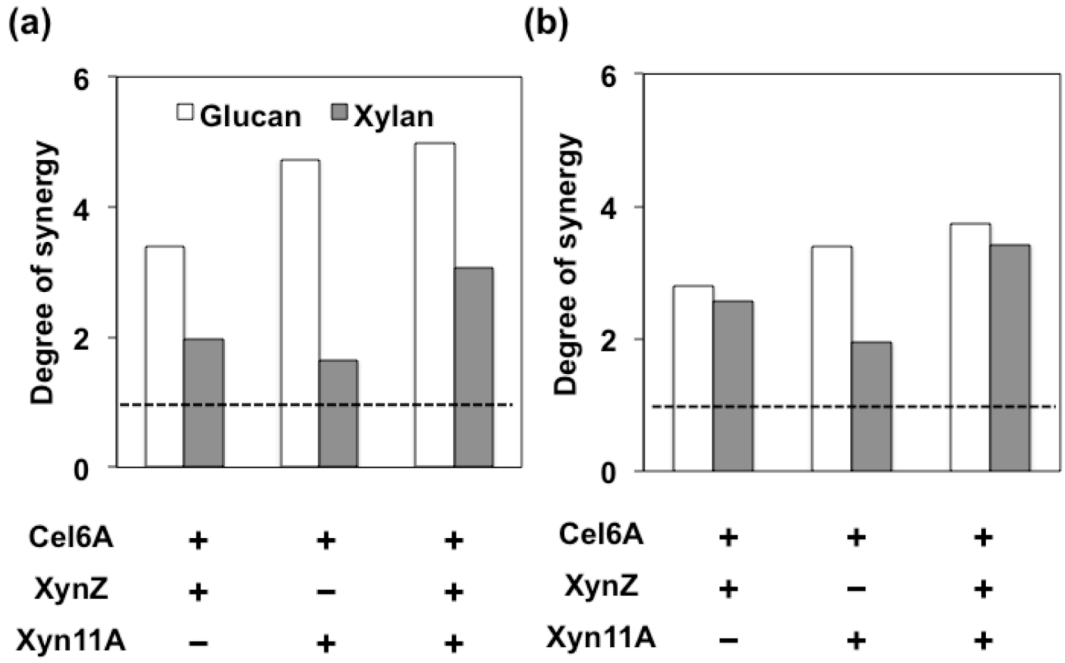

Fig. 2-12 Degree of synergy of endoglucanase and xylanase(s) for the conversion of glucan (white bar) and xylan (black bar) on (a) PAA pretreated bagasse and (b) [Emim][OAc] pretreated bagasse after 72 h of hydrolysis.

Reproduced from *Bioresour. Technol.*, 2015, 185, 158-164 with permission of Elsevier.

Furthermore, it was reported that the molecular structure of the enzyme could also affect the synergism. The lack of a CBM in xylanase Xyn11A from *C. flavigena* was shown to decrease the synergy between a xylanase and a cellulase (EG Cel7B from *T. reesei*) in the hydrolysis of alkaline pretreated bagasse [24]. In this study, for PAA pretreated bagasse, the combination of Cel6A + XynZ achieved a lower *DS* for glucan conversion (3.4), but a higher *DS* for xylan conversion (1.9) when compared with the results of combining Cel6A + Xyn11A, which had *DS* values for glucan and xylan conversion of 4.7 and 1.6, respectively. Likewise, for [Emim][OAc] pretreated bagasse, the combination of Cel6A and XynZ reached similar *DS* values for glucan and xylan conversion of 2.7 and 2.6, respectively. The

combination Cel6A + Xyn11A reached a higher *DS* value for glucan conversion (3.4) than the combination of Cel6A + XynZ, but a lower *DS* value for xylan conversion (1.9). As previously discussed, Xyn11A with a XBM converted more xylan than XynZ, which does not have a substrate binding module. Thus, more cellulose was exposed from the combination of Cel6A + Xyn11A. This combination showed high *DS* values for glucan conversion for both PAA and [Emim][OAc] pretreated bagasse. Correspondingly, glucan dissolution could create cleavage sites for xylanase. Thus, for XynZ without a CBM, this dissolution may potentially increase its efficiency and may explain the higher *DS* value for xylan conversion by the Cel6A + XynZ combination. On the other hand, for Xyn11A with a XBM, this improvement would not be that apparent, hence, the *DS* value for xylan conversion was lower. In conclusion, the presence of a substrate-binding module within a xylanase provides greater synergism for glucan conversion; the cellulose dissolution favored more the action of xylanase without a binding module. Not surprisingly, the highest *DS* values, for both glucan and xylan conversion, were achieved by the ternary mixture in the hydrolysis of PAA or [Emim][OAc] pretreated bagasse.

In summary, in the hydrolysis of PAA or [Emim][OAc] pretreated bagasse, it appears that not only the hemicellulose components and structure, and the cellulose crystallinity but also the molecular structure of the enzyme should be carefully considered to attain optimal synergism between a xylanase and a cellulase. These observations provide the basis for understanding the synergism of cellulases and xylanases on a pretreated lignocellulosic biomass and the development of more elaborated enzyme mixtures for the creation of a cost-effective and highly efficient biorefinery industry.

4. Conclusion

Synergism between cellulase and xylanase in the hydrolysis of bagasse was affected by structural and compositional differences between the substrates resulting from the different pretreatments. PAA pretreatment removed part of hemicellulose but left more crystalline cellulose, resulting in a high degree of synergy for glucan conversion. In contrast, [Emim][OAc] pretreatment likely disrupted less hemicellulose-cellulose associations but generated more amorphous cellulose, resulting in a high degree of synergy for xylan conversion. The molecular structure of enzymes also affected the synergism. Owing to the crosslinking of hemicellulose and cellulose, the removal of xylan favored glucan conversion, and vice versa.

Reference

[1] A.K. Chandel, S.S. da Silva, W. Carvalho, O. V. Singh, Sugarcane bagasse and leaves: foreseeable biomass of biofuel and bio-products, J. Chem. Technol. Biotechnol. 87 (2012) 11–20.

[2] R. Davis, L. Tao, E.C.D. Tan, M.J. Biddy, G.T. Beckham, C. Scarlata, Process design and economics for the conversion of lignocellulosic biomass to hydrocarbons : dilute-acid and enzymatic deconstruction of biomass to sugars and biological conversion of sugars to hydrocarbons, 2013.

[3] S. Lv, Q. Yu, X. Zhuang, Z. Yuan, W. Wang, Q. Wang, W. Qi, X. Tan, The influence of hemicellulose and lignin removal on the enzymatic digestibility from sugarcane bagasse, BioEnergy Res. 6 (2013) 1128–1134.

[4] A. Sant'Ana da Silva, S.-H. Lee, T. Endo, E.P.S. Bon, Major improvement in the rate and yield of enzymatic saccharification of sugarcane bagasse via pretreatment with the ionic liquid 1-ethyl-3-methylimidazolium acetate ([Emim] [Ac])., Bioresour. Technol. 102 (2011) 10505–10509.

[5] W. Hickman, Peracetic acid and its use in fibre bleaching, Rev. Prog. Color. Relat. Top. 32 (2002).

[6] L. Kham, Y. Le Bigot, M. Delmas, G. Avignon, Delignification of wheat straw using a mixture of carboxylic acids and peroxoacids. Ind. Crops Prod. 21, 9–15 (2005).

[7] R. Kumar, F. Hu, C. a Hubbell, A.J. Ragauskas, C.E. Wyman, Comparison of laboratory delignification methods, their selectivity, and impacts on physiochemical characteristics of cellulosic biomass., Bioresour. Technol. 130 (2013) 372–381.

[8] Uju, K. Abe, N. Uemura, T. Oshima, M. Goto, N. Kamiya, Peracetic acid-ionic liquid pretreatment to enhance enzymatic saccharification of lignocellulosic biomass., Bioresour. Technol. 138 (2013) 87–94.

[9] X. Zhao, K. Cheng, D. Liu, Organosolv pretreatment of lignocellulosic biomass for enzymatic hydrolysis., Appl. Microbiol. Biotechnol. 82 (2009) 815–827.

[10] X. Zhao, L. Wang, D. Liu, Effect of several factors on peracetic acid pretreatment of sugarcane bagasse for enzymatic hydrolysis, J. Chem. Technol. Biotechnol. 82 (2007) 1115–1121.

[11] M. Mora-Pale, L. Meli, T. V Doherty, R.J. Linhardt, J.S. Dordick, Room temperature ionic liquids as emerging solvents for the pretreatment of lignocellulosic biomass., Biotechnol. Bioeng. 108 (2011) 1229–1245.

[12] A. Brandt, J. Gräsvik, J.P. Hallett, T. Welton, Deconstruction of lignocellulosic biomass with ionic liquids, Green Chem. 15 (2013) 550.

[13] H. Liu, K.L. Sale, B.M. Holmes, B.A. Simmons, S. Singh, Understanding the Interactions of Cellulose with Ionic Liquids: A Molecular Dynamics Study, (2010) 4293–4301.

[14] S. Singh, B. a Simmons, K.P. Vogel, Visualization of biomass solubilization and cellulose regeneration during ionic liquid pretreatment of switchgrass., Biotechnol. Bioeng. 104 (2009) 68–75.

[15] P. Mäki-Arvela, I. Anugwom, P. Virtanen, R. Sjöholm, J.P. Mikkola, Dissolution of lignocellulosic materials and its constituents using ionic liquids—A review, Ind. Crops Prod. 32 (2010) 175–201.

[16] G. Cheng, P. Varanasi, R. Arora, V. Stavila, B.A. Simmons, M.S. Kent, S. Singh, Impact of ionic liquid pretreatment conditions on cellulose crystalline structure using 1-ethyl-3-methylimidazolium acetate, J. Phys. Chem. B. 116 (2012) 10049–10054.

[17] Z. Qiu, G.M. Aita, M.S. Walker, Effect of ionic liquid pretreatment on the chemical composition, structure and enzymatic hydrolysis of energy cane bagasse., Bioresour. Technol. 117 (2012) 251–256.

[18] S.H. Lee, T. V Doherty, R.J. Linhardt, J.S. Dordick, Ionic liquid-mediated selective extraction of lignin from wood leading to enhanced enzymatic cellulose hydrolysis., Biotechnol. Bioeng. 102 (2009) 1368–1376.

[19] P. Weerachanchai, J.-M. Lee, Recyclability of an ionic liquid for biomass pretreatment, Bioresour. Technol. 169 (2014) 336–343.

[20] L.W. Yoon, G.C. Ngoh, A.S. May Chua, M.A. Hashim, Comparison of ionic liquid, acid and alkali pretreatments for sugarcane bagasse enzymatic saccharification, J. Chem. Technol. Biotechnol. 86 (2011) 1342–1348.

[21] B.C. Saha, Hemicellulose bioconversion., J. Ind. Microbiol. Biotechnol. 30 (2003) 279–291.

[22] L. Saulnier, J.F. Thibault, Ferulic acid and diferulic acids as components of sugar-beet pectins and maize bran heteroxylans, J. Sci. Food Agric. 79 (1999) 396–402.

[23] A. Pollet, J. a Delcour, C.M. Courtin, Structural determinants of the substrate specificities of xylanases from different glycoside hydrolase families., Crit. Rev. Biotechnol. 30 (2010) 176–191.

[24] P. Pavón-Orozco, A. Santiago-Hernández, A. Rosengren, M.E. Hidalgo-Lara, H. Stålbrand, The family II carbohydrate-binding module of xylanase CflXyn11A from *Cellulomonas flavigena* increases the synergy with cellulase TrCel7B from *Trichoderma reesei* during the hydrolysis of sugar cane bagasse., Bioresour. Technol. 104 (2012) 622–630.

[25] J. Li, P. Zhou, H. Liu, C. Xiong, J. Lin, W. Xiao, Y. Gong, Z. Liu, Synergism of

cellulase, xylanase, and pectinase on hydrolyzing sugarcane bagasse resulting from different pretreatment technologies., Bioresour. Technol. 155 (2014) 258–265.
[26] A. Sluiter, B. Hames, R. Ruiz, C. Scarlata, J. Sluiter, D. Templeton, D. Crocker, Determination of Structural Carbohydrates and Lignin in Biomass, (2011).
[27] A. Sluiter, B. Hames, R. Ruiz, C. Scarlata, J. Sluiter, D. Templeton, Determination of Ash in Biomass, (2008).
[28] A. Sluiter, R. Ruiz, C. Scarlata, J. Sluiter, D. Templeton, Determination of extractives in biomass, (2008).
[29]F. Xu, Y.-C. Shi, D. Wang, X-ray scattering studies of lignocellulosic biomass: a review., Carbohydr. Polym. 94 (2013) 904–917.
[30] G.L. Miller, Use of dinitrosaIicyIic acid reagent for determination of reducing sugar, Anal. Chem. 31 (1959) 426–428.
[31] S. Yasuno, T. Murata, K. Kokubo, T. Yamaguchi, M. Kamei, Two-mode analysis by high-performance liquid chromatography of p-aminobenzoic ethyl ester-derivatized monosaccharides, Biosci. Biotech. Biochem. 61 (1997) 1944–1946.
[32] N. Andersen, K.S. Johansen, M. Michelsen, E.H. Stenby, K.B.R.M. Krogh, L. Olsson, Hydrolysis of cellulose using mono-component enzymes shows synergy during hydrolysis of phosphoric acid swollen cellulose (PASC), but competition on Avicel, Enzyme Microb. Technol. 42 (2008) 362–370.
[33] L.W. Yoon, T.N. Ang, G.C. Ngoh, A.S.M. Chua, Regression analysis on ionic liquid pretreatment of sugarcane bagasse and assessment of structural changes, Biomass and Bioenergy. 36 (2012) 160–169.
[34] G. Cheng, P. Varanasi, C. Li, H. Liu, Y.B. Melnichenko, B.A. Simmons, M.S. Kent, S. Singh, Transition of cellulose crystalline structure and surface morphology of biomass as a function of ionic liquid pretreatment and its relation to enzymatic hydrolysis., Biomacromolecules. 12 (2011) 933–941.
[35] E.M. Gomez del Pulgar, A. Saadeddin, The cellulolytic system of *Thermobifida fusca.*, Crit. Rev. Microbiol. 40 (2014) 236–247.
[36] P. V Harris, F. Xu, N.E. Kreel, C. Kang, S. Fukuyama, New enzyme insights drive advances in commercial ethanol production., Curr. Opin. Chem. Biol. 19 (2014) 162–170.
[37] F.M. Gírio, C. Fonseca, F. Carvalheiro, L.C. Duarte, S. Marques, R. Bogel-Łukasik, Hemicelluloses for fuel ethanol: A review., Bioresour. Technol. 101 (2010) 4775–4800.
[38] J. Zhang, L. Viikari, Impact of Xylan on Synergistic Effects of Xylanases and Cellulases in Enzymatic Hydrolysis of Lignocelluloses., Appl. Biochem. Biotechnol. 174 (2014) 1393–1402.

[39] M.J. Selig, E.P. Knoshaug, W.S. Adney, M.E. Himmel, S.R. Decker, Synergistic enhancement of cellobiohydrolase performance on pretreated corn stover by addition of xylanase and esterase activities., Bioresour. Technol. 99 (2008) 4997–5005.
[40] R. Kumar, C.E. Wyman, Effect of xylanase supplementation of cellulase on digestion of corn stover solids prepared by leading pretreatment technologies., Bioresour. Technol. 100 (2009) 4203–4213.
[41] P. Alvira, E. Tomás-Pejó, M. Ballesteros, M.J. Negro, Pretreatment technologies for an efficient bioethanol production process based on enzymatic hydrolysis: A review., Bioresour. Technol. 101 (2010) 4851–4861.

Chapter 3 Synergistic degradation of arabinoxylan by free and immobilized xylanases and arabinofuranosidase

1. Introduction

Hemicelluloses include a number of polysaccharides, of which xylans are the second most ubiquitous in nature. In recent years, biodegradation of hemicellulose has attracted a lot of attention in the industry, such as for the conversion of biomass to biofuels and value-added chemicals, enhancing the efficiency of delignification and the bleaching process in the pulp industry [1].

1.1 Degradation of arabinoxylans

Arabinoxylans are the main form of hemicellulose in plant cell walls, especially in cereal grains such as wheat. They consist of a xylan backbone with arabinose residues linked to its O-2 or O-3 positions [2]. The breakdown of xylan backbone by xylanase(s) is not efficient because of the presence of the mono- or di-substituted arabinose. Therefore, the removal of the arabinose side chains by supplementing with arabinofuranosidase (Araf) is a common method used to increase the efficiency of hemicellulose degradation (Fig. 3-1) [3]. Firstly, the depolymerzing enzyme, endoxylanase (EX) cuts the arabinoxylan into low polymerized arabino-xylooligomers (AXOS). Secondly, the debranching enzyme, some Arafs from GH43, GH51, GH54, or GH62, have the ability to digest the 1,3-linked arabinofuranoside side groups from disubstituted AXOS. Then the monospecific Arafs (GH43 and GH51) remove the rest 1,2- or 1,3-linked arabinose groups. Finally, in the presence of β-Xylosidases (BXL), the debranched AXOS can be completely degraded into xylose.

The cooperative activity between AFase and xylanase has been used to synergistically increase the release of soluble saccharides during the hydrolysis of arabinoxylan [4,5]. Yang and coworkers recently reported a bifunctional AFase from glycoside hydrolase (GH) family 51 that has the activity of both arabinofuranosidase and β-xylosidase. It worked synergistically with endoxylanase XynBE18 in the degradation of wheat arabinoxylan, increasing the production of sugar about 3-fold [6].

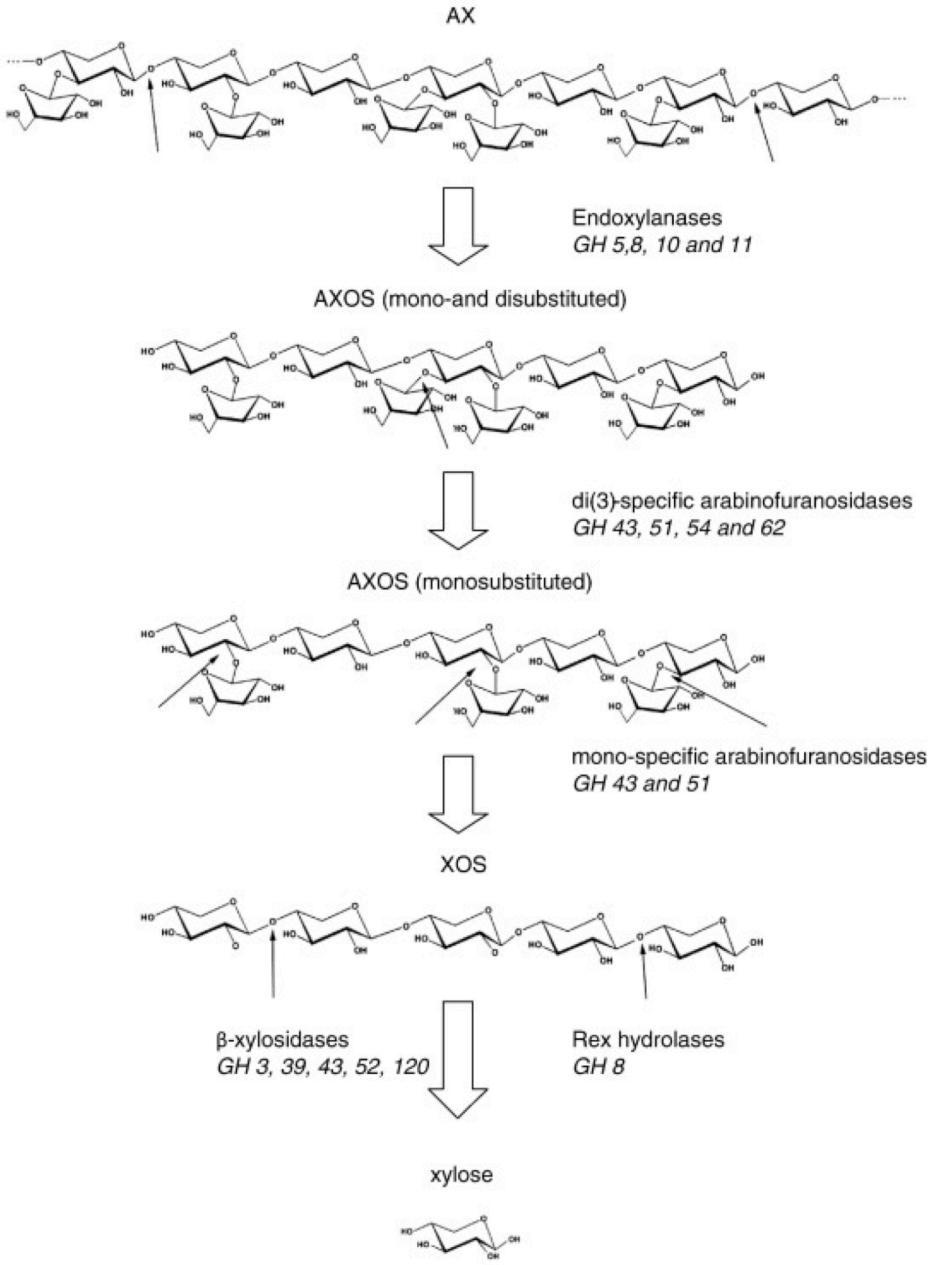

Fig. 3-1 Illustration of completely degradation of arabinoxylan [3]

3-Reprinted from *Biotechnol. Adv*. Vol. 32, Lagaert *et al*., β-Xylosidases and α-l-arabinofuranosidases: Accessory enzymes for arabinoxylan degradation, 316-332, Copyright 2014, with permission from Elsevier.

1.2 Immobilization of enzymes onto nano-materials

Many enzymes have been investigated and developed in an insoluble or immobilized form for academic interest and industrial use, owing to their advantages, such as enabling continuous usage, improved stability, activity and selectivity [7,8]. There are both physical and chemical ways to immobilize enzymes on various supports, which have been well summarized in previous reports [9-11]. For the application in xylan degradation, immobilization of xylanase has been investigated onto varied supports, such as multi-walled

carbon nanotubes [12], synthesized polymer [13], nanoporous gold [14], and resin [15]. Recently, the use of magnetic nanoparticles as supports are of particular interest because they possess both the advantages of the simple separation process of magnetic materials and the high surface area and mass transfer resistance of nanosized materials [16-20]. An increased thermal and pH stability and good reusability of the insoluble form of the enzyme was observed in all the studies compared with the corresponding soluble enzymes. However, enzymes immobilized on nano-sized materials are yet to be fully utilized on an industrial scale.

1.3 Studies of synergism in immobilized enzyme systems

Almost all the research on the synergism between enzymes has been conducted with free enzymes [21]. However, because the basic characteristics of enzymes might be altered upon immobilization onto solid supports, it is also important to investigate the synergism between immobilized enzymes. Tsai et al. observed 2-fold improvement of sugar production when co-immobilizing endoglucanase CelA and exoglucanase CelE onto CdSe-ZnS core-shell quantum dots through polyhistidine-metal coordination for hydrolysis of phosphoric-acid-swollen cellulose [22].

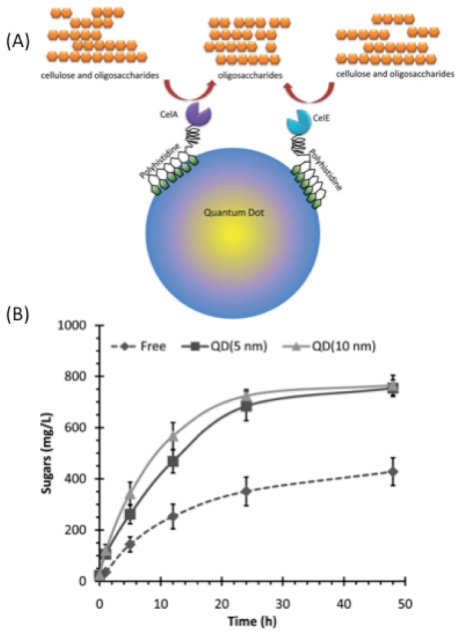

Fig. 3-2 Schematic illustration of polyhistidine-mediated enzyme-quantum dots conjugation and synergism between conjugated CelA and CelE onto 5 or 10 nm diameter QD. [22]

22-Reproduced from *Biotechnol. J.*, Tsai *et al.*, Vol. 8, Size-modulated synergy of cellulase clustering for enhanced cellulose hydrolysis, Copyright 2013, with permission of John Wiley & Sons, Ltd.

Recently, Yoshino group has developed a novel strategy for immobilization of proteins onto magnetic nanoparticles using magnetosome display systam with a magnetotactic bacterium, *Magnetospirillum magneticum*. EG and BGL were co-immobilized onto magntic nanoparticle via cohesin-dockerin system. Compared with single immobilized enzyme, enhanced reducing sugars yield was obtained in the case of co-immobilized enzymes in hydrolysis of soluble substrate, carboxymethyl cellulose (CMC) [23].

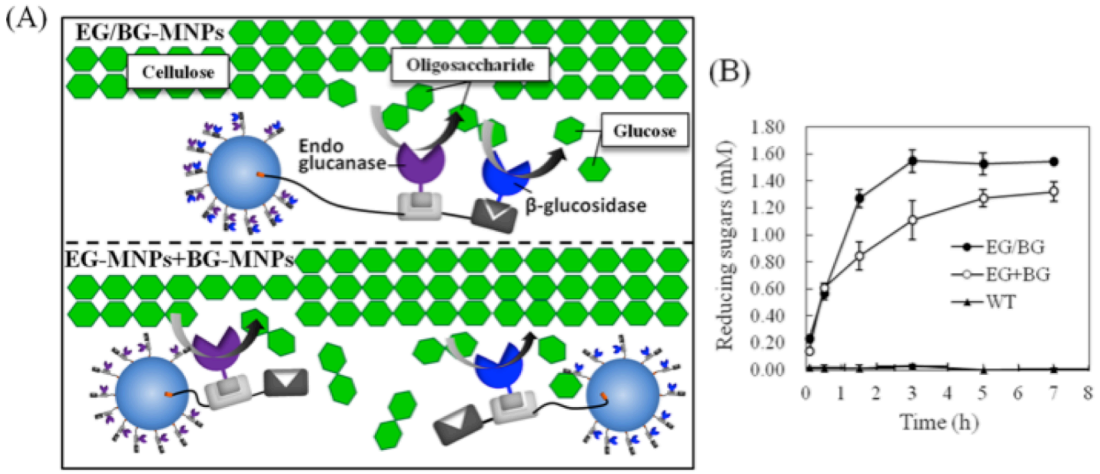

Fig. 3-3 (A) Schematic illustration of CMC degradation by Co-immobilized EG and BGL onto magnetic nanoparticles and single immobilized enzymes. (B) Enhanced reducing sugars production by Co-immobilized enzymatic system. [23]

1.4 Objective of this chapter

Although the synergism between immobilized enzymes have been already demonstrated, little has been studied and there is a need for the development of a recyclable and synergistic enzymatic system for (hemi)cellulose degradation. Therefore, we studied the degradation of arabinoxylan by enzymes in insoluble form, especially focusing on the change in synergism due to the recycling process. In the present study, we have explored the potential synergistic action of different enzyme formulations, free and immobilized enzymes, in hemicellulose degradation. Five EXs, XynZ from *Clostridium thermocellum*, belonging to GH10, and Xyn11A and Xyn10B from *Thermobifida fusca*, belonging to GH11 and GH10, respectively, and XlnB and XlnC from *Streptomyces lividans*, all belonging to GH11 were tested for their effectiveness in arabinoxylan degradation. The two EXs (XynZ and Xyn11A) that showed the highest conversion to reducing sugars among the five xylanases were selected and

investigated together with a family 51 Araf, Araf51A, from *C. thermocellum*. Subsequently, three enzymes were separately immobilized on commercial magnetic nanoparticles through covalent bonding. The immobilized enzymes were successfully recycled 10 times. Continued synergism between the enzymes immobilized on magnetic nanoparticles after 10 cycles was illustrated using arabinoxylan hydrolysis as a model system.

2. Materials and Methods

2.1 Substrates and enzymes

Insoluble wheat arabinoxylan was purchased from Megazyme (P-WAXYI, Wicklow, Ireland). It consists of 36% arabinose, 51% xylose, 6.5% glucose, 4.4% mannose, and 1.6% galactose. The magnetic nanoparticles decorated with N-hydroxysuccinimide groups (190±20 nm in diameter) were purchased from Tamagawa Seiki. Co., Ltd (Japan). The nanoparticles are composed of multiple ferrite particles in the size of 15-20 nm, and coated with a hydrophilic polymer, poly-GMA (glycidyl methacrylate), by seed polymerization.

The enzymes used in the present study, Xyn11A, Xyn10B, XlnB and XlnC were kind gifts from Professor Tanaka, Kobe University. XynZ and Araf51A were kind gifts from Professor Ichinose, Kyushu University. The detail information of these enzymes are listed below.

Table 3-1 The detail information of the enzymes used in present study

Enzyme	Classification	CBM	Microorganism	Mw (kDa)	pI	Family
XynZ	EX	-	*Clostridium thermocellum*	38	5.3	GH10
Xyn10B	EX	-	*Thermobifida fusca*	45	5.1	GH10
Xyn11A	EX	*XBM	*Thermobifida fusca*	36	9.5	GH11
XlnB	EX	CBM	*Streptomyces lividans*	36	9.3	GH11
XlnC	EX	-	*Streptomyces lividans*	26	8.4	GH11
Araf51A	Araf	-	*Clostridium thermocellum*	58	5.4	GH51

*XBM: bind to cellulose and xylan; EX: endoxylanase; Araf: arabinofuranosidase.

2.2 Enzyme immobilization on magnetic nanoparticles

The immobilization method followed the protocol provided by the manufacturer with minor modifications. Briefly, 1 μg/μL of the enzyme solution was prepared with immobilization buffer, which was 25 mM HEPES-NaOH (pH 7.9). Then the nanoparticles were washed with 50 μL of methanol and immobilization buffer successively, the liquid

phase was removed after centrifugation. The immobilization buffer (50 μL) and the prepared enzyme solution (50 μL) were added into a 1.5 mL tube and reacted at room temperature for 1 h and then incubated at 4 °C for 20 h with gentle rotating. After the reaction, the supernatant was removed by centrifugation. To mask the residue carboxyl groups on the nanoparticles, 250 μL of 1 M ethanolamine solution (pH 8.0) was added into the tube and reacted at 4 °C for 20 h with gentle rotating. After that, the enzyme-immobilized nanoparticles were washed three times with 50 mM phosphate buffer (pH 7.0), and resuspended in 200 μL phosphate buffer for further hydrolysis experiments.

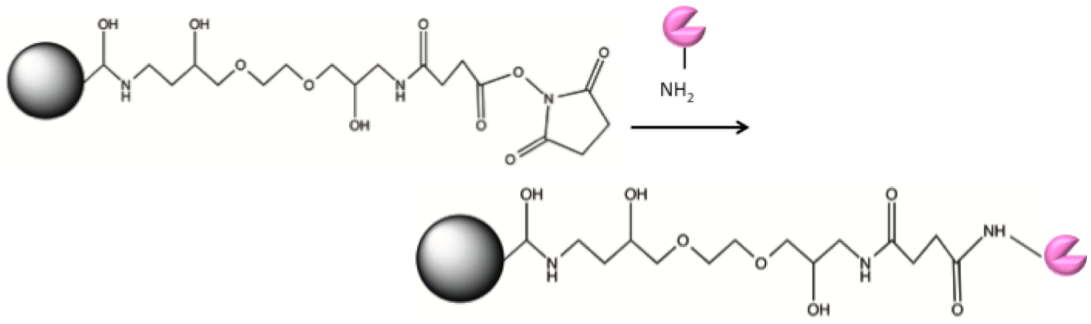

Fig. 3-4 Mechanism of enzyme immobilized on N-hydroxysuccinimide decorated magnetic nanoparticles

The amount of bound protein was determined by a bicinchoninic acid assay (BCA assay, Thermo Fisher Scientific). The immobilization efficiency was calculated using the following equation:

Immobilization efficiency (%)=Total amount of immobilized protein/Total amount of added protein×100%

2.3 Enzymatic hydrolysis and sugar analysis of hydrolysates

For the assay of free enzymes, the selection of proper EXs and optimization of the loading ratio together with Araf was performed. The hydrolysis experiments were performed with 0.25 wt% of the arabinoxylan at 50 °C in 2 mL of sodium phosphate buffer (50 mM, pH 7.0) and placed in a rotary shaker (TAITEC MBR-022UP, Japan) at 1000 rpm. In each tube the total enzyme loading was kept at 100 nM. For the binary mixtures, each enzyme loading was 50 nM, and for the ternary mixture, the enzymes were mixed at a specific ratio, but the total concentration was kept at 100 nM. After hydrolysis, the produced reducing sugars were analyzed by the dinitrosalicylic acid method (DNS assay) with xylose as the standard [24].

Briefly, 100 μL of reaction solution was mixed with 100 μL of DNS reagent, which containing 1.3M DNS, 1M potassium sodium tartrate, and 0.4 N NaOH, and incubated at 99 °C for 5 min. The reducing sugars were quantified colorimetrically at an absorbance of 540 nm. The soluble sugars were analyzed by high-performance liquid chromatography (HPLC) with a Shodex sugar KS-801 column (8.0×300 mm, Showa Denko Co., Tokyo, Japan) and a refractive index detector at 80 °C with HPLC-grade water as the eluent at a flow rate of 1 mL/min.

For investigation of the enzymes immobilized on nanoparticles, the saccharification experiments were performed using the same conditions, but with a final volume of 500 μL. Correspondingly, for the binary mixture each enzyme loading was 50 nM; for the ternary mixture, XynZ, Xyn11A and Araf51A were mixed at an optimized ratio of 2:2:1, which was obtained from the results of the free enzymes, with the total concentration kept at 100 nM. After hydrolysis, the concentrations of the reducing sugars were analyzed by using tetrazolium blue (TZ) assay [25]. After hydrolysis for 48 h, the enzymes immobilized on magnetic nanoparticles were separated using a magnet then washed with phosphate buffer three times. After that, a new substrate was introduced to the system. All the hydrolysis experiments were performed in triplicates. Values are averages of results from three independent trials; error bars indicate the standard deviation values.

2.4 Calculation of the degree of synergy (DS)

The calculation of the degree of synergy (DS) was performed using the equation:

$DS=Y_{1+2+3}/(\alpha Y_1+\beta Y_2+\gamma Y_3)$,

where α, β and γ correspond to the molar ratios of the enzymes. Y_{1+2+3}, indicates the yield of reducing sugars by the three enzymes working simultaneously, whereas Y_1, Y_2 and Y_3 indicate the yield of the reducing sugars achieved by each enzyme working individually. For all cases, single enzymes or combination of enzymes, the enzyme loading was kept at 100 nM.

3. Results and Discussion

3.1 Enzymatic hydrolysis of insoluble wheat arabinoxylan by free xylanases and free arabinofuranosidase

Five EXs, XynZ from *C. thermocellum*, Xyn11A and Xyn10B from *T. fusca*, XlnB and XlnC from *S. lividans*, were selected to investigate their performances in the hydrolysis of insoluble wheat arabinoxylan. Afterwards, the concentration of the reducing sugars was measured by DNS assay. The reducing sugars we measured here indicate the total amount of

sugars including the monomeric and oligomeric forms, which were estimated by DNS method.

As shown in Fig. 3-5, XynZ hydrolyzed the highest amount of reducing sugars (1.5 mM) from the substrate after 24 h, followed by Xyn11A (1.4 mM). The high conversion of substrate to reducing sugars achieved by XynZ or Xyn11A, might be the result of their different structural features. XynZ was purified from *C. thermocellum*, which is an anaerobic bacterium, producing lignocellulose hydrolyzing enzymes in the form of cellulosomes. The full length of XynZ includes a feruloyl esterase domain, a cellulose-binding module (CBM) from family 6 and GH10 xylanase domain. We have only expressed the xylanase catalytic domain of XynZ, since it has higher activity against insoluble birchwood xylan than that of intact enzyme [26]. Conversely, Xyn11A has a special CBM, so-called XBM, that can bind to both cellulose and xylan, thus increasing the interactions between xylan and enzymes [27]. Our previous works also showed that these two EXs are highly active in the hydrolysis of pretreated bagasse [28,29].

Interestingly, xylanases from different families showed different patterns in enzymatic saccharification of insoluble wheat arabinoxylan. All the xylanases from family 11, which are Xyn11A, XlnB and XlnC, produced more reducing sugars in the initial stage of hydrolysis than the xylanases from family 10, such as Xyn10B and XynZ. It has been suggested that GH10 xylanase has a greater affinity to highly branched xylan, whereas GH11 xylanases preferably cleave in the unsubstituted regions of the xylan backbone [30,31]. Thus, at the beginning of the hydrolysis process, GH 11 xylanase acts on the unsubstituted sites and the concentration of reducing sugars would not change as much even if the time period was extended. Similar observation was reported by using xylanases from these two families to degrade wheat bran [32].

Surprisingly, Araf51A, from *C. thermocellum*, showed little conversion to the reducing sugars under the described conditions. Taylor and co-workers have previously demonstrated that Araf51A is an intracellular enzyme that shows relatively lower activity on polymeric wheat arabinoxylan than on an artificial substrate, PNP-Araf, and short soluble oligosaccharides [33].

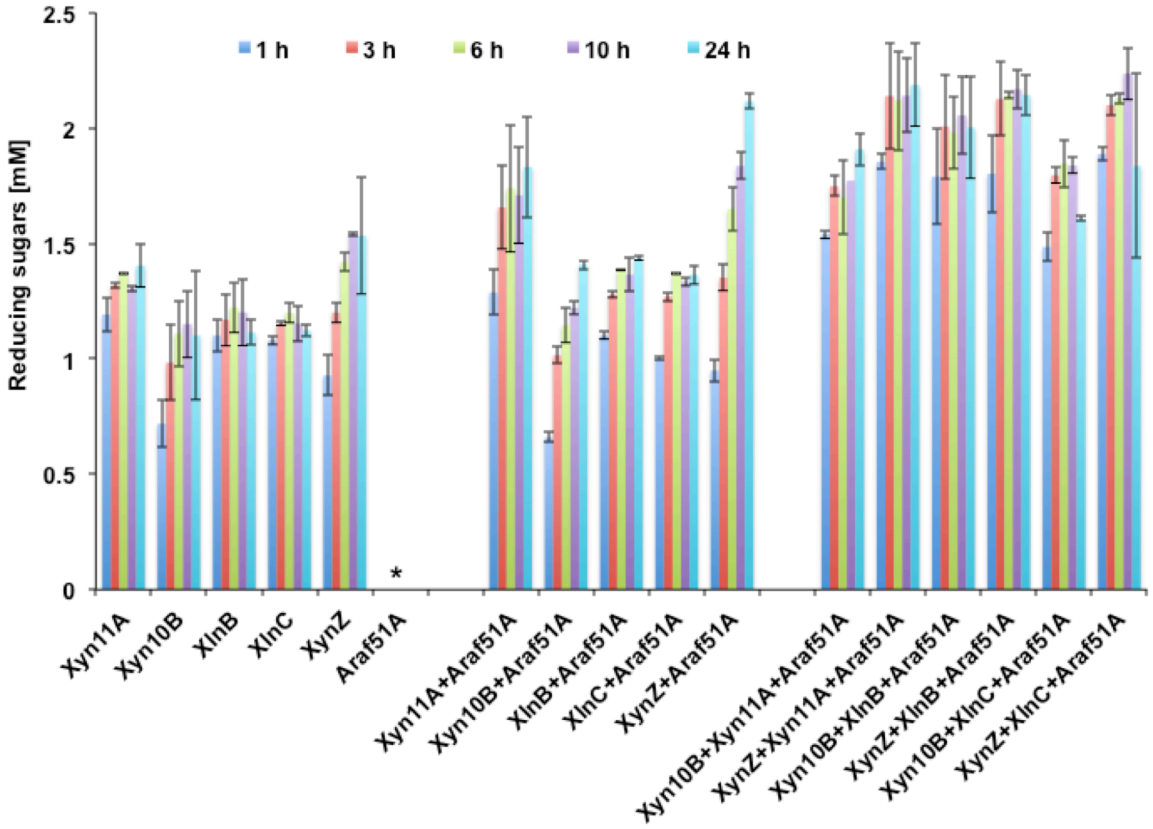

Fig. 3-5 Determination of reducing sugar concentration after 1, 3, 6, 10, and 24 h hydrolysis of arabinoxylan by individual or combinations of endoxylanases, XynZ, Xyn11A, Xyn10B, XlnB and XlnC, with arabinofuranosidase, Araf51A. The total enzyme loading was kept at 100 nM with working volume of 2 mL. For the binary mixtures, each enzyme loading was 50 nM, and for the ternary mixture, each enzyme loading was 33 nM. The concentration of reducing sugars was measured by DNS assay with xylose as standard. The error bars represent the standard deviations from three independent trials. Asterisk symbol (*) represents the concentration of reducing sugars converted by Araf51A alone was below the detection limit of DNS assay.

Meanwhile, the hydrolytic performance of xylanase(s) together with Araf51A, with a loading ratio of 1:1, for the hydrolysis of arabinoxylan was also evaluated. First, binary combination, that is each individual xylanase combined with Araf51A, were tested. In general, all the combinations displayed a higher conversion to the reducing sugar than the single

enzymes. In particular, the combination of XynZ and Araf51, and Xyn11A and Araf51A, had the highest production of reducing sugars, approximately 2 mM after 24 h hydrolysis of arabinoxylan. This proves that the addition of Araf51A is benign to the action of xylanase. Moreover, the concentration of reducing sugars converted by ternary mixture of enzymes (loading ratio of 1:1:1) was quantified to select the best combination. As our previous data has already shown the synergistic effect between GH10 and GH11 xylanases in the hydrolysis of hemicellulose content in pretreated bagasse [28], in the present experiments we only combined family 10 and 11 xylanases with Araf51A, with the aim of achieving the highest conversion to sugar. As expected, after addition of xylanases from different GH families, the concentration of the reducing sugars produced by the enzyme mixture was improved. Among these, not surprisingly, the combination of XynZ and Xyn11A with the addition of Araf51A resulted in the highest amount of reducing sugars. Therefore, XynZ, Xyn11A, as well as Araf51A were selected to conduct further experiments.

3.2 Synergism between free enzymes, XynZ, Xyn11A and Araf51A

Because of its complex structure, lignocellulosic biomass, in most cases, needs a consortium of enzymes to degrade collaboratively. The synergism between enzymes is a reflection of the degree of collaboration between two or more enzymes during the degradation of a substrate. The degree of synergy (DS) is a direct and quantitative way of evaluating the cooperation between enzymes. The value of DS is calculated by dividing the observed activity of a consortium of enzymes with the sum of the activities of the same enzymes, but working separately. If the DS value is greater than one, it means that synergism exist between the enzymes. Conversely, if DS is less than one, it indicates there is no synergy between the enzymes and they are probably competing with each other for binding sites on the substrate.

As shown in Fig. 3-5, with the addition of Araf51A, more sugars were released, compared with the amount of reducing sugars produced by each enzyme working individually. For example, when used alone, XynZ and Xyn11A produced 1.5 mM and 1.4 mM reducing sugars, respectively, after 24 h hydrolysis. With the addition of Araf51A, the amount of reducing sugars increased to 2.1 mM and 1.8 mM, respectively. This suggests that a synergistic effect exists between endoxylanase and arabinofuranosidase.

3.2.1 Impact of synergism on soluble sugars production

The soluble sugars released from the hydrolysis of arabinoxylan by individual or combined enzymes after 24 h were analyzed by HPLC. Note that higher polymerized oligomers have not been detected (Fig. 3-6).

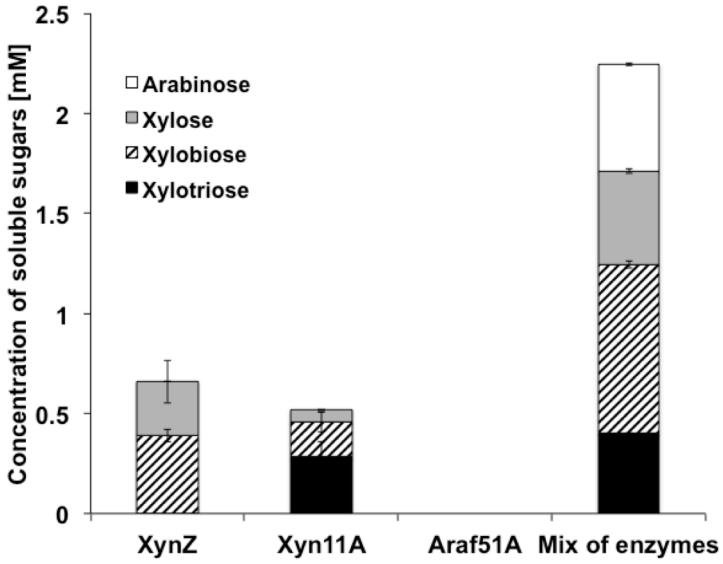

Fig. 3-6 The concentration of soluble sugars after 24 h hydrolysis of arabinoxylan by individual or mixed enzymes, XynZ, Xyn11A and/or Araf51A, measured by HPLC. The error bars represent the standard deviations from three independent trials.

Reproduced from *Biochem. Eng. J.*, 2016, 114, 268-275 with permission of Elsevier.

Smaller polymeric products were generated in the hydrolysis of arabinoxylan by XynZ, which belongs to GH10, whereas the products liberated by the action of Xyn11A were mostly xylotriose and xylobiose. This observation is in good agreement with a previous report [32]. A small amount of arabinose was detected when only Araf51A was used for the hydrolysis of arabinoxylan. But when XynZ and Xyn11A were supplemented with Araf51A, 0.53 mM of arabinose was released. Conversely, higher concentration of soluble xylose and short xylo-oligomers were released after mixing xylanases with Araf51A. In particular, the production of xylotriose, xylobiose and xylose increased by 42%, 50% and 40%, respectively, compared with the sum

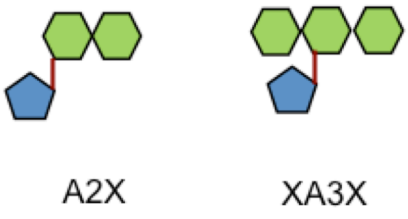

Fig. 3-7 Schematic illustration of the products released by xylanases activity

of those sugars produced by XynZ and Xyn11A individually. Earlier studies have reported that there are soluble products generated from the action of xylanases on arabinoxylan, such as xylobiose with arabinose, linked at the non-reducing end (A2X) from GH10 xylanases, and xylotriose with arabinose linked at the central xylose (XA3X) from GH11 xylanases [31]. Consequently, these are the ideal substrates for Araf51A; by the action of Araf51A, these short soluble oligomers can be digested into arabinose and release xylotriose and xylobiose simultaneously. Besides, with the debranching action of Araf51A, more xylan backbone was exposed to the xylanase, and in turn, more xylose and short xylo-oligomers could be detected.

3.2.2 Effect of enzyme ratio on synergism between free enzymes

Because of the high efficiency of XynZ and Xyn11A in the hydrolysis of arabinoxylan together with Araf51A, different molar ratios of these three enzymes were tested to investigate the relationship between the enzyme loading and the conversion to reducing sugars (Fig. 3-8A). The ratios of XynZ, Xyn11A and Araf51A were chosen as 1:1:2, 1:1:1 and 2:2:1, respectively, but the total loading was kept constant at 100 nM. A similar amount of reducing sugars was obtained when XynZ, Xyn11A and Araf51A, were mixed at different ratios. The mixture of enzymes at a ratio of 2:2:1 converted slightly more sugars than the enzymes loaded at a ratio of 1:1:2 or 1:1:1. As mentioned before, Araf51A catalyzes the α-1,2- or α-1,3-arabinofuranosyl residues of the side chain, as a debranching enzyme, liberating a smaller amount of sugars than xylanase, which is a depolymerizing enzyme. More sugar could be generated with a higher proportion of xylanases. The degree of synergy between xylanases and Araf was also affected by the enzyme-loading ratio (Fig. 3-8B). The DS value increased with the increase of the Araf proportion in the enzyme mixture. As shown in Fig. 3-8B, the a ratio of XynZ/Xyn11A/Araf51A=1:1:2 resulted in the highest DS. However, a high DS value did not correspond to a higher reducing sugars concentration. The addition of less xylanase resulted in less degradation of the xylan main chain. Therefore, because of the high conversion to reducing sugars, subsequent experiments were conducted at a XynZ/Xyn11A/Araf51A ratio of 2:2:1.

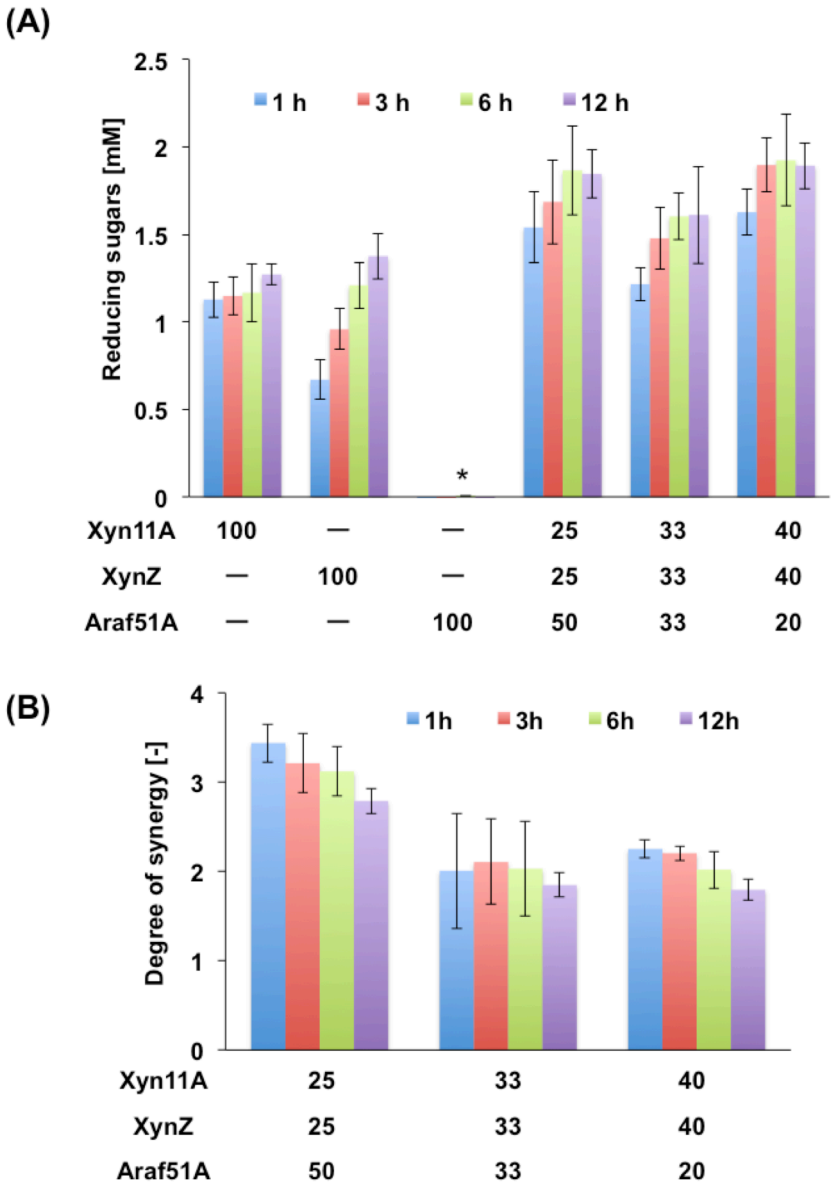

Fig. 3-8 (A) The optimization of the loading of enzymes mixture for the hydrolysis of arabinoxylan. Total enzyme loading was 100 nM in 2 mL working volume. (B) The degree of synergy (DS) of xylanases and arabinofuranosidase for hydrolysis of arabinoxylan under different enzyme-loading ratios.

Reproduced from *Biochem. Eng. J.*, 2016, 114, 268-275 with permission of Elsevier.

3.3 Immobilization of hemicellulases on magnetic nanoparticles

There are physical and chemical ways to immobilize enzymes on solid support. Physical

adsorption, based on hydrophobic and van der Waals interactions, is generally characterized as weak binding methods, and the enzyme(s) could not stably fix on the support [11]. Conversely, the enzyme immobilization through chemical reaction is strong that proteins are covalently bound to appropriately modified supports through functional side groups exposed on protein surface. By far, the reactive groups coupling with amine-containing molecules are the most common choice for protein immobilization. Solid supports surface covering suitable functional group, such as N-hydroxysuccinimide ester, epoxy, aldehyde or sulfonyl chloride, can readily interact with amino group of proteins to form amide bonds [34].

Three enzymes were immobilized individually on commercial magnetic nanoparticles using covalent bonding. Using commercial succinylated magnetic nanoparticles with an average diameter of 200 nm, the enzyme was readily conjugated using a common activation chemistry method; the N-hydroxysuccinimide (NHS) activated carboxylate group primarily coupled with α-amines at the N-terminals and the ε-amines of lysine side chains [34]. Consequently, a new and stable amide linkage was created. As shown in Table 3-2, the amount of enzymes bound on the magnetic nanoparticles was different. Immobilization efficiency of Xyn11A was 44.8%, whereas only 22.4% and 16.4% of XynZ and Araf51A was bound, respectively. One possible reason might be the difference in the isoelectric point (pI) of the enzymes. Because the activated carboxylate groups make the nanoparticles negatively charged after hydrolysis, a closer proximity could be formed if the enzyme is positively charged at the given pH. In the present study, XynZ, Xyn11A and Araf51A have an isoelectric point of 5.2, 9.5 and 5.4, respectively. Thus, only Xyn11A is positively charged in the buffer solution at a pH of 7.9. Because of the electrostatic adsorption between the positively charged protein and negatively charged carboxyl group, more Xyn11A was bound. Johnsson and colleagues have compared the immobilization of one small protein with a high pI of 9.3, ribonuclease A, and one medium-sized protein with low pI of 5.1, *Staphylococcus aureus* protein A, on an NHS activated gold surface. The highest amount of protein was immobilized when the solution pH was lower than the pI of the protein, which reveals the importance of electrostatic attraction forces in the immobilization process [35]. Xyn11A is the smallest of the three enzymes. Thus, with a protein loading mass of 50 μg, more Xyn11A was added in the immobilization solution; as a result, more Xyn11A was available for immobilization.

Table 3-2 Immobilization efficiency of proteins on the magnetic nanoparticles and properties of the enzymes

Enzyme	Immobilization efficiency (%)	Theoretical isoelectric point	Molecular weight (kDa)
XynZ	22.4 ± 2.2	5.2	38.0
Xyn11A	44.8 ± 6.2	9.5	36.4
Araf51A	16.4± 5.8	5.4	57.7

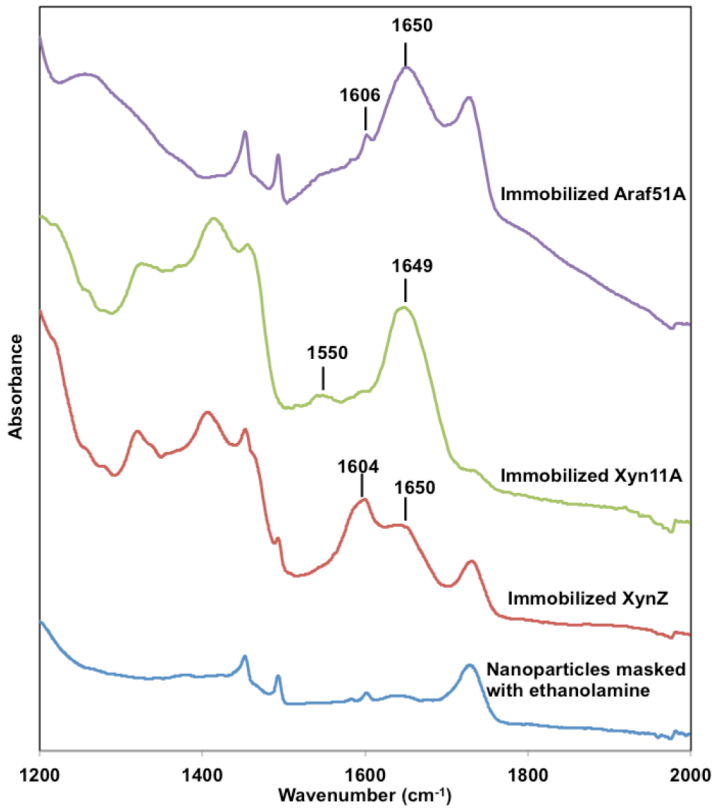

Fig. 3-9 Characterization of enzymes after immobilization on the magnetic nanoparticles by Fourier transform infrared spectroscopy (FTIR).

Reproduced from *Biochem. Eng. J.*, 2016, 114, 268-275 with permission of Elsevier.

The enzymes in the free and immobilized form were characterized. The Fourier transform infrared spectroscopy (FTIR) results confirmed the successful immobilization of the enzymes on the nanoparticles (Fig. 3-9). In the case of free enzymes, the characteristic bands at approximately 1650 and 1541 cm^{-1} were assigned to Amide I and II, respectively, which are the two prominent vibration bands of the protein backbone [36]. In the last step of the immobilization, the unreacted carboxyl groups were masked with ethanolamine to form an amide bond. The difference between the nanoparticles reacted with ethanolamine and enzyme

was also demonstrated by FTIR. After the immobilization of XynZ on the nanoparticles, the Amide I band at 1650 cm^{-1} was clearly observed and the Amide II band shifted to 1604 cm^{-1}, whereas these bands were not observed in the case of the magnetic nanoparticles masked with ethanolamine. Similar observations were made in the case of Xyn11A and Araf51A.

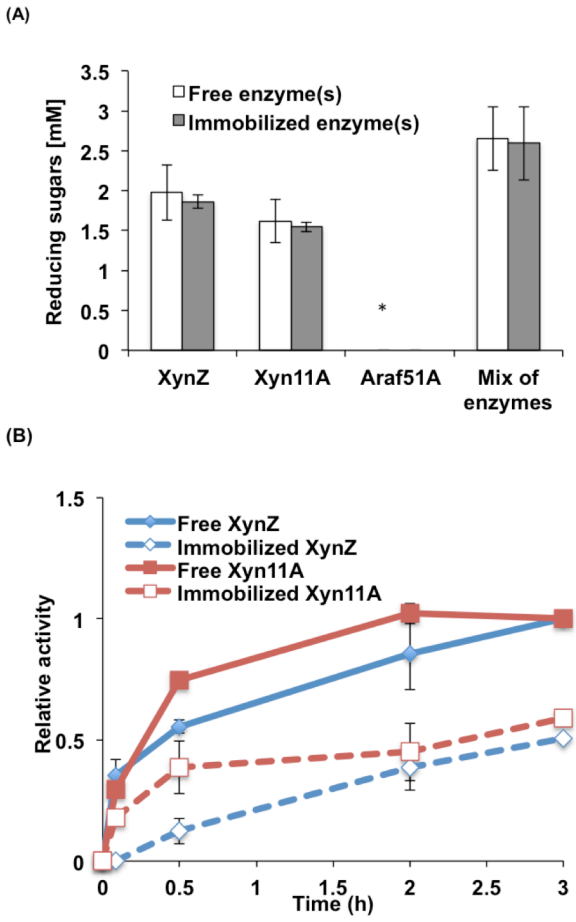

Fig. 3-10 Comparison of free enzymes and enzymes immobilized on magnetic nanoparticles at the initial stage of hydrolysis process. The relative activities were based on the amount of reducing sugars converted by free XynZ or free Xyn11A, determined at 6 h after the first cycle. The experiments were conducted in triplicates.

Reproduced from *Biochem. Eng. J.*, 2016, 114, 268-275 with permission of Elsevier.

Thereafter, the performance of the free enzyme and the enzyme immobilized on nanoparticles in the hydrolysis of insoluble arabinoxylan was investigated (Fig.3-10A). After hydrolysis for 48 h, comparable amounts of reducing sugars were obtained using the free enzymes and immobilized enzymes, although the initial stage of the conversion by the immobilized enzymes was slow (Fig. 3-10B). The reason might be the slower rate of substrate diffusion in the conjugated system owing to steric hindrance from the solid support [37]. It is

also worth mentioning that the immobilized enzyme showed a similar trend to the free enzyme in the hydrolysis process, whereby xylanase from GH11 converted a higher amount of sugars in the initial stage, whereas xylanase from GH10 gradually degraded the insoluble substrate. This result indicated that enzymes immobilized on nanoparticles have the potential to be used in the hydrolysis of (hemi)cellulosic biomass, with similar features as the free enzymes, and with the advantage of being reused.

3.4 A recyclable and synergistic enzyme system for hemicellulase degradation

The recyclability of the immobilized enzymes was evaluated by using it multiple times. After the first hydrolysis, the immobilized enzymes were separated using a magnet, washed, and a fresh substrate was introduced. As illustrated in Fig. 3-11, 10 cycles of hydrolysis were performed. Since the concentration of arabinose was below the detection limit of TZ assay used in this study, the amount of reducing sugars produced by immobilized Araf51A alone could be negligible. We thus set the value of Y_3 as zero for the calculation of DS. Not surprisingly, in all cases, for individual or a mixture of immobilized enzymes, the highest conversion was achieved in the first cycle. An apparent loss of activity was observed after each cycle, with the largest reduction after the first cycle. The amount of reducing sugars produced by immobilized XynZ, immobilized Xyn11A and mixture of immobilized enzymes dropped by 58%, 42% and 35%, respectively, after the first cycle, probably owing to the disassociation of weakly bound enzymes. Only the strongly bound enzymes were retained after the first cycle. After 10 cycles, the amount of reducing sugars produced by the individual enzymes, XynZ and Xyn11A, fell to 21% and 25% of the amount of sugars produced in the first cycle, respectively; the amount of reducing sugars produced by the mixture of immobilized enzymes was 42% of that from the first cycle. This drop in the conversion to sugar might be because of both dissociation and deactivation of the enzymes. Jordan and co-workers covalently immobilized commercial cellulase on magnetic nanoparticles and recycled cellulase six times until the activity decreased to 10% of initial cycle. Moreover, they observed a noticeable drop of 47.5% of enzyme activity after the first cycle [38,39].

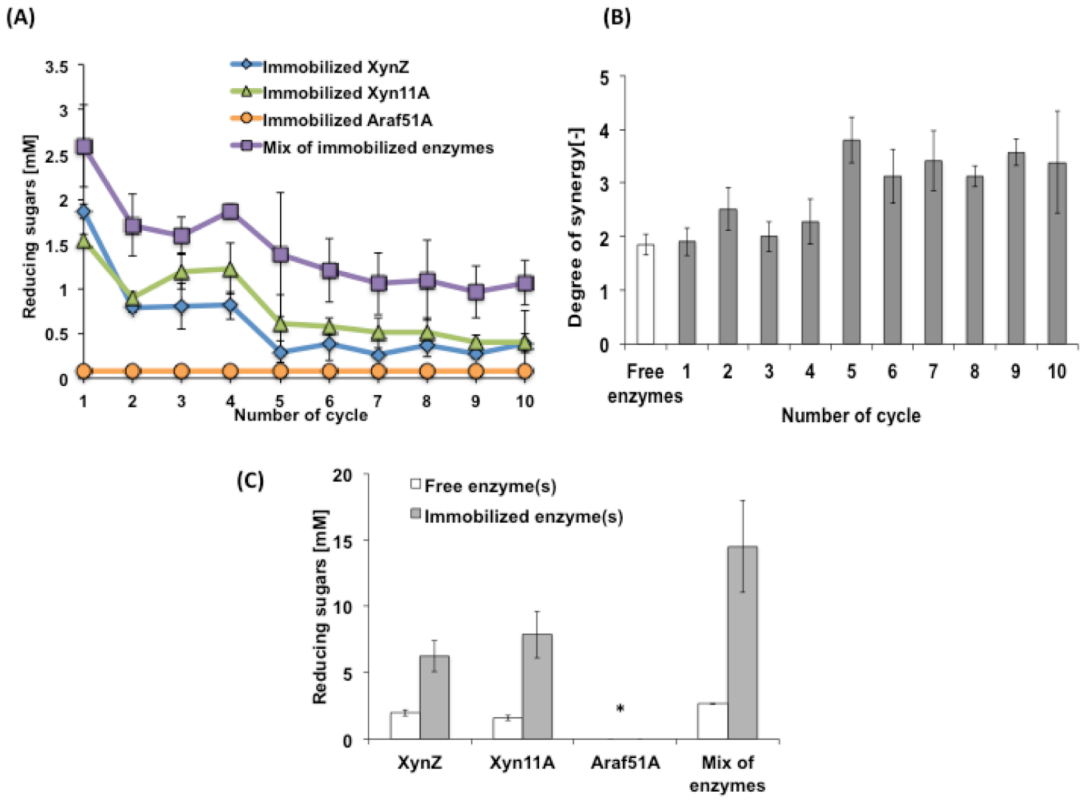

Fig. 3-11 (A) The amount of reducing sugars converted by individual or a mixture of immobilized enzymes in the hydrolysis of arabinoxylan for 48 h after 10 cycles. For immobilized Araf51A, the detection limit of TZ assay in this study (0.08 mM) was shown. (B) The degree of synergy (DS) of xylanases and arabinofuranosidase for hydrolysis of arabinoxylan after 48 h. The white bar represents the DS of free enzymes; the grey bars represent the DS values of enzymes immobilized on nanoparticles after 10 cycles. (C) The amount of reducing sugars converted by free enzymes (white bar); and sum of sugar production converted by immobilized enzymes after 10 cycles (gray bar). Asterisk symbol (*) represents the concentration of reducing sugars converted by Araf51A alone was below the detection limit of TZ assay.

Reproduced from *Biochem. Eng. J.*, 2016, 114, 268-275 with permission of Elsevier.

The degree of synergy (DS) between immobilized xylanases and Araf after 48 h of hydrolysis of insoluble wheat arabinoxylan were calculated (Fig. 3-11B). After ten times recycling of the immobilized enzymes, the DS value increased from 1.9 (cycle 1) to 3.4 (cycle 10). As shown in Fig. 3-11A, the conversion of reducing sugars by each individual enzyme, through ten cycles, was decreased, especially from cycle 1 to cycle 5, and there was a substantial loss in the conversion of reducing sugars for the immobilized XynZ. However, the

concentration of reducing sugars released by the collaborative action of the enzymes in the mixture did not decrease as much, probably because of the synergism between the enzymes, which were still active. Based on the equation of DS, in which synergism is a function of the ratio of reducing sugars converted by enzyme mixture and individual enzyme components, the value of DS would increase mathematically with the large decrease of the denominator, as the significant loss in reducing sugars by XynZ, from cycle 1 to cycle 5. Nevertheless the synergism between Araf and EXs improved the production of the reducing sugars through all ten cycles. This indicates the potential application of enzymes immobilized on inorganic solid supports for the synergistic degradation of hemicellulose.

In most studies, the hydrolysis experiments with free enzymes can only be performed once, owing to the poor recoverability of the free enzymes. However, with the same initial enzyme loading, enzymes immobilized on nanoparticles could be recycled several times. Fig. 3-11C shows the comparison of the total amount of sugars produced by free enzymes after one cycle and by the enzymes immobilized on nanoparticles after ten cycles. The free XynZ and Xyn11A produced 2.0 and 1.6 mM sugars, respectively, after 48 h hydrolysis of arabinoxylan. Correspondingly, with the same enzyme loading, immobilized XynZ and Xyn11A produced 6.2 and 7.9 mM sugars, respectively, after 10 cycles. The mixture of free enzymes produced 2.7 mM reducing sugars after hydrolysis of insoluble arabinoxylan for 48 h, whereas the corresponding mixture of immobilized enzymes produced a 5.5-fold increase of reducing sugars after 10 cycles.

In summary, clear synergism was observed between EXs from GH10 and GH11, and Araf in the hydrolysis of insoluble arabinoxylan. More importantly, continued synergism was observed between the same enzymes after they were immobilized on magnetic nanoparticles. Because of the recyclability, a 5.5-fold increase in the amount of sugar was obtained after 10 cycles compared with free enzymes. These remarkable improvements in the production of sugars demonstrate that immobilized enzymes can be used to reduce enzyme loadings and lower the production costs in industries that use enzymes. Although the technology of enzyme recovering through nanoparticle immobilization is not mature enough to be transferred into production scale, the presenting recyclable and synergistic enzyme system could provide as a reference for the cost-effective enzyme utilization study.

4. Conclusions

Two purified recombinant EXs, XynZ and Xyn11A, were shown to degrade insoluble arabinoxylan with a high conversion to reducing sugars. The selected xylanases worked synergistically with Arabinofuranosidase and converted the highest amount of sugars at a

ratio of XynZ:Xyn11A:Araf51A=2:2:1. After immobilization of the enzymes on magnetic nanoparticles through covalent bonding, the immobilized enzymes were recycled 10 times. Continued synergism between the enzymes immobilized on magnetic nanoparticles after 10 cycles was illustrated. Our results indicate efficient utilization of the interaction between Arabinofuranosidase and xylanases for the degradation of natural polymers, which can be used to lower the production costs in industries that utilize enzymes.

References

[1] B.C. Saha, Hemicellulose bioconversion., J. Ind. Microbiol. Biotechnol. 30 (2003) 279–291.

[2] M.L.T.M. Polizeli, A.C.S. Rizzatti, R. Monti, H.F. Terenzi, J.A. Jorge, D.S. Amorim, Xylanases from fungi: properties and industrial applications., Appl. Microbiol. Biotechnol. 67 (2005) 577–591.

[3] S. Lagaert, A. Pollet, C.M. Courtin, G. Volckaert, β-Xylosidases and α-l-arabinofuranosidases: Accessory enzymes for arabinoxylan degradation, Biotechnol. Adv. 32 (2014) 316–332.

[4] T. Hashimoto, Y. Nakata, Synergistic degradation of arabinoxylan with α-L-arabinofuranosidase, xylanase and β-xylosidase from soy sauce koji mold, *Aspergillus oryzae*, in high salt condition, J. Biosci. Bioeng. 95 (2003) 164–169.

[5] A. Valls, P. Diaz, F.I. Javier Pastor, S. V Valenzuela, A newly discovered arabinoxylan-specific arabinofuranohydrolase. Synergistic action with xylanases from different glycosyl hydrolase families, Appl. Microbiol. Biotechnol. 100 (2015) 1743–1751.

[6] W. Yang, Y. Bai, P. Yang, H. Luo, H. Huang, K. Meng, P. Shi, Y. Wang, B. Yao, A novel bifunctional GH51 exo-α-l-arabinofuranosidase/endo-xylanase from Alicyclobacillus sp. A4 with significant biomass-degrading capacity, Biotechnol. Biofuels. 8 (2015) 197.

[7] B.J. Johnson, W. Russ Algar, A.P. Malanoski, M.G. Ancona, I.L. Medintz, Understanding enzymatic acceleration at nanoparticle interfaces: Approaches and challenges, Nano Today. 9 (2014) 102–131.

[8] R. DiCosimo, J. McAuliffe, A.J. Poulose, G. Bohlmann, Industrial use of immobilized enzymes, Chem. Soc. Rev. 42 (2013) 6437−6474.

[9] U.T. Bornscheuer, Immobilizing Enzymes : How to Create More Suitable Biocatalysts, Angew. Chemie Int. Ed. 42 (2003) 3336–3337.

[10] C. Garcia-Galan, A. Berenguer-Murcia, R. Fernandez-Lafuente, R.C. Rodrigues, Potential of different enzyme immobilization strategies to improve enzyme performance, Adv. Synth. Catal. 353 (2011) 2885–2904.

[11] R.A. Sheldon, S. Van Pelt, Enzyme immobilisation in biocatalysis: why, what and how, Chem. Soc. Rev. 42 (2013) 6223–6235.

[12] S. Shah, M.N. Gupta, Simultaneous refolding, purification and immobilization of xylanase with multi-walled carbon nanotubes, Biochim. Biophys. Acta - Proteins Proteomics. 1784 (2008) 363–367.

[13] M. Sardar, I. Roy, M.N. Gupta, Simultaneous purification and immobilization of *Aspergillus niger* xylanase on the reversibly soluble polymer Eudragit™ L-100, Enzyme

Microb. Technol. 27 (2000) 672–679.
[14] X. Yan, X. Wang, P. Zhao, Y. Zhang, P. Xu, Y. Ding, Xylanase immobilized nanoporous gold as a highly active and stable biocatalyst, Microporous Mesoporous Mater. 161 (2012) 1–6.
[15] Y.S. Lin, M.J. Tseng, W.C. Lee, Production of xylooligosaccharides using immobilized endo-xylanase of Bacillus halodurans, Process Biochem. 46 (2011) 2117–2121.
[16] E.P. Cipolatti, M.J. a. Silva, M. Klein, V. Feddern, M.M.C. Feltes, J.V. Oliveira, J.L. Ninow, D. de Oliveira, Current status and trends in enzymatic nanoimmobilization, J. Mol. Catal. B Enzym. 99 (2014) 56–67.
[17] H. Shahrestani, A. Taheri-Kafrani, A. Soozanipour, O. Tavakoli, Enzymatic clarification of fruit juices using xylanase immobilized on 1,3,5-triazine-functionalized silica-encapsulated magnetic nanoparticles, Biochem. Eng. J. 109 (2016) 51–58.
[18] A. Landarani-Isfahani, A. Taheri-Kafrani, M. Amini, V. Mirkhani, M. Moghadam, A. Soozanipour, A. Razmjou, Xylanase Immobilized on Novel Multifunctional Hyperbranched Polyglycerol-Grafted Magnetic Nanoparticles: An Efficient and Robust Biocatalyst, Langmuir. 31 (2015) 9219–9227.
[19] M. Royvaran, A. Taheri-Kafrani, A. Landarani Isfahani, S. Mohammadi, Functionalized superparamagnetic graphene oxide nanosheet in enzyme engineering: A highly dispersive, stable and robust biocatalyst, Chem. Eng. J. 288 (2016) 414–422.
[20] A. Soozanipour, A. Taheri-Kafrani, A. Landarani Isfahani, Covalent attachment of xylanase on functionalized magnetic nanoparticles and determination of its activity and stability, Chem. Eng. J. 270 (2015) 235–243.
[21] J.S. Van Dyk, B.I. Pletschke, A review of lignocellulose bioconversion using enzymatic hydrolysis and synergistic cooperation between enzymes--factors affecting enzymes, conversion and synergy., Biotechnol. Adv. 30 (2012) 1458–1480.
[22] S.L. Tsai, M. Park, W. Chen, Size-modulated synergy of cellulase clustering for enhanced cellulose hydrolysis, Biotechnol. J. 8 (2013) 257–261.
[23] T. Honda, T. Tanaka, T. Yoshino, Stoichiometrically Controlled Immobilization of Multiple Enzymes on Magnetic Nanoparticles by the Magnetosome Display System for Efficient Cellulose Hydrolysis, Biomacromolecules. 16 (2015) 3863–3868.
[24] G.L. Miller, Use of dinitrosaIicyIic acid reagent for determination of reducing sugar, Anal. Chem. 31 (1959) 426–428.
[25] C.K. Jue, P.N. Lipke, Determination of reducing sugars in the nanomole range with tetrazolium blue, J. Biochem. Biophys. Methods. 11 (1985) 109–115.
[26] M. Sajjad, M.I.M. Khan, N.S. Akbar, S. Ahmad, I. Ali, M.W. Akhtar, Enhanced

expression and activity yields of *Clostridium thermocellum* xylanases without non-catalytic domains., J. Biotechnol. 145 (2010) 38–42.

[27] D. Irwin, E.D. Jung, D.B. Wilson, Characterization and sequence of a *Thermomonospora fusca* xylanase., Appl. Environ. Microbiol. 60 (1994) 763–770.

[28] G.A.L. Gonçalves, Y. Takasugi, L. Jia, Y. Mori, S. Noda, T. Tanaka, H. Ichinose, N. Kamiya, Synergistic effect and application of xylanases as accessory enzymes to enhance the hydrolysis of pretreated bagasse, Enzyme Microb. Technol. 72 (2015) 16–24.

[29] L. Jia, G.A.L. Gonçalves, Y. Takasugi, Y. Mori, S. Noda, T. Tanaka, H. Ichinose, N. Kamiya, Effect of pretreatment methods on the synergism of cellulase and xylanase during the hydrolysis of bagasse, Bioresour. Technol. 185 (2015) 158–164.

[30] J. Hu, V. Arantes, A. Pribowo, J.N. Saddler, The synergistic action of accessory enzymes enhances the hydrolytic potential of a "cellulase mixture" but is highly substrate specific., Biotechnol. Biofuels. 6 (2013) 112.

[31] A. Pollet, J. a Delcour, C.M. Courtin, Structural determinants of the substrate specificities of xylanases from different glycoside hydrolase families., Crit. Rev. Biotechnol. 30 (2010) 176–191.

[32] J. Beaugrand, G. Chambat, V.W.K. Wong, F. Goubet, C. Rémond, G. Paës, S. Benamrouche, P. Debeire, M. O'Donohue, B. Chabbert, Impact and efficiency of GH10 and GH11 thermostable endoxylanases on wheat bran and alkali-extractable arabinoxylans., Carbohydr. Res. 339 (2004) 2529–2540.

[33] E.J. Taylor, N.L. Smith, J.P. Turkenburg, S. D'Souza, H.J. Gilbert, G.J. Davies, Structural insight into the ligand specificity of a thermostable family 51 arabinofuranosidase, Araf51, from *Clostridium thermocellum.*, Biochem. J. 395 (2006) 31–37.

[34] F. Rusmini, Z. Zhong, J. Feijen, Protein immobilization strategies for protein biochips, Biomacromolecules. 8 (2007) 1775–1789.

[35] B. Johnsson, S. Löfås, G. Lindquist, Immobilization of Proteins to a Carboxymethyldextran-Modified Gold Surface for Biospecific Interaction Analysis in Surface Plasmon Resonance Sensors, Anal. Biochem. 198 (1991) 268–277.

[36] J. Kong, S. Yu, Fourier transform infrared spectroscopic analysis of protein secondary structures, Acta Biochim. Biophys. Sin. (Shanghai). 39 (2007) 549–559.

[37]U. Hanefeld, L. Gardossi, E. Magner, Understanding enzyme immobilisation, Chem. Soc. Rev. 38 (2009) 453–468.

[38] J. Jordan, C. Theegala, Probing the limitations for recycling cellulase enzymes immobilized on iron oxide (Fe3O4) nanoparticles, Biomass Convers. Biorefinery. 4 (2014) 25–33.

[39] J. Jordan, C.S.S.R. Kumar, C. Theegala, Enzymatic Preparation and characterization of cellulase-bound magnetite nanoparticles, J. Mol. Catal. B Enzym. 68 (2011) 139–146.

Chapter 4 Construction of a novel polymeric proteinaceous scaffold for ratio-controllable binary artificial hemicellulosome

1. Introduction

1.1 Synergistic action by assembling enzymes on a scaffold

Cellulosome, secreted by some anaerobic cellulolytic microorganisms, a natural huge enzyme assembly mediated by cohesin-dockerin interaction, has attracted much attention in the area of biocatalysis and bioengineering. Since a number of enzymes locate closely on a protein scaffold, the proximity of enzymes enables high synergistic effect to accelerate a specific reaction rate [1]. With the advancement of genetic engineering and conjugation technologies, artificial cellulosomes have been proposed to mimic this natural enzyme assembly [2,3]. A common strategy is to carefully design the spatial organization of enzymes to decrease the distance between two protein components and avoid the reactants diffusing to the bulk solution, as a consequence, promote the kinetic driving force that facilitates the reaction (Fig. 4-2) [4].

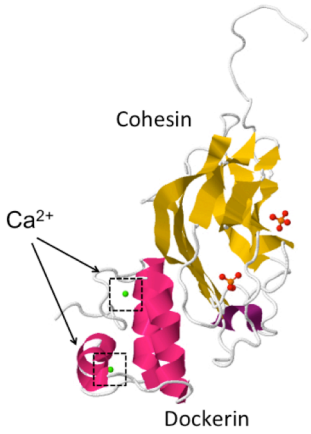

Fig. 4-1 Structure of cohesin-dockerin complex (PDB 2CCL).

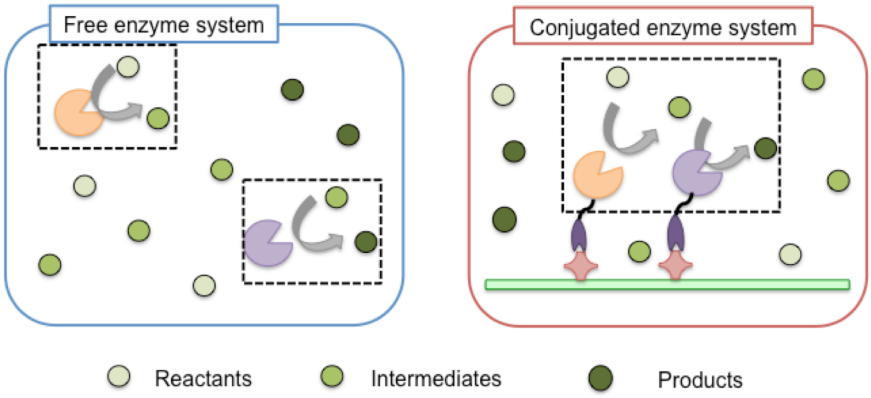

Fig. 4-2 Schematic illustration of free enzyme system and conjugated enzyme system.

1.2 Approaches of site-specific protein crosslinking

As described in introduction, a variety of chemical methodologies are proposed to crosslink

proteins, however, careful selection of chemistry is required to avoid the structural perturbation during the protein crosslinking process. Compared to the chemical coupling reaction, enzyme mediated crosslinking approaches are mild and site-specific [5]. Several potential catalytic tools for site-specific protein crosslinking, listed below, have been introduced in biotechnological fields.

1.2.1 Sortase A

In addition to the cohesin-dockerin system, other approaches for modulating enzyme and scaffold have also been demonstrated. Sortase A catalyzes the crosslinking reaction by cleaving between threonine and glycine in a C-terminal LPXTG motif and forming a peptide bond with an N-terminal polyglycine tag of another molecule [6]. Previous studies have shown the conjugation of bio-macromolecules like enzymes, antibody, aptamer on to protein nanoparticles [7], polystyrene nanoparticles [8] through the catalysis of sortase A.

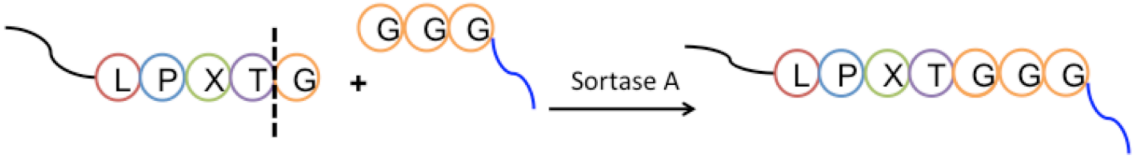

Fig. 4-3 Schematic diagram of Sortase A-catalyzed crosslinking reaction.

1.2.2 Transglutaminase

Another widely used strategy is transglutaminase-mediated conjugation of protein, where catalyzing acyl transfer between acyl-donor glutamine and acceptor lysine residues of proteins and form the isopeptide bond [9]. Mori and coworkers have conjugated an endoglucanase containing a transglutaminase recognizable lysine tag (MRHKGS) onto DNA scaffold containing benzyloxycarbonyl-L-glutaminylglycine moieties (Z-QG) via microbial transglutaminase catalysis, and obtained 5.7-fold improvement of reducing sugars than free enzyme did [10].

Fig. 4-4 The acyl transfer reaction between glutamine and lysine catalyzed by transglutaminase (TGase).

Avidin is a tetrameric protein existed in chicken egg white, it forms a stable non-covalent bond (K_d = 10^{-13} – 10^{-15} M) with its small molecule partner, biotin. One streptavidin is capable for binding four molecules of biotin [11]. This technique is widely used in affinity chromatography for protein purification, and the signal amplification for enzyme-linked immunosorbent assay (ELISA), immunoprecipitation, cell-surface labeling and so on. Recently, Mori *et al*. have labeled an endoglucanase Cel5A and a cellulose-binding module (CBM) with a newly designed tetra-biotin ligand by transglutaminase-mediated crosslinking reaction, and then constructed self-assembled one-dimensional enzyme conjugates [12]. The saccharification efficiency was improved 2.6-fold by assembling different protein units compared to the free enzymes.

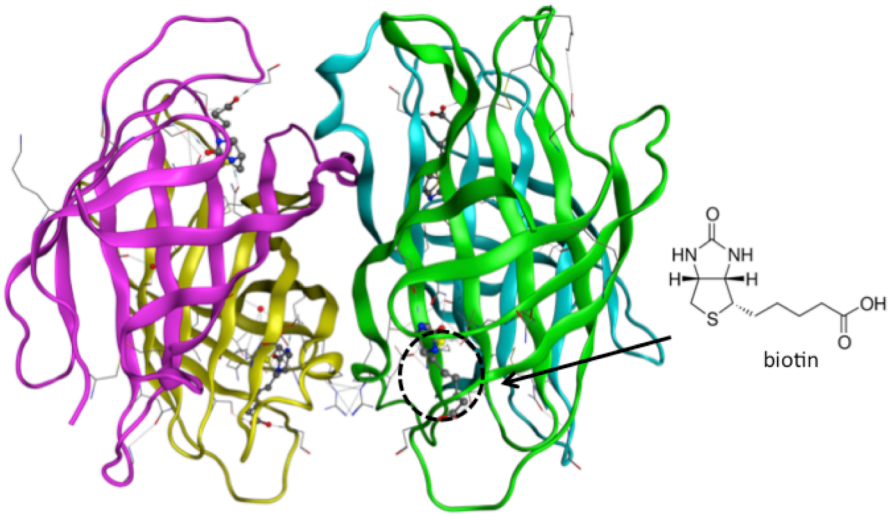

Fig. 4-5 Structure of streptavidin and biotin. (PDB 2AVI)

1.2.3 Horseradish peroxidase

Horseradish peroxidase (HRP) is one of most important enzymes that widely used in many biochemical and biomedical area [13]. The enzyme catalyzes the redox reactions between hydrogen peroxide and a reducing substrate, such as aromatic phenols, phenolic acids, indoles, amines and sulfonates [14]. HRP contains Fe(III) protoporphyrin IX (referred as heme group) and two calcium ions. The heme group is non-covalently attached through the coordination of His^{170} to the iron center and the carboxylate side-chain of Asp^{247} helps to control imidazolate character of His^{170} ring [15]. The mechanism of HRP that catalyzes the reducing substrate in the presence of H_2O_2 is:

$$H_2O_2 + 2AH_2 \rightarrow 2H_2O + 2AH\bullet$$

where, AH_2 and AH• represent a reducing substrate and its radical product, respectively [13].

Recently, HRP has been used in site-specific crosslinking of functional proteins.

Minamihata and coworkers constructed a hyperbranched protein G polymer by crosslinking two Tyr-containing tags (Y-tag, GYGGGG at N- termini and GGGGY at C-termini) fused with protein G [16].

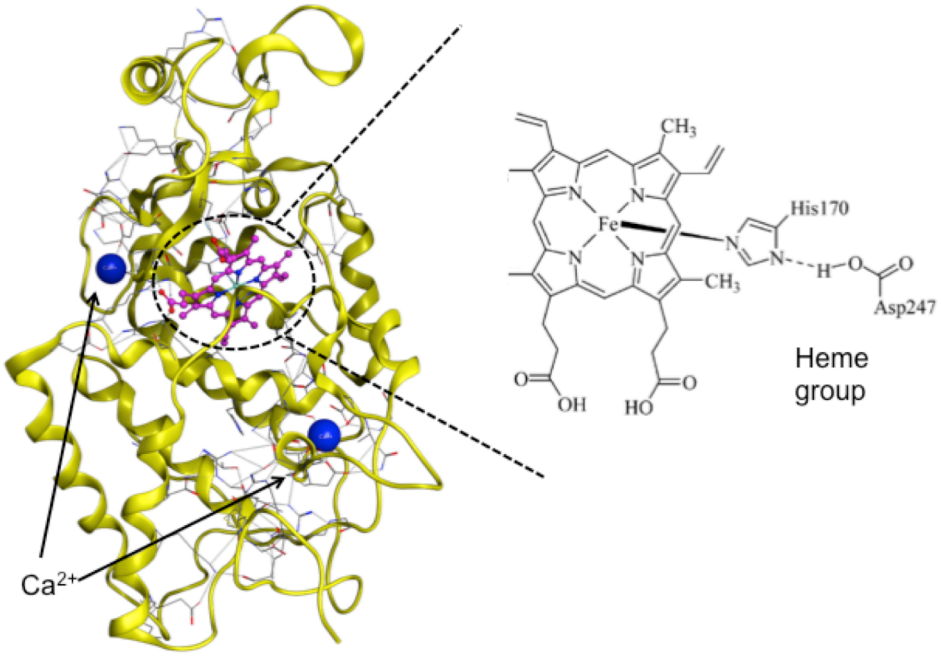

Fig. 4-6 Structure of HRP and heme group (PDB 1H5A).

1.2.4 SpyCatcher/SpyTag system

Recently, another protein ligation system has been explored in biology from *Streptococcus pyogenes*, so-called SpyCatcher-SpyTag, a 14 kDa protein and 13-amino acid-residue peptide (sequence: AHIVMVDAYKPTK) [17]. The isopeptide bond would be formed spontaneously between the lysine residue (Lys^{31}) of SpyCatcher and asparatic acid (Asp^{117}) residue of SpyTag under a wide range of temperatures, pH values and buffer types by simply mixing SpyCatcher and SpyTag. The conjugation examples that employs SpyCatcher-SpyTag including hydrogel preparation [18], protein cyclization [19] and immobilization of enzyme on cell [20]. However, it has not yet been sufficiently explored in the application for the design of new biocatalysts, despite the ease of the conjugation technique.

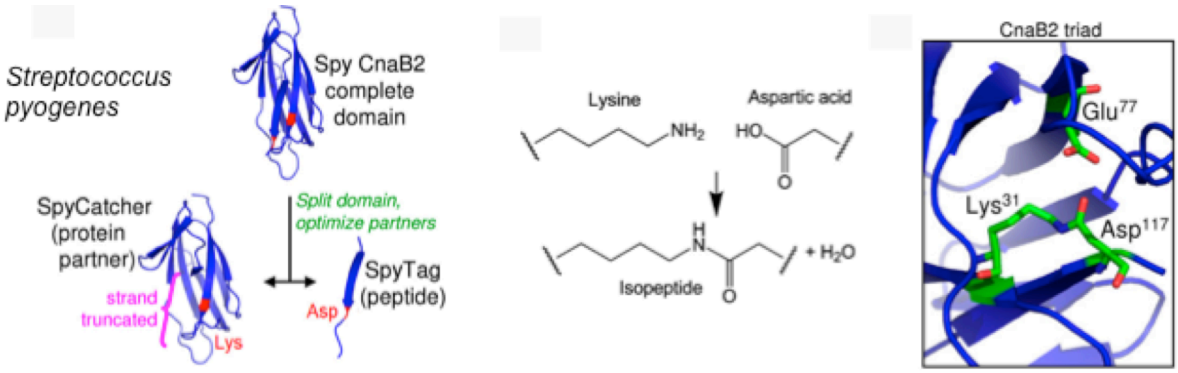

Fig.4-7 Schematic illustration of isopeptide formation between SpyCatcher and SpyTag [17]

17-Reprinted from Proc. Natl. Acad. Sci. U.S.A Vol. 109, Zakeri et al., peptide tag forming a rapid covalent bond to a protein, through engineering a backerial adhesin., Copyright 2012, with permission from National Academy of Sciences.

1.3 Objective of this chapter

Most of natural scaffolds observed in cellulosomal system contain about six to nine cohesins. Recently, it was shown that enzymes conjugated on a longer scaffold presenting nine cohesin modules exhibited better synergistic effect than a truncated scaffold that contains two cohesin modules in the hydrolysis of Avicel [21]. However, expression of a large recombinant scaffold protein in a standard host organism is difficult because of the difficulty of proper protein folding and the full retention of protein function.

In this chapter, a SpyCatcher polymer scaffold was prepared by using HRP-catalyzed crosslinking reaction, and the potential of this protein polymer as a scaffold of artificial hemicellulosome was validated. Several SpyTagged proteins, green fluorescence protein (GFP-ST), xylanase (XynZ-ST) and arabinofuranosidase (Araf51A-ST) from *Clostridium thermocellum* were successfully expressed. The SpyCatcher polymer prepared by HRP-catalyzed Y-tag mediated protein polymerization was conducted (Step 1, Fig. 4-8). The SpyTagged proteins were then assembled onto the SpyCatcher polymer scaffold via SpyCatcher-SpyTag interaction (Step 2, Fig. 4-8). Finally, the catalytic efficiency of this artificial hemicellulosome in hydrolysis of soluble arabinoxylan was investigated.

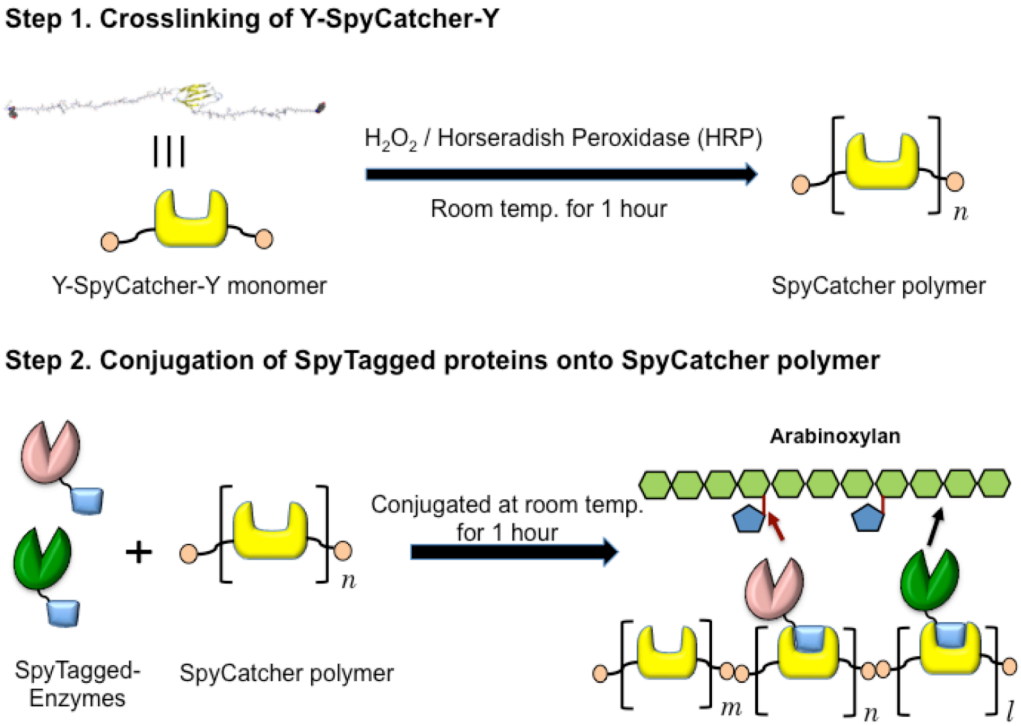

Fig. 4-8 Schematic illustration of the formation of SpyCatcher polymer by HRP reaction and fabrication of artificial cellulosome via SpyCatcher-SpyTag interaction

2. Materials and Methods

2.1 Expression and purification of recombinant proteins

The recombinant plasmids carrying the genes of Y-SpyCatcher-Y, EGFP-ST, XynZ-ST and Araf51A-ST were constructed by Dr. Kosuke Minamihata in Kyushu University.

E. coli strain BL21 (DE3) was transformed with the expression plasmids for each proteins and inoculated onto Luria–Bertani (LB) agar medium supplemented with ampicillin (100 mg/L) and grown overnight. A single colony was picked up and inoculated into 3.5 mL of LB medium containing the same antibiotics and cultured for overnight with shaking (180 rpm) at 37 °C. The overnight culture was transferred into 500 mL or 1 L of Terrific Broth (TB) medium supplemented with ampicillin (100 mg/L). Cells were grown with shaking (180 rpm) at 37 °C until the OD600 reached a value of 0.8. The culture was then cooled to 17 °C with addition of isopropyl β-D-1-thiogalactopyranoside at a concentration of 1 mM and kept culturing with shaking at 150 rpm for overnight. The cells were then harvested by centrifugation at 3500 ×*g* for 10 min, and washed with PBS three times. Finally, the washed cells were resuspended in 10 mM sodium phosphate buffer (pH 7.4), and kept at −20 °C until use.

The cell suspension was thawed on ice and disrupted by sonication in an ice-cold water bath for 10 min with a cooling period of 5 min after first 5 min of sonication. After removing the cell debris by centrifugation at 10,000 ×*g* for 15 min, cell-free supernatants were filtered through a 0.45 μm membrane followed by a 0.22 μm membrane filter. Then the filtered supernatants were undergone His-tag affinity chromatography using HisTrap HP column from GE Healthcare BioSciences (Uppsala, Sweden) at 4 °C. Fractions containing target protein were collected and desalted into 10 mM sodium phosphate buffer (pH 7.4) on PD-10 Sepharose columns. The desalted solution was further purified by anion-exchange chromatography using HiTrap Q HP column (GE Healthcare BioSciences, Uppsala, Sweden). All chromatography experiments were conducted on a BioLogic DuoFlow chromatography system (Bio-Rad Laboratories, Inc., Hercules, CA, USA). The concentrations of purified proteins were measured using bicinchoninic acid assay (BCA assay, Thermo Fisher Scientific, Rockford, IL, USA).

2.2 The crosslinking reaction of Y-SpyCatcher-Y by HRP reaction and Conjugation of protein onto SpyCatcher-polymer

Thirty micromolar of Y-SpyCatcher-Y was mixed with appropriate amount of HRP and H_2O_2 to induce the crosslinking reaction in 10 mM Tris-HCl (pH8.0). The mixture was incubated at room temperature for 1 h, and the samples were analyzed by SDS-PAGE.

To construct the artificial cellulosome, 3 μM of enzyme(s), XynZ-ST and/or Araf51A-ST, were conjugated onto 15 μM of SpyCatcher polymer at ratio of 4:1, 2:1, 1:1, 1:2, 1:4, in 50 mM phosphate buffer (pH 7.0) under room temperature for 1 hour.

2.3 Characterization of SpyCatcher polymer

The confirmation of SpyCatcher polymer was done by using size-exclusion chromatography (SEC). The samples, Y-SpyCatcher-Y monomer and SpyCatcher polymer, were separately subjected to SEC column of HiLoad 16/600 Superdex 200 pg (GE Healthcare BioSciences, Uppsala, Sweden). The peaks of Y-SpyCatcher-Y monomer and SpyCatcher polymer were monitored under 280 nm.

To investigate the binding capacity of SpyCatcher polymer, 100 μM of GFP-ST was mixed with 20 μM of SpyCatcher polymer in 50 mM phosphate buffer (pH 7.0) under room temperature for 1 hour in dark room. Afterwards, the extra amount of GFP-ST was removed by SEC, and the high molecular weight fraction was collected. The SpyCatcher polymer was incubated with HRV 3C (Takara Bio Inc.) and thrombin (Wako Pure chemical Industries, Ltd., Japan) at loading of 0.5 U/10 μg protein in 10 mM Tris-HCl (pH 8.0) at 4 °C for overnight.

The capacity was estimated by comparing the band intensities of GFP-ST conjugated SpyCatcher monomer and un-conjugated SpyCatcher monomer in SDS-PAGE analysis by using the software of YabGelImage based on the following equation:

$$\text{Binding capacity of SpyCatcher polymer} = (I_{GSC} / Mw_{GSC}) / (I_{GSC} / Mw_{GSC} + I_{SC} / Mw_{SC}) \times 100\%$$

where I_{GSC} and I_{SC} represent the band intensities of GFP-SpyCatcher monomer and SpyCatcher monomer estimated by YabGelImage, respectively. Mw_{GSC} and Mw_{SC} are the molecular weights of GFP-conjugated SpyCatcher monomer and unbounded Y-SpyCatcher-Y monomer, respectively.

2.4 Enzymatic activity assay of free and conjugated enzyme

The activity of free enzyme and conjugated enzyme was evaluated by hydrolysis experiments with 0.25 wt% of the model substrate, xylan from beechwood (Tokyo Chemical Industry, CO. Ltd., Japan), at 50 °C in 2 mL of sodium phosphate buffer (50 mM, pH 7.0) and placed in a rotary shaker (TAITEC MBR-022UP, Japan) at 1000 rpm. After hydrolysis, the amount of produced reducing sugars were measured by the dinitrosalicylic acid method (DNS assay) with xylose as standard [22]. One unit of xylanase activity is defined as the amount of enzyme that produces 1 μmol of reducing sugars per minute.

2.5 The enzymatic hydrolysis of free and conjugated enzyme on arabinoxylan

The saccharification experiments were carried out with 0.25 wt% of soluble arabinoxylan (low viscosity, Megazyme, Wicklow, Ireland), under a final volume of 500 μL in sodium phosphate buffer (50 mM, pH 7.0). The enzyme loadings were 30 nM, respectively. After hydrolysis reaction at 50 °C for 10 min, 30 min, 1 h, 2 h and 3 h, the concentrations of the reducing sugars were analyzed by using tetrazolium blue (TZ) assay [23]. Also, after hydrolysis reaction of 3 h, the composition of soluble sugars were analyzed by high-performance liquid chromatography (HPLC) with a Shodex sugar KS-801 column (8.0×300 mm, Showa Denko Co., Tokyo, Japan) and a refractive index detector at 80 °C with HPLC-grade water as the eluent at a flow rate of 1 mL/min.

3. Results and Discussion

3.1 HRP-mediated crosslinking reaction of Y-SpyCatcher-Y to obtain SpyCatcher polymer

Y-SpyCatcher-Y was designed to have two Y-tags (YGGGG at N-termini and GGGGY at C-termini), flanked by digestive sequences recognized by human rhinovirus 3C (HRV 3C)

protease and thrombin (Fig. 4-9).

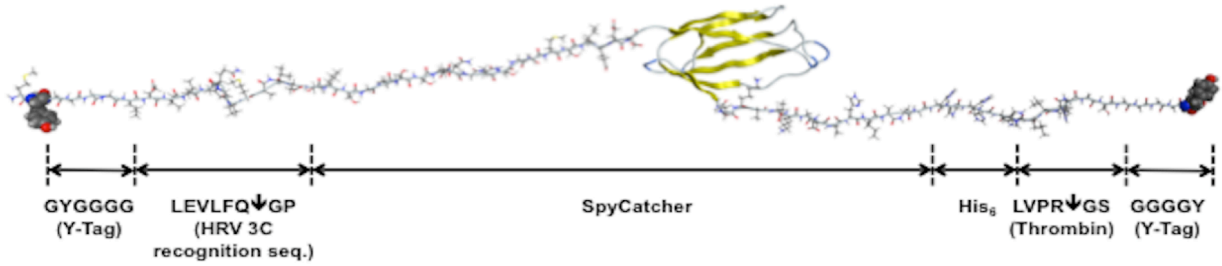

Fig. 4-9 Molecular image of Y-SpyCatcher-Y. The structure was produced by Molecular Operating Environment (MOE, version 2014.0901) software.

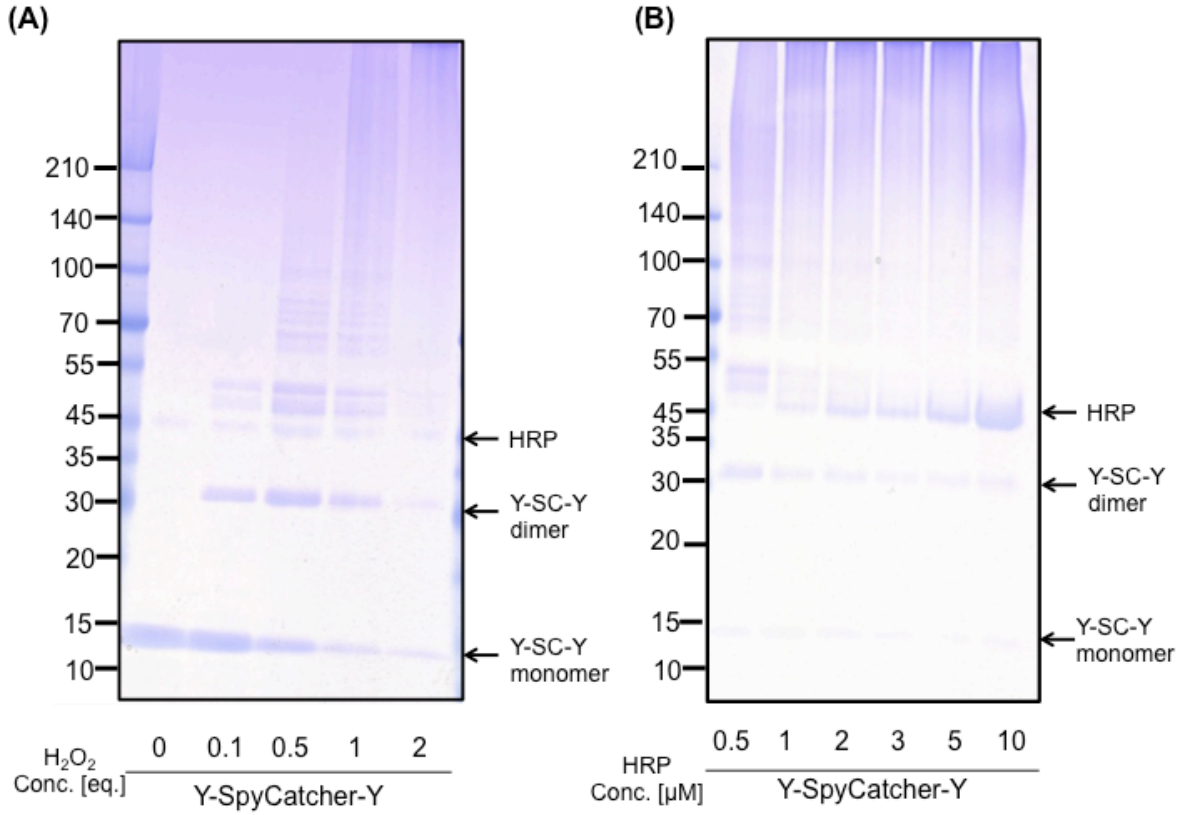

Fig. 4-10 Optimization of the H_2O_2 concentration (A) and Horseradish peroxidase concentration (B) of HRP-catalyzed tyrosine coupling reaction. The concentration of Y-SpyCatcher-Y monomer was 30 μM. All the experiment performed in 10 mM Tris-HCl buffer (pH 8.0) and under room temperature for 1 hour.

Firstly, the optimal condition of tyrosine coupling reaction catalyzed by HRP was investigated. It was revealed that 1 μM of HRP and 2 eq. (60 μM) of H_2O_2 against Y-SpyCatcher-Y were needed to completely crosslink 30 μM of Y-SpyCatcher-Y monomer

(Fig. 4-10). In the previous study, the amount of HRP and H_2O_2 needed to crosslink all of the dual Y-tagged protein G was 0.1 μM and 1 eq. against the Y-tagged protein G, respectively [16]. The difference of the optimum conditions of protein polymerization using HRP and Y-tag between this study and the previous study is probably due to the structural difference of the protein to be polymerized. Protein G displays its N- and C-termini at the completely opposite side of its structure, while SpyCatcher possesses N- and C-termini relatively in close position. Additionally, as shown in Fig. 4-9, Y-SpyCatcher-Y has very long additional Y-tag sequences, especially the N-terminal Y-tag, as a consequence of the flexible domains of SpyCatcher of- N- and C-termini, of which no tertiary structures were obtained (PDB ID of 4MLI). Thus it can be assumed that Y-SpyCatcher-Y might form intramolecular crosslinking between the two Y-tags at the N- and C-termini due to close proximity of the termini and also long and flexible Y-tags.

3.2 Characterization of the SpyCatcher polymer

Size-exclusion chromatography (SEC) was applied to further characterize the formation of SpyCatcher polymer. In a good agreement with the result of SDS-PAGE, the peak of Y-SpyCatcher-Y monomer in SEC disappeared after crosslinking reaction (Fig. 4-11).

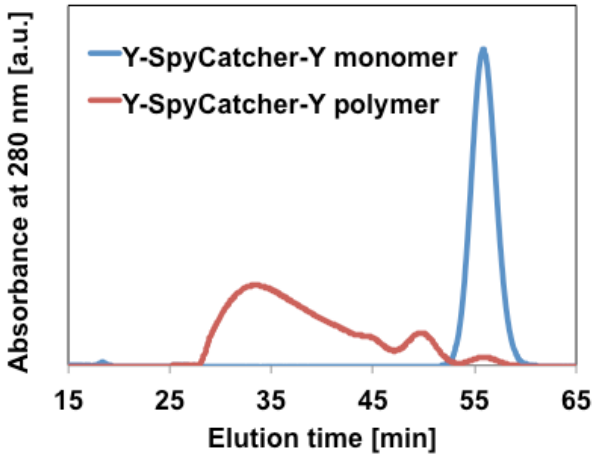

Fig. 4-11 The size-exclusion chromatography of Y-SpyCatcher-Y before and after crosslinking.

After the success of formation of SpyCatcher polymer, the binding capacity of SpyCatcher polymer for conjugation of SpyTagged protein molecules was evaluated. Green fluorescence protein fused with SpyTag (GFP-ST) was selected as a model. Excess amount of GFP-ST was added into the SpyCatcher solution. After that, unbound GFP-ST was separated by SEC and the higher molecular weight fraction was collected (Fig. 4-12, lane B). Protease treatments of both HRV 3C and thrombin on SpyCatcher polymer and GFP-conjugated SpyCatcher

polymer were conducted. After treated with protease, a main band at 15 kDa corresponding to SpyCatcher monomer, and some faint bands at around 30 kDa and 45 kDa, representing SpyCatcher dimer and trimer, respectively, were observed in digestion of SpyCatcher polymer (Fig. 4-12 lane C). This result showed that the treatment by HRV 3C and thrombin could efficiently digest the polymer into monomeric building blocks. Conversely, the treatment was applied to digest the GFP-SpyCatcher polymer. The formation of a major band corresponding to GFP conjugated on SpyCatcher monomer was observed (Fig. 4-12, lane A). Based on the rough comparison of band intensities between GFP-SpyCatcher monomer and SpyCatcher monomer, over 50% of GFP-ST was conjugated onto SpyCatcher polymer. This result suggests that the SpyCatcher polymer has the high loading capacity in conjugation of SpyTagged molecules.

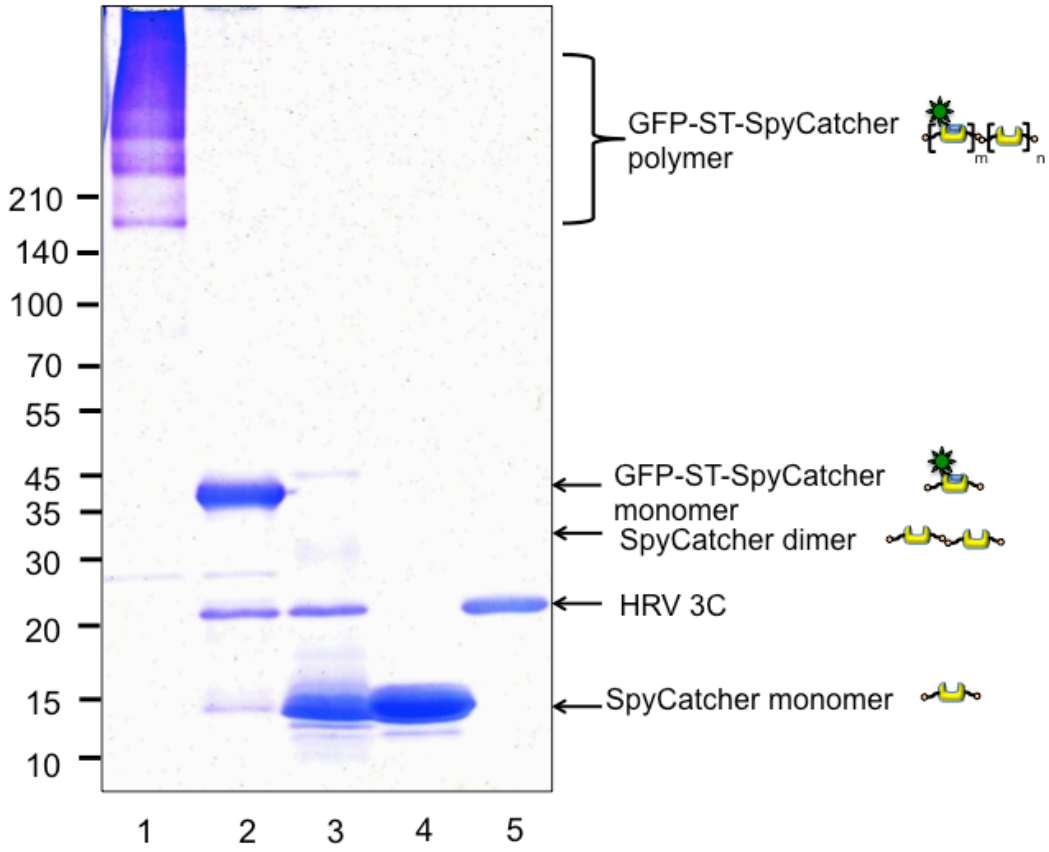

Fig. 4-12 The protease treatment of SpyCatcher polymer and GFP-conjugated SpyCatcher polymer. Lane 1, GFP-conjugated SpyCatcher polymer after SEC; lane 2, after HRV 3C and thrombin treated GFP-conjugated SpyCatcher polymer; lane 3, after HRV 3C and thrombin treated SpyCatcher polymer; lane 4, SpyCatcher monomer; lane 5, HRV 3C.

3.3 Application of SpyCatcher polymer as a scaffold of artificial hemicellulosome

The feasibility of SpyCatcher polymer as a scaffold of artificial hemicellulosome was

explored. SpyCatcher polymer and the SpyTagged enzyme, XynZ-ST, were mixed with different molar ratios to obtain the best conjugation efficiency. As shown in Fig. 4-13, the optimum ratio of XynZ-ST and SpyCatcher polymer was 1:5, requiring excess SpyCatcher for complete conjugation of XynZ-ST. Since the SpyCatcher polymer is in a hyperbranch-like structure and thus the SpyCatcher domains entangled inside of the polymer structure are not available for conjugation, the ratio of SpyCatcher to SpyTagged enzymes needed for complete conjugation of the enzymes was not exactly 1:1. Comparing with the result of conjugating GFP-ST (Fig. 4-12), more SpyCatcher polymer was needed for conjugation of XynZ-ST. This maybe due to the difference of molecular weight of these two proteins (XynZ-ST: 42 kDa; GFP-ST: 29 kDa), implying the binding capacity of SpyCatcher polymer is largely dependent on the size of conjugated protein.

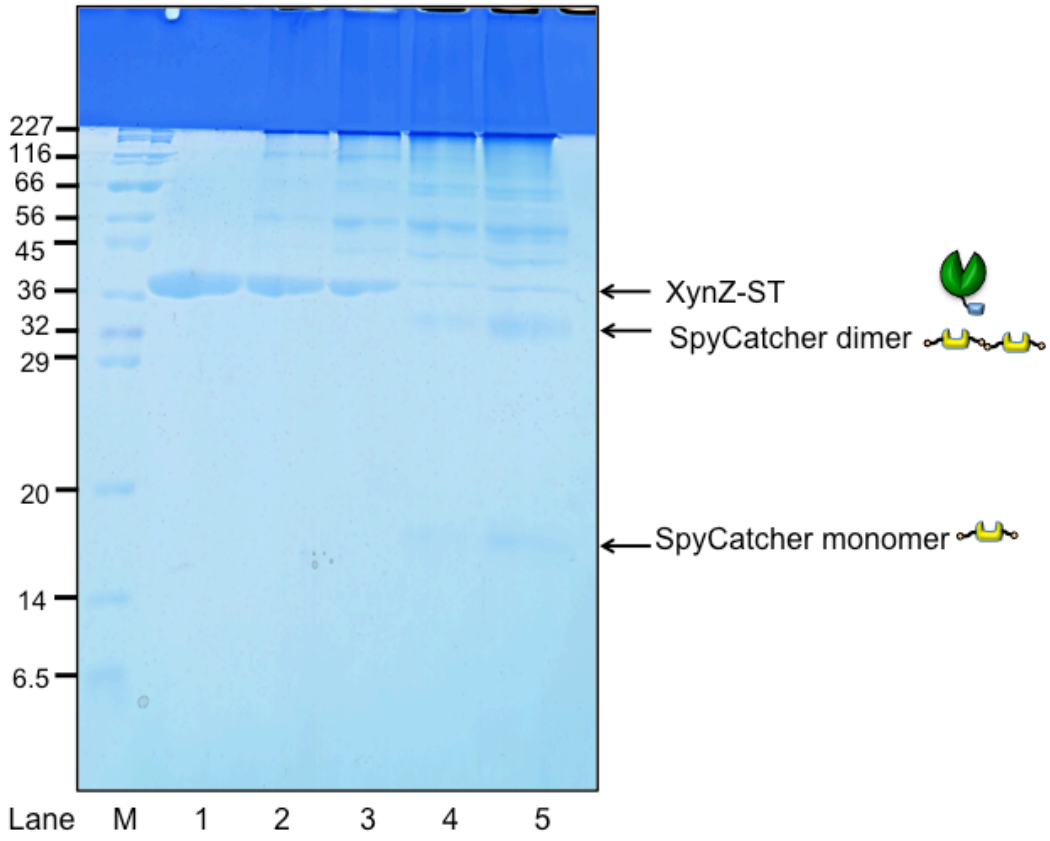

Fig. 4-13 The optimization of conjugation ratio of SpyTagged-XynZ and SpyCatcher polymer. Lane M, marker; Lane 1, SpyTagged XynZ; Lane 2, SpyTag-XynZ/SpyCatcher polymer = 1:1; Lane 3, SpyTag-XynZ/SpyCatcher polymer = 1:2; Lane 4, SpyTag-XynZ/SpyCatcher polymer = 1:5, Lane 5, SpyTag-XynZ/SpyCatcher polymer = 1:10.

After successful conjugation of XynZ-ST onto SpyCatcher polymer, the activity test of free XynZ-ST and the conjugated XynZ-ST onto SpyCatcher polymer was carried out (Table 1). Interestingly, after conjugated onto SpyCatcher polymer, the activity of XynZ-ST improved from 45.8 U/mg enzyme to 65.1 U/mg enzyme, indicating that this simple enzyme assembly not only has the same diffusion efficiency as single free enzyme, but also, to some extent, it can improve the production of reducing sugars in substrate hydrolysis. Previous reports also have shown the enhanced production of sugars by superamolecular enzyme assembly than the free enzymes. Mori *et al.* have site-specifically assembled tetrabiotin-labeled endoglucanase, Cel5A, and a carbohydrate binding module (CBM) onto streptavidin, and observed 2.6-fold improvement of overall Avicel degradation activity in the artificial cellulosome compared with unconjugated enzyme [25]. Recently, Chen and coworker conjugated endoglucanase CelA onto E2 core of the pyruvate dehydrogenase complex from *Bacillus stearothermophilus* by sortase A ligation. Similarly, the activity of CelA increased after conjugated to E2 [26]. The possible reason of the improvement of XynZ-ST activity after conjugated onto SpyCatcher polymer might be the spatial proximity between the enzymes, as a consequence, increase the local concentration of the enzymes attacking the polymeric substrate. Besides, the conjugated XynZ-ST showed similar activity loss as free enzyme during the heat treatment at 65 °C or 70 °C for 1 hour (Table 1). Taken together, the results showed that SpyTagged enzyme can be site-specifically conjugated onto SpyCatcher polymer scaffold and it has the possible capability to improve the enzymatic activity.

Table 4-1 The activity of free XynZ-ST and SpyCatcher polymer conjugated XynZ-ST on beechwood xylan after incubation at 65 °C and 70 °C for 1 hour

Enzyme activity (U/mg of enzyme)	No heat treatment	65 °C	70 °C
Free XynZ-ST	45.8 ± 13.2	40.7 ± 4.6	26.5 ± 5.0
Conjugated XynZ-ST	65.1 ± 12.3	53.1 ± 7.8	30.7 ± 3.3

Given that the identical affinity between SpyTag fused molecules to SpyCatcher, it can be expected that SpyCatcher polymer might be capable of assembling different molecules at arbitrary ratio. Two SpyTagged-hemicelluases, XynZ-ST and Araf51A-ST, were selected to conjugate on the present polymer scaffold. The ratio of SpyTagged enzymes to SpyCatcher polymer was kept at 1:5 as optimized before, the different ratio of XynZ-ST and Araf51A-ST was set and the conjugation with SpyCatcher polymer was evaluated. XynZ-ST and Araf51A-ST with different ratio (4:1, 2:1, 1:1, 1:2 and 1:4) were added into SpyCatcher

polymer solution, and the final concentrations of SpyTagged enzymes and SpyCatcher polymer were 3 μM and 15 μM, respectively. After 1 hour of conjugation at room temperature, the formation of two enzymes-polymer assembly was confirmed by SDS-PAGE (Fig. 4-14).

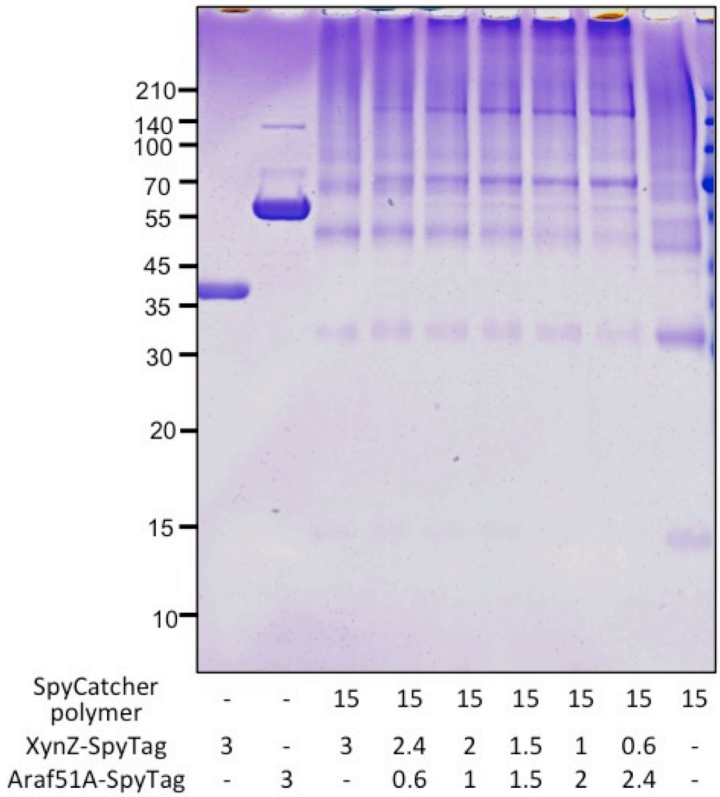

Fig. 4-14 SDS-PAGE of XynZ-ST and Araf51A-ST conjugated on SpyCatcher polymer. Lane 1, XynZ-ST; Lane 2, Araf51A-ST; Lane 3, XynZ-ST conjugated on SpyCatcher polymer; Lane 4 - 8, XynZ-ST and Araf51A-ST mixed with the molar concentration shown below and conjugated on SpyCatcher polymer; Lane 9, SpyCatcher polymer.

The assemblies with different XynZ-ST/Araf51A-ST ratio were then subjected to catalytic activity assay using soluble arabinoxylan as substrate. When the saccharification started the initial phase (10 minutes), for all the combinations, the conjugated enzyme(s) yielded higher amount of reducing sugars than free SpyTagged enzyme(s) (Fig. 4-15A). The reducing sugars conversion by conjugated XynZ-ST increased 45%, comparing with free XynZ-ST. This result was also in good agreement of the activity test as described earlier (Table 1), where the conjugated XynZ-ST showed higher activity than free XynZ-ST. Furthermore, the best improvement of reducing sugars production was the combination of XynZ-ST/Araf51A-ST=1:4, the concentration of reducing sugars increased 1.63-fold, after

the formation of artificial cellulosome. Conversely, after 3 hours of hydrolysis (Fig. 4-15B), combination of XynZ-ST/Araf51A-ST = 2:1, both free and conjugated, released highest reducing sugars, 5.3 mM and 5.6 mM, respectively. Similar as the result of 10 min, the combination of XynZ-ST/Araf51A-ST =1:4 again got the highest improvement (53%) after conjugated onto the SpyCatcher polymer.

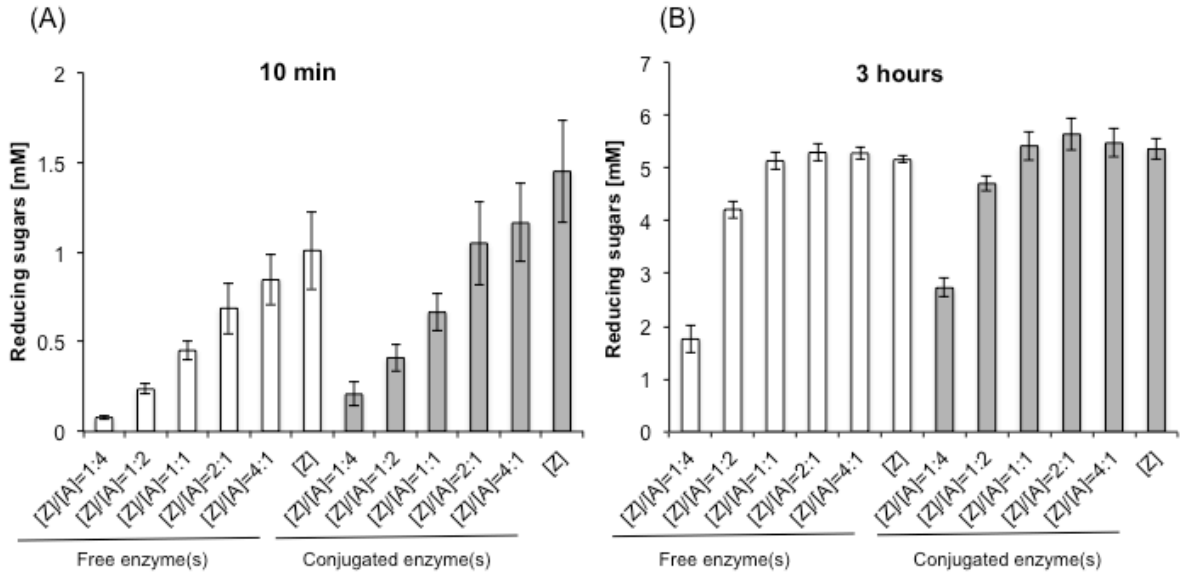

Fig. 4-15 Determination of reducing sugars concentration after (A) 10 min and (B) 3 h hydrolysis of soluble arabinoxylan by free or conjugated of SpyTagged-endoxylanases, XynZ-ST ([Z]), and SpyTagged-arabinofuranosidase, Araf51A-ST ([A]). The total enzyme loading was kept at 30 nM. The concentration of reducing sugars was measured by TZ assay with xylose as standard. The error bars represent the standard deviations from three independent trials.

Subsequently, the composition of soluble sugars released from the actions of XynZ-ST and Araf51A-ST on arabinoxylan was identified by HPLC analysis. Note that higher polymerized oligomers and substituted sugars have not been detected. The relationship between Araf51A-ST proportion and the production of soluble sugars, xylotriose, xylobiose, xylose and arabinose, during the hydrolysis of soluble arabinoxylan by free or conjugated enzymatic assemblies was shown (Fig. 4-16 and Fig. 4-17). Generally, the enzyme assemblies showed better conversion than free enzymes, when the proportion of Araf51A-ST was high. This observation is also in a good agreement with the reducing sugars conversion.

The release of xylotriose and xylose were proportionally decreased with the Araf51A-ST

percentage (Fig. 4-16). When using XynZ-ST alone, the main product in arabinoxylan hydrolysis was xylotriose. After 3 hours hydrolysis, free XynZ-ST and conjugated XynZ-ST obtained 0.50 mM and 0.57 mM of xylotriose, respectively. While the concentration of xylobiose and xylose were only around 0.3 mM and 0.2 mM, respectively, by either free or conjugated XynZ-ST (Fig. 4-16 and Fig. 4-17B).

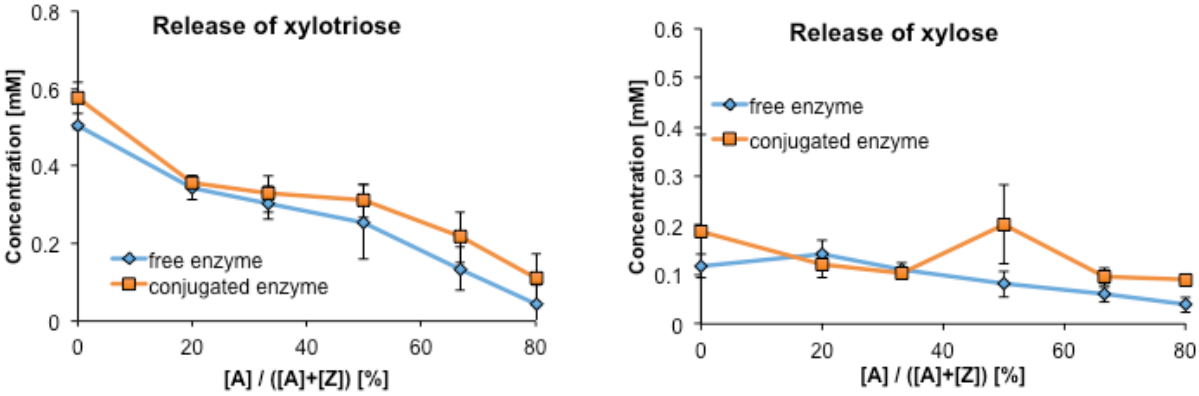

Fig. 4-16 The concentration of xylotriose and xylose after 3 h hydrolysis of soluble wheat arabinoxylan by free or conjugated enzymes, XynZ-ST ([Z]) and Araf51A-ST ([A]), measured by HPLC. The total enzyme loading was kept at 30 nM. The error bars represent the standard deviations from three independent trials.

In contrast, the release of xylobiose and arabinose showed a different trend. Initially, with the increase of arabinofuranosidase proportion, the concentration of xylobiose was increased and reached the plateau by the enzyme mixture containing 20% of Araf51A-ST (Fig. 4-17B). When the proportion of Araf51A-ST increased from 20% to 80%, the xylobiose converted by free enzymes dropped from 0.48 mM to 0.01 mM. However, in the case of conjugated enzymes, xylobiose concentration started to decrease only after Araf51A-ST proportion was over 50%. Conversely, in the case of released arabinose, the highest concentration (0.35 mM) was obtained by free enzyme mixture containing 20% of Araf51A-ST. Higher amount of arabinose (0.46 mM) was released by conjugated enzyme mixture containing 50% of Araf51A-ST.

As illustrated, the hydrolytic products released by XynZ-ST could classified as two parts, unsubstituted sugars and substituted sugars (Fig. 4-17A). The mainly released substituted sugar is A^2X, which is arabinose substituted at the non-reducing end of xylobiose [27]. As suggested from previous researches, the arabinofuranosidase used in current study,

Araf51A-ST, only has the activity on short oligomers rather than long polymer substrate [28,29]. Thus, the endo-type XynZ-ST depolymerzing arabinoxylan chain plays major role in the release of short oligomers from hydrolysis of arabinoxylan. When conjugate XynZ-ST and Araf51A-ST together, because of the proximity of Araf51A-ST to XynZ-ST, Araf51A-ST would not need to move a relatively longer distance to recognize its favorable substrates, which is generated by neighboring XynZ-ST. However, this advantage can be obvious only in the beginning of saccharification assay or in the case of low XynZ-ST proportion, since the products of XynZ-ST reaction dominate the soluble sugars produced in the solution.

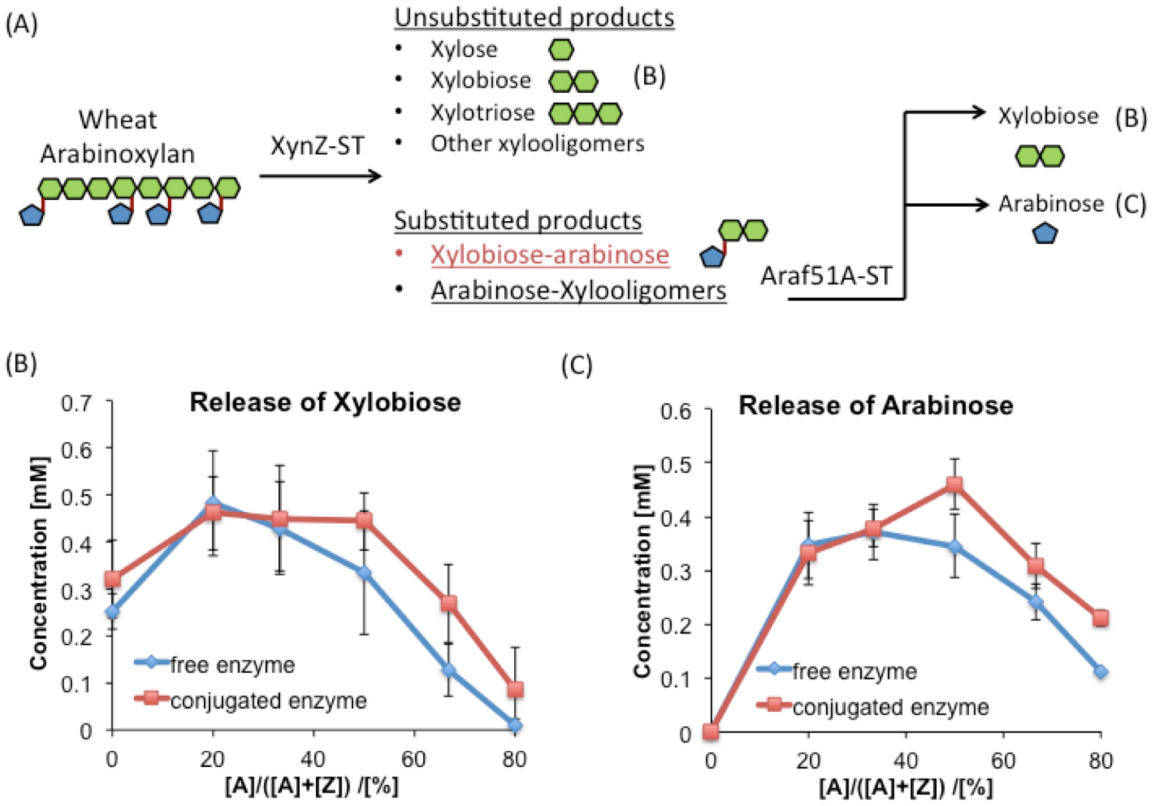

Fig. 4-17 (A) Schematic illustration of the hydrolytic products from action of XynZ-ST and Araf51A-ST on wheat arabinoxylan. The concentration of (B) xylobiose and (C) arabinose after 3 h hydrolysis of soluble wheat arabinoxylan by free or conjugated enzymes, XynZ-ST ([Z]) and Araf51A-ST ([A]), measured by HPLC. The total enzyme loading was kept at 30 nM. The error bars represent the standard deviations from three independent trials.

Taking the above-mentioned findings into consideration, it is confirmed that the functional SpyCatcher polymer possesses a promising potential as an artificial scaffold to assemble different kinds of enzymes. Further studies could be performed to apply this enzyme

assembly into the degradation of insoluble substrate and lignocellulosic biomass. Besides, it is also interesting to apply this functional protein assembly with careful design in other biochemical and biomedical area, such as improving the drug loading capacity [30] and the signal amplification for improving detection limit of enzyme-linked immunosorbent assay (ELISA) [31,32].

4. Conclusion

A feasible and functional crosslinked SpyCatcher polymer was constructed via HRP-mediated protein crosslinking reaction. The present proteinaceous polymer possesses the advance of site-specific interaction between SpyCatcher-SpyTag, thus a variety of molecules fused with SpyTag, including fluorescence protein and enzymes, could be easily conjugated onto this polymer. The potential applications of this SpyCatcher polymer as an artificial scaffold were explored. The proximity after enzyme site-specifically conjugated onto protein scaffold showed enhanced sugars conversion, especially at the low concentration of intermediate substrate. These remarkable improvements revealed that the SpyCatcher polymer owns a promising future that can be widely used in biochemical and biomedical area.

Reference

[1] E.A. Bayer, R. Lamed, M.E. Himmel, The potential of cellulases and cellulosomes for cellulosic waste management, Curr. Opin. Biotechnol. 18 (2007) 237–245.

[2] G. Gonçalves, Y. Mori, N. Kamiya, Biomolecular assembly strategies to develop potential artificial cellulosomes, Sustain. Chem. Process. 2 (2014) 19.

[3] S.P. Smith, E. a Bayer, Insights into cellulosome assembly and dynamics: from dissection to reconstruction of the supramolecular enzyme complex., Curr. Opin. Struct. Biol. 23 (2013)

[4] R. Chen, Q. Chen, H. Kim, K. Siu, Q. Sun, S. Tsai, W. Chen, Biomolecular scaffolds for enhanced signaling and catalytic efficiency, Curr. Opin. Biotechnol. 28 (2014) 59–68.

[5] S. Avvakumova, M. Colombo, P. Tortora, D. Prosperi, Biotechnological approaches toward nanoparticle biofunctionalization, Trends Biotechnol. 32 (2014) 11–20.

[6] H. Ton-That, G. Liu, S.K. Mazmanian, K.F. Faull, O. Schneewind, Purification and characterization of sortase, the transpeptidase that cleaves surface proteins of Staphylococcus aureus at the LPXTG motif., Proc. Natl. Acad. Sci. U. S. A. 96 (1999) 12424–12429.

[7] Q. Sun, Q. Chen, D. Blackstock, W. Chen, Post-Translational Modification of Bionanoparticles as a Modular Platform for Biosensor Assembly, ACS Nano. 9 (2015) 8554–8561.

[8] Y. Hata, T. Matsumoto, T. Tanaka, A. Kondo, C-Terminal-oriented Immobilization of Enzymes Using Sortase A-mediated Technique, Macromol. Biosci. 15 (2015) 1375–1380.

[9] M. Kitaoka, M. Mitsumori, K. Hayashi, Y. Hiraishi, H. Yoshinaga, K. Nakano, K. Miyawaki, S. Noji, M. Goto, N. Kamiya, Transglutaminase-Mediated in Situ Hybridization (TransISH) System: A New Methodology for Simplified mRNA Detection, Anal. Chem. 84 (2012) 5885–5891.

[10] Y. Mori, S. Ozasa, M. Kitaoka, S. Noda, T. Tanaka, H. Ichinose, N. Kamiya, Aligning an endoglucanase Cel5A from Thermobifida fusca on a DNA scaffold: potent design of an artificial cellulosome., Chem. Commun. (Camb). 49 (2013) 6971–6973.

[11] E.P. Diamandis, T.K. Christopoulos, The biotin-(strept)avidin system: principles and applications in biotechnology., Clin. Chem. 37 (1991) 625–636.

[12] Y. Mori, H. Nakazawa, G.A.L. Gonçalves, T. Tanaka, M. Umetsu, N. Kamiya, One-dimensional assembly of functional proteins: toward the design of an artificial cellulosome, Mol. Syst. Des. Eng. 22 (2016).

[13] N.C. Veitch, Horseradish peroxidase: A modern view of a classic enzyme, Phytochemistry. 65 (2004) 249–259.

[14] N.E. Domeradzka, M.W. Werten, F.A. de Wolf, R. de Vries, Protein cross-linking tools

for the construction of nanomaterials, Curr. Opin. Biotechnol. 39 (2016) 61–67.
[15] A.M. Azevedo, V.C. Martins, D.M.F. Prazeres, V. Vojinović, J.M.S. Cabral, L.P. Fonseca, Horseradish peroxidase: A valuable tool in biotechnology, Biotechnol. Annu. Rev. 9 (2003) 199–247.
[16] K. Minamihata, S. Yamaguchi, K. Nakajima, T. Nagamune, Tyrosine Coupling Creates a Hyperbranched Multivalent Protein Polymer Using Horseradish Peroxidase via Bipolar Conjugation Points, Bioconjug. Chem. 27 (2016) 1348–1359.
[17] B. Zakeri, J.O. Fierer, E. Celik, E.C. Chittock, U. Schwarz-Linek, V.T. Moy, M. Howarth, Peptide tag forming a rapid covalent bond to a protein, through engineering a bacterial adhesin., Proc. Natl. Acad. Sci. U. S. A. 109 (2012) E690–E697.
[18] F. Sun, W.-B. Zhang, A. Mahdavi, F.H. Arnold, D.A. Tirrell, Synthesis of bioactive protein hydrogels by genetically encoded SpyTag-SpyCatcher chemistry., Proc. Natl. Acad. Sci. U. S. A. 111 (2014) 11269–11274.
[19] J. Wang, Y. Wang, X. Wang, D. Zhang, S. Wu, G. Zhang, Enhanced thermal stability of lichenase from *Bacillus subtilis* 168 by SpyTag/SpyCatcher-mediated spontaneous cyclization, Biotechnol. Biofuels. 9 (2016) 79.
[20] Z. Botyanszki, P.K.R. Tay, P.Q. Nguyen, M.G. Nussbaumer, N.S. Joshi, Engineered Catalytic Biofilms : Site-Specific Enzyme Immobilization onto E . coli Curli Nanofibers, Biotechnol. Bioeng. 112 (2016) 2016–2024. d
[21] K. Hirano, S. Nihei, H. Hasegawa, M. Haruki, N. Hirano, Stoichiometric Assembly of Cellulosome Generates Maximum Synergy for the Degradation of Crystalline Cellulose, as Revealed by *In Vitro* Reconstitution of the *Clostridium thermocellum* Cellulosome., Appl. Environ. Microbiol. 81 (2015) AEM.00772-15.
[22] G.L. Miller, Use of dinitrosaIicyIic acid reagent for determination of reducing sugar, Anal. Chem. 31 (1959) 426–428.
[23] C.K. Jue, P.N. Lipke, Determination of reducing sugars in the nanomole range with tetrazolium blue, J. Biochem. Biophys. Methods. 11 (1985) 109–115.
[24] H.P. Erickson, Size and shape of protein molecules at the nanometer level determined by sedimentation, gel filtration, and electron microscopy, Biol. Proced. Online. 11 (2009) 32–51.
[25] Q. Sun, W. Chen, HaloTag mediated artificial cellulosome assembly on a rolling circle amplification DNA template for efficient cellulose hydrolysis, Chem. Commun. 52 (2016). 6701–6704.
[26] Q. Chen, Q. Sun, N.M. Molino, S.-W. Wang, E.T. Boder, W. Chen, Sortase A-mediated multi-functionalization of protein nanoparticles, Chem. Commun. 51 (2015) 12107–12110.
[27] A. Pollet, J. a Delcour, C.M. Courtin, Structural determinants of the substrate

specificities of xylanases from different glycoside hydrolase families., Crit. Rev. Biotechnol. 30 (2010) 176–191.
[28] E.J. Taylor, N.L. Smith, J.P. Turkenburg, S. D'Souza, H.J. Gilbert, G.J. Davies, Structural insight into the ligand specificity of a thermostable family 51 arabinofuranosidase, Araf51, from *Clostridium thermocellum.*, Biochem. J. 395 (2006) 31–37.
[29] L. Jia, G.A.L.G. Budinova, Y. Takasugi, S. Noda, T. Tanaka, H. Ichinose, M. Goto, N. Kamiya, Synergistic degradation of arabinoxylan by free and immobilized xylanases and arabinofuranosidase, Biochem. Eng. J. 114 (2016) 268–275.
[30] K. Cai, X. He, Z. Song, Q. Yin, Y. Zhang, F.M. Uckun, C. Jiang, J. Cheng, Dimeric Drug Polymeric Nanoparticles with Exceptionally High Drug Loading and Quantitative Loading Efficiency, J. Am. Chem. Soc. 137 (2015) 3458–3461.
[31] Y.W. Chu, B.Y. Wang, H.-S. Lin, T.-Y. Lin, Y.-J. Hung, D.A. Engebretson, W. Lee, J.R. Carey, Layer by layer assembly of biotinylated protein networks for signal amplification., Chem. Commun. (Camb). 49 (2013) 2397–2399.
[32] S.M. Hsu, L. Raine, H. Fanger, Use of avidin-biotin-peroxidase complex (ABC) in immunoperoxidase techniques: a comparison between ABC and unlabeled antibody (PAP) procedures., J. Histochem. Cytochem. 29 (1981) 577–580.

Chapter 5 Conclusions

Lignocellulosic biomass is an ideal feedstock for producing bioethanol, due to the advantages of ubiquitous distribution and abundant harvest. However, because of its rigid and complex structure, the complete degradation via enzymatic hydrolysis needs a variety of enzymes working synergistically in addition to various pretreatment techniques of lignocellulosic biomass. The aim of this work is to implement enzymatic strategies in ligocellulosic substrate hydrolysis that improves the degradation efficiency with less enzyme loading.

In Chapter 2, the effect of pretreatment with peracetic acid (PAA) or an ionic liquid (1-ethyl-3-methylimidazolium acetate, [Emim][OAc]) on the synergism between endoglucanase and endoxylanases in the hydrolysis of bagasse was investigated. Under the same pretreatment conditions, PAA pretreatment was more efficient at removing the hemicellulose from substrate, while ionic liquid pretreatment was more capable at decreasing the crystallinity of cellulose. The differences of the physical structure and chemical components of pretreated bagasse and the molecular architecture of enzymes were shown great impacts on synergism. More specifically, the hemicellulose content, especially arabinan, and the cellulose crystallinity of bagasse were found to affect the cellulase-xylanase synergism. A higher synergism (above 3.4) was observed for glucan conversion, at low levels of arabinan (0.9 %), during the hydrolysis of PAA pretreated bagasse. In contrast, [Emim][OAc] pretreated bagasse, showed lower cellulose crystallinity and achieved higher synergism (over 1.9) for xylan conversion. Ultimately, the combination of Cel6A and Xyn11A resulted in higher synergism for glucan conversion than the combination of Cel6A with XynZ-C, because of Xyn11A has a XBM that binds to both cellulose and xylan while XynZ does not.

Based on the result of Chapter 2, the substituent of xylan backbone, arabinose, has impeded the degradation of xylan, thus, in Chapter 3, arabinofuranosidase was investigated to degrade the hemicellulose together with endoxylanase. Two endoxylanases and an arabinofuranosidase were selected and immobilized on commercial magnetic nanoparticles through covalent bonding. Although the immobilized enzyme showed lower efficiency in degradation of insoluble wheat arabinoxylan than free enzymes at initial phase of hydrolysis process, free and immobilized enzymes showed a similar conversion to reducing sugars after hydrolysis for 48 h. Moreover, the immobilized enzymes were successfully recycled for 10 times. As a result, a 5.5-fold increase in the production of sugars was obtained with a mixture of enzymes immobilized after 10 cycles in total compared with free enzymes. Importantly, a

sustainable synergism between arabinofuranosidase and endoxylanases in the hydrolysis of insoluble substrate was observed even in the immobilized forms.

In Chapter 4, inspired by a naturally occurring multienzyme system, cellulosome, for degrading lignocellulose in a synergistic manner, an artificial binary enzyme conjugate system was developed based on the SpyCatcher-SpyTag system. An artificial proteinaceous scaffold, hyperbranched SpyCatcher polymer, was prepared by enzymatic protein polymerization catalyzed by horseradish peroxidase. Taking the advantage of SpyCatcher-SpyTag interaction, two SpyTagged enzymes were site-specifically conjugated onto the SpyCatcher polymer, yielding a binary enzyme complex. The ratio-controllable binary conjugated enzyme complex exhibited higher sugar conversion than free enzymes in the case of high Araf51A proportion sample, possibly due to the spatial proximity between the conjugated enzymes.

The present study only focuses on the clarifying the factors that affect the synergism between several purified enzymes on specific substrate and the synergistic effect between enzymes which are in different forms. Since the enzymatic strategies demonstrated in the present work were only tested on the simple pretreated bagasse and model substrates, it is necessary to further apply these systems, combining with other beneficial enzymes, in degradation of real substrate, lignocellulosic biomass.

Besides, in the present study, enzymes immobilized on magnetic nanoparticles have shown a good synergistic effect in hydrolysis of insoluble substrates. In the future, we can probably either decrease the diameter of the nanoparticles to achieve a higher diffusion rate or increase the enzyme binding sites on the scaffold by means of immobilizing polymer adaptors, to further improve the enzymatic efficiency.

Moreover, we have constructed a SpyCatcher scaffold with high conjugation capacity and close proximity between conjugated enzymes. With the ease to co-localize proteins via SpyCatcher-SpyTag system, this proteinaceous scaffold could serve as an universal scaffold and may be used to assemble other enzymes involved in biochemical cascade reactions, such as glucose oxidase (GOx) and horseradish peroxidase (HRP) for biosensing, and alcohol dehydrogenases (ADHs) and ketoreductases (KREDs) for biosynthesis. With the careful design of the spatial organization and loading process, this scaffold also may be used as a module that amplifies the signal intensity, as a result, improves the detection sensitivity of biosensors.

Acknowledgements

This thesis includes the works I have done in Department of Applied Chemistry, Faculty of Engineering, Kyushu University, Japan, from October 2013 to March 2017.

Firstly, I would like to express my sincere appreciation to my supervisor, Professor Noriho Kamiya. Professor Kamiya is greatly passionate towards science and a man with a wealth of knowledge. He always encourages me to expand my vision and supports my every decision. He guides me to start the journey of doing biology science and shares lots of the experiences and knowledge with me. I will never forget all the discussions and talks we had in lab. My sincere thanks also goes to Professor Masahiro Goto, for all the comments in lab seminars and all the helps and encouragements he gave to me.

Besides my supervisors, I would like to thank Professor Masahiro Kishida as my thesis committee. Thank you for your insightful comments and reviews.

Many thanks to Assistant Professor Rie Wakabayashi and Assistant Professor Kosuke Minamihata for all the expert advices, discussions and supports. Special thanks also goes to Assistant Professor Fukiko Kubota, who always takes good care of my study and life.

I would like to thank Associate Professor Hirofumi Ichinose from Faculty of Agriculture, Kyushu University, and Associate Professor Tsutomu Tanaka from Faculty of Engineering, Kobe University, for kindly support the enzymes I used in the present thesis.

Special thanks goes to Dr. Geisa Budinova who introduced me to all the basic techniques of biology and gave expert advices while I prepare the papers and invited me to many activities. I will never forget all those lovely moments. Appreciations also goes to my other labmates, the graduated students Dr. Yutaro Mori, Mr. Yusaku Takasugi, and Mr. Takafumi Saeki, and Dr. Yukiho Hosomomi, Dr. Mari Takahara and students belong to BioCatalysis group: Mr. Hiroki Kawashima, Mr. Naoki Fujimoto, Mr. Takashi Matsuzaki, and Mr. Yusuke Tanaka for all your kind helps and suggestions. It is a pleasure that I can work with you guys. Thanks to Dr. Zhigang Zhao, Dr. Kounosuke Hayashi, Mr. Qingliang Kong, Dr. Momoko Kitaoka, Ms. Sakurako Shiroishi, Ms. Mayu Fukuda I enjoyed the time we spend together. All of you made my PhD life colorful.

In the past three and half years, I was financially supported by China Scholarship Council (CSC). I would like to thank CSC for giving me this chance to study abroad and learned lots of useful techniques and knowledge.

Last but not least, I would like to thank my parents for all their unconditional love and supports throughout the whole journey. I love you all.

Lili Jia